THE STUDY OF N-GLYCANS USING HILIC, ION MOBILITY, AND MASS SPECTROMETRY

by

HOANG KIM NGAN THAI

(Under the Direction of Ron Orlando)

ABSTRACT

The existence of different isomers makes the study of N-glycan a challenging task. Hydrophilic Interaction Liquid Chromatography paired with Mass Spectrometry (HILIC-MS) is one of the well-known methods in glycomics. Having a single separation dimension limits HILIC-MS ability to distinguish some isomers. Ion mobility spectrometry (IMS) is a high-resolution gas phase separational technique that can be combined with HILIC-MS to increase the resolving power of the system without compromising the efficiency of HILIC separation. The HILIC-IMS-MS system provides better separation for N-glycan isomers, improving the ability to identify individual components in complex carbohydrate mixtures.

The work presented in this dissertation highlights the application of HILIC, IMS, and MS for the study of N-glycans. In Chapter 3, HILIC-MS was employed to examine the quantitative results of N-glycans labeled with different tags. The quantification of N-glycans using liquid chromatography (LC) – MS was found to be impacted by the chosen derivative tag. The ability of HILIC-MS/MS to distinguish glycan isomers was evaluated in Chapter 4. Separations were achieved between linkage and branched isomers. Chapter

5 describes the analysis of immunogenic N-glycans containing α -linked Galactose (α -Gal), HILIC-MS/MS could not separate α -Gal glycan from its non- α -Gal isomer. IMS successfully enabled the separation between α -Gal glycan and its non- α -Gal isomer. Because the high resolving power of IMS complements the performance of HILIC-MS for isomeric separation, a database (Chapter 6) was created that includes HILIC retention time, ion mobility collision cross section (CCS), and mass to charge (m/z) data of 205 procainamide labeled N-glycans. The database acts as a resource for data analysis of unknown samples.

An orthogonality study was performed to evaluate the resolving power obtained by combining different LC modes of separations with IMS-MS (Chapter 7). For glycan, porous graphitic carbon (PGC)-IMS-MS has higher peak capacity compared to HILIC-IMS-MS. Similar study performed on peptide shows that HILIC-IMS-MS has higher peak capacity than reserved phase (RP)-IMS-MS.

INDEX WORDS: Hydrophilic Interaction Liquid Chromatography, Mass

Spectrometry, Ion Mobility Spectrometry, N-glycan, Isomeric

Separation, Database, Orthogonality

THE STUDY OF N-GLYCANS USING HILIC, ION MOBILITY, AND MASS SPECTROMETRY

by

HOANG KIM NGAN THAI

BS, Youngstown State University, 2021

A Dissertation Submitted to the Graduate Faculty of The University of Georgia in Partial Fulfillment of the Requirements for the Degree

DOCTOR OF PHILOSOPHY

ATHENS, GEORGIA

2025

© 2025

Hoang Kim Ngan Thai

All Rights Reserved

THE STUDY OF N-GLYCANS USING HILIC, ION MOBILITY, AND MASS ${\tt SPECTROMETRY}$

by

HOANG KIM NGAN THAI

Major Professor: Committee: Ron Orlando Jon Amster Kelly Hines

Electronic Version Approved:

Ron Walcott Vice Provost for Graduate Education and Dean of the Graduate School The University of Georgia August 2025

DEDICATION

To my beloved family in Vietnam, thank you for having supported me throughout my educational journey. I would like to send a special thanks to my mom, my dad, and my grandma. I understand raising a child with the widest dream to become a scientist is not something you run into every day, especially in Vietnam. Mom, you have been there every step of this long journey, always making sure to be my constant support. This work is a declaration to your dedication and love. To my dad, thank you for always being there when I need you. I remember everything you have done for me, and I will forever treasure them. Grandma, you were the voice that advocated me to pursue my dream in the USA. I could never be thankful enough for your love and support. I hope I have made you both proud, Mom, Dad & Grandma.

To my husband (Brendon) and parents-in-law, thank you for being my second family here in the USA. To Appa and Omma, thank you for welcoming me into your home and family. I am grateful for all the support that you both have given me throughout these past years. Brendon, you have been my constant emotional support and always been there for me no matter what. While this journey is challenging, I am less lonely and more motivated because of your love and encouragement. It is time for us to get start on the life we have always dreamed and talked about. I am forever thankful to get to know you and have you in my life.

ACKNOWLEDGEMENTS

I would like to thank my advisor, Dr. Ron Orlando. Thank you for all the patience and dedication that you have for me. You have patiently taught me how to solve problems and think more critically in research. You are the best advisor that I could ever have asked for. Your guidance helped me to become the scientist I am today, and I am forever grateful. I would also like to thank Dr. Kelly Hines for helping to sharpen my scientific logic with constructive questions and feedback. To Dr. Jon Amster, thank you for giving me insightful suggestions and questions that encourage me to shape better thinking.

Thank you to the University of Georgia for admitting me into the PhD program in the Chemistry Department. To the Complex Carbohydrate Research Center, MobilIon, Agilent, and Bristol Myers Squibb (BMS), thank you for providing me with all the resources and support to complete this degree. Thank you to all the former and current group members that have taught, helped, and worked with me.

TABLE OF CONTENTS

| Pag | ţе |
|---|-----|
| CKNOWLEDGEMENTS | .V |
| IST OF TABLESv | ii |
| IST OF FIGURESvi | .11 |
| HAPTER | |
| 1 INTRODUCTION | .1 |
| 2 LITERATURE REVIEW | 6 |
| 3 N-LINKED GLYCAN QUANTITATION, IS RELATIVE QUANTITATION | |
| ALTERED BY LABEL CHOICE? | 0 |
| 4 SEPARATION OF N-GLYCAN ISOMERS VIA HILIC, ION MOBILITY AND | |
| MASS SPECTROMETRY | 4 |
| 5 USING HIGH RESOLUTION ION MOBILITY FOR THE SEPARATION OF α - | |
| GAL CONTAINING GLYCANS FROM THEIR NON- α-GAL ISOMERS5 | 6 |
| 6 A THREE-DIMENSIONAL DATABASE OF N-GLYCANS INCLUDES HILIC | |
| RETENTION TIME, ION MOBILITY COLLISION CROSS SECTION, AND | |
| MASS TO CHARGE FROM MASS SPECTROMETRY | 3 |
| 7 ORTHOGONALITY OF SEPARATION IN LIQUID CHROMATOGRAPHY, ION | |
| MOBILITY, AND MASS SPECTROMETRY10 | 0 |
| 8 CONCLUSION11 | 7 |
| FFFRENCES 12 | 1 |

LIST OF TABLES

| Paş | ge |
|--|----|
| Table 6.1: Procainamide-labeled N-glycans database with m/z, HILIC retention time in GU, and | d |
| ion mobility traveling-wave CCS information | 36 |

LIST OF FIGURES

| Page |
|--|
| Figure 3.1: HILIC analysis of N-glycans released from IgG2 (Frankenmab), IgG4 (Natalizumab), |
| and human serum IgG when labeled with ProA, 2AA, and 2-AB30 |
| Figure 3.2: The relative quantitation of doubly protonated glycans31 |
| Figure 3.3: The relative quantitation of multiple protonated species, including M + H, M + 2H, |
| and M + 3H32 |
| Figure 3.4: The relative quantitation of glycans calculated via the peak area of multiple |
| protonated species and sodium adducts, including $M + H + Na$, $M + 2H + Na$, and $M + H$ |
| + 2Na |
| Figure 4.1: The tandem mass spectrum of A3G3(Neu5Ac)1(1 α 2-6-Gal) (M+2H m/z = 1258.99) |
| and A3G3(Neu5Ac)1(1 α 2-3-Gal) (M+2H m/z = 1258.99) |
| Figure 4.2: The unassigned extracted ion chromatogram (EIC) of A3G3(Neu5Ac)3 and the fully |
| assigned EIC of A3G3(Neu5Ac)3 where the N-glycans were identified using Townsend |
| et al data, ³⁰ HILIC retention rules, and tandem mass spectrometry48 |
| Figure 4.3: The tandem mass spectrum of A3G3(Neu5Ac)3 at 31.06 min and 31.56 min49 |
| Figure 4.4: The EICs for A3G3(Neu5Ac)1(Neu5Gc)1 (M+3H m/z = 942.02), A3G3(Neu5Ac)2 |
| (M+3H m/z = 936.68), A3G3(Neu5Gc)1 $(M+3H m/z = 844.99)$, and A3G3(Neu5Ac)1 |
| (M+3H m/z = 839.66)50 |
| Figure 4.5: The EIC at M+2H m/z = 1332.03 of the A3G3(Neu5Ac)1F glycan and the tandem |
| mass spectra of the two detected chromatographic peaks |

| Figure 4.6: Possible positional isomers of A3G3(Ne5Ac)1F (1 α 2-3-Gal) that is not a |
|---|
| polyLacNAc species53 |
| Figure 4.7: The mobiligrams of A3G3(Neu5Ac)1F (1 α 2-3-Gal) glycan and |
| A2G2(LacNAc)1(Neu5Ac)1F (1 α2-3-Gal) glycan |
| Figure 5.1: HILIC analysis of major N-glycans released from Cetuximab |
| Figure 5.2: Extracted ion chromatograms (EICs) of $m/z = 1003.9$ from the β 1-3,4 Galactosidase |
| digested Cetuximab, the α 1-3,4,6 Galactosidase digested Cetuximab and standard |
| Cetuximab68 |
| Figure 5.3: The tandem mass spectrum of the precursor ion at $m/z = 1003.9$ from Cetuximab and |
| human serum IgG69 |
| Figure 5.4: The mobiligrams of $m/z = 1003.9$ from Adalimumab (IgG1), human serum IgG, and |
| Cetuximab70 |
| Figure 5.5: HILIC-IMS-MS results showing the ion mobility traces of the ion at 1003.9 m/z units |
| from Cetuximab, obtained before digestion, after β1-3,4 Galactosidase digestion, and |
| after α1-3,4,6 Galactosidase digestion71 |
| Figure 6.1: Procainamide-labeled dextran is used as an external calibrant to convert retention |
| time in minutes into glucose unit (GU)96 |
| Figure 6.2: The CCS calibration errors of dextran ladder from GU9 to GU19 using two different |
| fitting functions including: logarithmic fit and quadratic polynomial fit97 |
| Figure 6.3: A three-dimensional plotted space of the procainamide labeled glycans database |
| composed of HILIC retention time in GU, ion mobility values in CCS, and m/z data98 |
| Figure 6.4: An in-house N-glycan identification protocol using the assistance of the developed |
| N-glycan database99 |

| Figure 7.1: Two-dimensional plots of N-glycan data collected from HILIC-IMS-MS | 113 |
|--|-----|
| Figure 7.2: The normalized plots of N-glycan data collected from PGC-IMS-MS | 114 |
| Figure 7.3: The normalized plots of peptide data obtained from HILIC-IMS-MS and RP-IMS | S- |
| MS platforms | 115 |

CHAPTER 1

INTRODUCTION

Changes in N-linked glycosylation are found to be correlated with numerous diseases.¹⁻⁴ Cancer research has delved into utilizing some abnormal changes of glycoforms as biomarkers for early-stage diagnosis. ^{1,5} The advancement in drug development has also brought more attention to the study of N-glycans. Administrating biotherapeutic products with a high abundance of non-human glycoforms can lead to severe negative effect on patients. ⁶⁻⁹ The characterization of N-glycans plays a crucial role in guaranteed safety and efficacy of biotherapeutic products. Hydrophilic Interaction Liquid Chromatography (HILIC) paired with Mass Spectrometry (MS) is one of the popular methods in glycomics. ¹⁰⁻¹³ HILIC-MS enables characterization of challenging profiles of N-glycans human samples, 14-16 or monoclonal antibodies (mAbs). 17-19 The first part of this work focus on differentiating glycan isomers using HILIC paired with tandem mass spectrometry (MS/MS). Isomeric separation via HILIC-MS/MS depends mainly on only HILIC, which limits the ability to resolve some isomers. Ion mobility spectrometry (IMS) is emerging as a powerful separational technique for carbohydrates with separational timescale within milliseconds, ²⁰ making IMS a great candidate to be paired with HILIC-MS for improvement in resolving power without compromising HILIC separation efficiency. The second half of this work discusses the advantages of HILIC-IMS-MS in N-glycan study. A database of 205 common N-glycan species in biotherapeutics was developed with HILIC retention time, ion mobility collision cross section, and mass to charge data. The

orthogonality of multidimensional systems involved IMS were evaluated to assess the resolving power of each developed system.

Chapter 3 discusses Liquid chromatography - mass spectrometry (LC-MS) quantitative results of N-glycans labeled with different tags including Procainamide (ProA), 2aminobenzamide (2AB), and 2-aminobenzoic acid (2AA). Derivatizing N-glycans helps to avoid complications in chromatographic analysis²¹ and increase ionization efficiency in MS.²²⁻²⁵ Reductive animation is one of the common derivative methods in N-glycan quantification. There are various reductive animation tags available for derivatization. The quantitative results from LC-MS are expected to be consistent despite different tags chosen for quantification. Each tag has a unique structure and carries distinct chemical properties, which can produce dissimilarities in quantification. Chapter 3 examines differences observed amongst the relative quantitation of differently labeled glycans. Discussion focusses on different aspects that can produce inconsistency in quantification using LC-MS. Frankenmab (IgG2), Natalizumab (IgG4), and Human Serum IgG were the three main glycoprotein sources chosen for the study. All labeled glycans were run under similar LC-MS conditions to guarantee consistency amongst experiments. The profile of N-glycans were characterized prior to quantification. The relative abundance (%) of N-glycans was calculated based on the characterized glycan profiles.

Chapter 4 demonstrates the application of HILIC-MS/MS in separating N-glycan isomers. Overexpression of some N-glycans has been proposed as potential biomarkers in cancer studies. The abnormal increase in abundance of $\alpha 2$,6-linkages Neu5Ac N-glycans^{26,27} or polyLacNAc glycan^{28,29} was found to associate with tumorigenesis. PolyLacNAc species are glycans composed of the repeating pattern of Gal-($\beta 1$ -4)-GlcNAc on antennae. Fetuin is a well-known glycoprotein source with a high variety of complex sialylated glycans including Neu5Ac-

(α2-3/6)-Gal glycans, Neu5Ac-(α2-6)-GlcNAc glycans, and Neu5Gc-(α2-3/6)-Gal. ^{30, 31} Chinese Hamster Ovary (CHO) cells is a popular cell line used in synthesizing biotherapeutics products. ^{32, 33} Glycoforms in CHO cells involve arrays of different N-glycans with complex structures. Chapter 4 displays some exciting separation of sialylated isomers and polyLacNAc glycans detected in Fetuin and CHO cells. The achieved separations indicate HILIC-MS is a powerful tool in differentiating challenging profile of N-glycan isomers. A preliminary study combining ion mobility spectrometry (IMS) with HILIC-MS for N-glycan characterization was conducted. The study shows promising results of IMS complements the separation of HILIC and provides additional fingerprint data for identification.

Chapter 5 studies the separation of Gal-(α 1-3)-Gal (α -Gal) glycans from their non- α -Gal isomers using high resolution ion mobility. Clinical research found that biotherapeutic products with high abundance in glycans containing α -Gal linkage can lead to severe allergic reaction in patients. Humans lack the ability to produce α -Gal glycan and a novel IgE antibody (Ab) is directed against the existence of α -Gal glycans. He detection of α -Gal glycans plays a crucial role in ensuring the safety in biotherapeutics. The glycoforms of Cetuximab have high abundance in α -Gal containing glycans and was chosen as the α -Gal positive control of this study. HILIC-MS/MS was initially used to identify α -Gal containing glycans from non- α -Gal species. While HILIC-MS/MS attained the separation of α -Gal species with the Galactose number exceeds the antenna number, HILIC-MS/MS could not distinguish α -Gal species with Galactose number equals to the antenna number. A different system involves a combination of a high-resolution ion mobility (IMS), and HILIC-MS was used for the characterization of α -Gal glycans. The separation between non- α -Gal glycan and its α -Gal isomer was achieved via IMS.

The study reveals the ability of IMS in identifying challenging immunogenic α -Gal glycan in the presence of their non- α -Gal isomers.

Chapter 6 discusses the development of procainamide labeled N-glycan database. HILIC-IMS-MS has been demonstrated as a powerful system in the characterization of N-glycans. Most of the current databases only include data from one of the participating dimensions such as Glycostore 35 only reports LC retention time data or Glycomob 36 includes only ion mobility data. The available databases are independent databases that report data of N-glycan with different derivatization and cannot be linked together for identification purposes. This study developed a comprehensive database that comprises 205 procainamide labeled N-glycans with HILIC retention time in glucose unit, ion mobility data in CCC, and mass to charge (m/z) data from MS. A list of glycoprotein sources was carefully chosen to characterize information of N-glycans commonly found in biotherapeutic products. The database also includes immunogenic glycans such as ($\alpha 2$ -3/ $\alpha 2$ -6) Neu5Gc-glycan and α -Gal containing glycan. The three-dimensional N-glycan database is a useful toolbox during data analysis that provides detailed characterization profile of N-glycans with information on linkage or branched isomers.

Chapter 7 evaluates the orthogonality of different multidimensional systems used in glycomics and proteomics. Peak capacity is a common metric to measure separation efficiency.

37, 38 The combination of multiple separational systems enables improvement of peak capacity, which can significantly increase the overall resolving power of the system. The utilization of LC-IMS-MS has gained attention in many research areas for high resolving power and efficiency.

41 This study examines the orthogonality of three LC-IMS-MS systems including: HILIC-IMS-MS, porous graphitized carbon (PGC)-IMS-MS, and reversed phase (RP)-IMS-MS. The orthogonality of HILIC-IMS-MS and PGC-IMS-MS in N-glycan analysis was assessed. The

orthogonal study of peptide examines the behavior of HILIC-IMS-MS and RP-IMS-MS. The study of orthogonality allows better assessment of resolving power of different LC-IMS-MS systems. Researchers can utilize orthogonal information in choosing an ideal system for analysis.

CHAPTER 2

LITERATURE REVIEW

Glycosylation

Glycosylation is the most common protein post translational modification. 42-44 This process involves the attachment of polysaccharides to a protein at a specific amino acid. There are four classifications including O-glycosylation, N-glycosylation, C-glycosylation, and GPI-anchored attachment. 42, 45 O-glycosylation and N-glycosylation are two most common forms of glycosylation. O-glycosylation is the result of sugar attaching to oxygen atom in the hydroxyl group of Serine (Ser) or Threonine (Thr). 42, 46 O-glycan can be further categorized based on the initial sugar linked to the amino acid. 46 N-linked glycoprotein formed via the bonding of N-acetylglucosamine (GlcNAc) to nitrogen atom of Asparagine amino acid. 47 N-glycan is divided into three groups: high mannose, hybrid, and complex glycan. 47 Glycosylation participates in many biological functions such as immune response, signaling pathway, protein stability, and folding. 42 Abnormal changes of glycosylation correlate with numerous diseases such congenital disorders of glycosylation, cancer, infectious, and chronic inflammatory diseases. 45, 46 *N-linked Glycosylation*

N-linked glycosylation involves the addition of sugars to the peptide backbone at the asparagine (Asn) amino acid. $^{47-49}$ The chain of N-glycan sugars commonly starts with the formation of β 1-4 linkage between N-acetylglucosamine (GlcNAc) and the nitrogen atom of Asn. Most N-glycans with GlcNAc- β 1-4-Asn core linkage share the same biosynthesis pathway that begins with the synthesis of dolichol-P-P-GlcNAc₂Man₉Glc₃ in the ER lumen.

Oligosaccharyltransferase (OST) then binds to the newly formed dolichol-P-P-GlcNAc₂Man₉Glc₃ to transfer GlcNAc₂Man₉Glc₃ onto Asn-X-Ser/Thr in proteins and release Dol-P-P in the process. The pathway continues with the cleavage of glucoses via α -glucosidases I and II, leaving the glycan chain with GlcNAc₂Man₉ (Man₉). From there, the α1-2 linkages between mannoses are cleaved to transform Man9 into GlcNAc₂Man₅ (Man5). It is worth noting the removal process of α1-2 linkages between mannoses suggests that Man9 and Man5 are the two unique high mannose glycans exit in only one structure, no isomers formed throughout the process. The formation of hybrid and complex glycans is initiated by Nacetylglucosaminyltransferase (MGAT1) transferring GlcNAc residue to the C-2 position of the Mannose attached to the α 1-3 branch. ⁴⁷⁻⁴⁹ Different enzymes such as Mannosidase, Nacetylglucosaminyltransferase, Galactosyltransferases, Fructosyltransferase, and Sialyltransferases start to add or trim monosaccharide residue, which create different structures of N-glycans. 47, 50 The diversity of an N-glycan structure depends on the number of antenna GlcNAc, antenna Gal, attached sialic acids (Neu5Ac or Neu5Gc), and the identification of glycosidic linkages.

Involvement of N-Glycans in Biotherapeutics

The alterations in abundance of some specific glycan structure have been explored as potential biomarkers for cancer diagnosis.¹⁻⁴ Sialic acids are often attached to galactose or N-acetylgalactosamine residues at the reducing end via α2,3 or α2,6 linkages.⁵¹⁻⁵³ Sialic acids play a key role in cell communication due to their exposure location.^{52,53} Elevation in abundance of α-2,6 Neu5Ac glycan was detected in cancerous samples and proposed as potential biomarkers.
^{26,27} Another example of glycan in biomarker study is the overexpression of Poly-N-acetyllactosamine (polyLacNAc) glycans. PolyLacNAc glycans are species with Gal-(β1-4)-

GlcNAc disaccharides (LacNAc) repeating on antennae.⁵⁴ The progress of tumor was found to correlate with the increase in abundance of polyLacNAc species. ^{28, 29} The highlighted examples demonstrate the involvement of glycans in numerous diseases, particularly cancer.

The evolution in synthesizing biotherapeutic products from non-human sources has brought more attention to non-human immunogenic glycoforms. Some non-human glycans detected in biotherapeutic products can cause negative impact when administrated into patients. A popular example is the Gal-(α 1-3)-Gal (α -Gal) immunogenicity. The immunogenicity of α -Gal species was first reported in a clinical study of a biotherapeutic drug called Cetuximab. Humans lack the ability to produce N-glycan with α -Gal modification. A novel IgE antibody (Ab) was discovered to direct against the detected α -Gal glycans in Cetuximab, causing hypersensitivity reaction in patients. Another popular case of immunogenic glycans is the existence of glycans with N-glycolylneuraminic acid (Neu5Gc). Neu5Gc is created via the conversion of N-acetylneuraminic acid (Neu5Ac) using CMP-Neu5Ac hydroxylase enzyme. Human lost the ability to make CMP-Neu5Ac hydroxylase enzyme through evolution and cannot produce Neu5Gc. Anti-Neu5Gc activity has been reported in healthy human or human-like models, indicating the potential risk Neu5Gc posed. 57,58

N-glycan Release

The analysis of N-glycan starts with releasing of glycan from the peptide backbone. Chemical and enzymatic release are the two common methods employed in glycan analysis. Hydrazine and β-elimination are the two most well-known chemical approaches.⁵⁹ N-glycan linkage is cleaved via hydrolysis under alkeline condition in β-elimination.⁶⁰ Hydrazine method uses anhydrous hydrazine to remove the linkage of between GlcNAc and Asn.⁶¹ Chemical approaches involves highly toxic chemicals and can result in unpredicted modification of the

released glycan, ⁵⁹⁻⁶¹ which makes chemical application a less popular choice compared to enzymatic method. Some of the enzymes used in enzymatic cleavage include Endo H, Endo F, Endo D, PNGaseA, and PNGaseF. ^{47, 59, 62} Each of these enzymes have their own limitations in cleaving some type of glycans or large species. PNGaseF is the most widely used enzyme due to its ability in cleaving most N-glycans including large and complex species with the only exceptions for non-mammalian glycans containing a 1,3-core fucose. ^{47, 59}

Derivatization of N-glycan

Derivatization is highly recommended in the analysis of N-glycan. Released N-glycan has a non-reducing end of GlcNAc residue that produces β - and α -anomer. The conversion between anomers results in multiple peaks in chromatographic profile and complicate the analysis of N-glycan. Derivatization of N-glycan can transform the unreduced GlcNAc into sugar alditols, which avoid complications in chromatographic profile and increase ionization efficiency in mass spectrometry. Analytical methods utilize fluorescence detectors cannot detect native glycan due to the absence of chromophore or fluorophore group. Some derivatization methods label the reducing end glycan with fluorescence tags to enable detection in fluorescence analysis. Another popular platform for glycomics study is mass spectrometry. The glycosidic bonds of glycan are fragile and can easily be broken down during electrospray ionization in mass spectrometry, resulting in a decrease in ionization efficiency and increase in limit of detection.

Permethylation is a derivatization method that works well for glycomics study using mass spectrometry platforms.^{24, 63, 64} Permethylation is the process where all active hydrogens of the glycan structure are converted to methyl groups using iodomethane. All hydrophilic hydroxyl groups in glycan are replaced with methoxy groups, which led to the increase in hydrophobicity

for permethylated glycans.²⁴ Permethylation was first introduced by Purdie and Irvine,⁶⁵ but the procedures were laborious with a lot of hazardous chemicals involved. The permethylation procedure was later optimized by Ciucanu and Kerek, 66 utilizing iodomethane in dimethyl sulfoxide (DMSO) containing powdered sodium hydroxide to perform permethylation of glycans. While more development has been done to increase permethylation yield, Ciucanu and Kerek protocol are the standard method for permethylation in glycomics studies. Sialic acid with carboxyl groups struggle to ionize and decrease the overall protonation of highly sialylated glycan. These carboxyl groups are converted into methyl ester, which significantly increases the ionization efficiency of sialylated glycans. Permethylation is one of the most effective derivatization methods to eliminates the low ionization of sialylated species.²⁴ Research also reported that permethylated glycan enables structure identification by tandem mass spectrometry and overcome fucose migration issues detected in gas-phase.⁶⁴ The separation of permethylated glycans with high hydrophobicity has been well-studied in reversed phase liquid chromatography. 63, 67, 68 While these studies successfully detect complex glycans, limitations in isomeric separations are observed as the differences in hydrophobicity were not effective enough to distinguish some challenging isomers. 13 Research also demonstrated the distinguishment of permethylated glycans using porous graphitized carbon mode, suggesting a new approach in permethylated glycan separation.^{64, 69, 70}

Reductive animation is another popular mode derivatization approaches. A condensation reaction is performed between a chosen fluorescence tag with amine group and the aldehyde group of the nonreduced GlcNAc. A reductive reaction is performed after, converting the resulted imine or Schift base to a secondary amine via reducing agent such as NaBH₄ or Na[BH₃CN].²² Reductive animation only modified the reducing end with the addition of an

amine tag, which reserves the hydrophilicity of glycans. The reserved hydrophilicity enables the separation of challenging glycan isomers using hydrophilic interaction liquid chromatography.

Some traditional tags such as 2-aminobenzamide (2-AB), 2-aminobenzoic acid (2-AA), and 2-aminopyridine (PA) are often used in N-glycan analysis using liquid chromatography paired with detectors. 22, 24 Studies using mass spectrometry as detector technique typically prefer fluorescence tags with tertiary amine group that has high ionization efficiency in positive ion acquisition mode such as procainamide (ProA), InstantPC, and RapiFluor-MS (RFMS). 24 InstantPC and RFMS allow high through application, but these tags are not cost-effective for research as they require purchasing expensive N-glycan kit from the vendor. ProA produces effective ionization efficiency and does not require purchase of vendor labeling kit, which is cost-effective for applications in research. Reductive animation provides significant benefits to analytical methods using liquid chromatography or mass spectrometry platforms and has been applied widely in N-glycan analysis.

Mass Spectrometry in Glycans Analysis

Mass spectrometry (MS) is a widely used platform for the characterization of N-glycans. ⁷¹⁻⁷³ MS identify molecules by measuring their mass to charge (m/z). Analytes are introduced into an ion source to generate charged particles for analysis. The charged ions travel through mass analyzer where ions are separated based on their m/z prior to arriving at the detector. ^{74, 75} The detector measures the ion intensity of separated ions via electronic currents. ⁷⁶ Mass spectrum is generated for analysis with the ion intensity (y-axis) and m/z (x-axis).

Tandem mass spectrometry (MS/MS) produces fragment ions that are used to assist in structural identification of unknown glycan. Some common fragmentation techniques such as low/high collision-induced dissociation (CID), electron capture dissociation (ECD), and electron

transfer dissociation (ETD) have been utilized in carbohydrate identification. ⁷⁷ CID remains the more popular option for glycan analysis. ⁷⁷ Glycan can be fragmented through the glycosidic linkage or cross-link cleavages. While protonated carbohydrates generate glycosidic cleavage, metal-adducted oligosaccharides are prone to produce cross-link fragment ions under the influence of low energy CID. ^{78, 79} Electron-based dissociation methods such as ECD and ETD generally reported to produce extensive abundance in cross-link cleavage. ^{80, 81} Glycosidic cleavage produces fragment ions focusing on composition information, but ions resulted from cross-link cleavage provide more detail on linkage identification. Cross-link fragment ion assists MS to characterize linkage or branching position of glycan structure. ^{80, 81} Applications of tandem mass spectrometry have demonstrated fragment ions benefit MS-based analysis greatly in characterizing N-glycans. ⁸⁰⁻⁸³

Ionization Methods

Two most popular soft ionization methods in carbohydrate analysis are Matrix-Assisted Laser Desorption/Ionization (MALDI) and Electrospray Ionization (ESI). 77, 84, 85 MALDI utilizes laser to desorbs and ionizes samples under high vacuum. Samples are required to be mixed with a chosen matrix that enables the absorption of laser energy. 86 High throughput applications of N-glycans analysis have demonstrated MALDI-MS is a powerful tool that enables the analysis of high complex N-glycan profiles. 87-89 MALDI paired with mass spectrometry imaging (MSI) emerges as a valuable tool in biotherapeutics, particularly tissue analysis. MALDI-MSI can directly analyze glycans on the surface of tissue, which allows glycan profiling of tumor- and non-tumor regions. 90, 91 Electrospray Ionization (ESI) applies high electric energy to transform liquid sample into charged droplets. High temperature and stream of drying gas induces evaporation, and ions are ejected from the charged droplets. The emitted ions are often generated

as multiple charged species. 92 ESI is widely used as an ionization source for online liquid chromatography/capillary electrophoresis separation paired with MS. The application of ESI-MS with online separation method has enabled identification of challenging glycan profiles. 93-95

Mass Analyzer

Mass analyzer is a sensitive component that plays a crucial role in differentiating ions. Different mass analyzers are available for glycan analysis including ion trap (IT), orbitrap, Fourier transform ion cyclotron resonance (FT-ICR), quadrupole, and time-of-flight (TOF). 96 Ion trap is one of the classic mass analyzers used in carbohydrate analysis. 97,98 Ion trap uses direct current (DC) and radio frequency (RF) potential to trap ions in a confined space before ejecting ions for detection. 99, 100 FT-ICR and Orbitrap also "trap" ions for analysis. FT-ICR works by trapping ions in a strong magnetic field where ions move in circular motion. RF electric field excites the ions and push them toward the detector plate. Excited ions continue to orbit and generate unique image currents on the detector plate. Fourier transforms the time-domain image current into frequency domain, which are then converted into m/z ratios. 101, 102 Orbitrap on the other hand traps ions in an electrostatic field where ions orbit around the central spindle electrode. A special conical shape of electrode at the same time introduces an axial electric field that pushes ions and initiates harmonic axial oscillations. The axial oscillations generate unique image currents, which are later Fourier-transformed into the frequency domain and converted into m/z data. 102, 103 While FT-ICR provides higher resolution and mass accuracy, Orbitrap operates more simple without the need of superconducting magnet and is a more poplar mass analyzer in glycomics study. 96, 104 Quadrupole is another popular mass analyzer in glycan analysis. Quadrupole consists of four circular metal rods where DC and RF are employed to create an electric field. Ions outside a desired m/z range when oscillates in the electric field will

collide into the rods and not reach the detector.¹⁰⁵ Some modern applications of quadrupole mass analyzer are triple quadrupole mass spectrometry (QQQ) or quadrupole - time of flights mass spectrometry (Q-TOF). QQQ instrument consists of three quadrupoles where the first quadrupole selects precursor ions, the second quadrupole contains a collision cell that produces fragment ions, and the resulting fragment ions are filtered in the third quadrupole. QQQ is a unique mass spectrometry platform that provides absolute quantification.¹⁰⁶ Quadrupole can often be combined with TOF mass analyzer to create an identification system that filters, fragments, and detects ions. TOF measures the time travel of ions in a fixed distance and converts the collected flight time into m/z ratio. TOF offers ultra-fast mass analysis with a wide range of m/z and great ion transmission.¹⁰⁷ Quadrupole combined with TOF enables both high selectivity of ions and rapid analysis, which is ideal for high throughput identification. Q-TOF is a valuable platform that has been applied widely in characterizing complex glycan profiles.^{82, 108, 109} *Liquid Chromatography*

Liquid chromatography (LC) is a separation technique that separates a mixture into individual analytes. Separation in LC is driven by the interaction of analytes with the mobile phase and stationary phase. A chromatographic column is described as being made up of theoretical plates¹¹⁰ where the high number of theoretical plates represents high separation efficiency. Assuming the length of the column remains unchanged, the height of the theoretical plates can be altered to optimize the number of plates in a chromatographic column.¹¹¹ The smaller the height of theoretical plates equivalent with a higher the number of plates. The elements impacting the height of theoretical plates can be described via Van Deemter equation¹¹¹:

$$H = A + \frac{B}{\mu} + C\mu$$
 Equation 1

Eddy diffusion (A) describes different paths that an analyte can travel in the column. The packing of the column directly impacts eddy diffusion where poor packing creates multiple paths and results in wider analyte elution. Longitudinal diffusion (B) is the diffusion of analytes from high to low concentration areas phase, which results in band broadening. The faster the mobile phase velocity (u) or often known as flow rate, the smaller the impact of longitudinal diffusion. Resistance to mass transfer (C) illustrates the movement of an analyte between the stationary phase and the mobile phase. Analyte can travel inside the stationary phase and a slow flow rate results in slow existing of analyte, creating peak broadening. Increasing of mobile phase velocity enables fast existing of analyte from the stationary phase and avoid peak broadening.

Liquid chromatography is often paired with MS in glycomics study. There are several LC techniques that have been paired with MS to characterize N-glycans: reversed phase liquid chromatography, porous graphitized carbon, and hydrophilic interaction liquid chromatography. ¹³

Reversed Phase Liquid Chromatography (RPLC) separate analytes through the hydrophobic interaction between the analyte and the stationary phase. The RP stationary phase used in glycan analysis is often made of long chain hydrocarbons called C₁₈ (octadecylsilane) linked with silica particles. Molecules with higher hydrophobicity interact and retain longer on the RP column. N-glycan is a chain of monosaccharide residue with high hydrophilicity, which does not interact well with the nonpolar stationary phase of RP. Hydrophobic derivatization of N-glycan is necessary to increase the hydrophobicity of glycan the structure and enable better interaction with the stationary phase. N-glycan is a common choice of hydrophobic derivatization where the hydroxyl groups are converted to methoxy group. S-4

Research has reported that RPLC combined with MS/MS enable successful analysis of glycans released from complex matrices such as human milk, 115 mouse brain tissue, 116 or cell lines. 117

One of the limitations of RPLC in glycan analysis is the ability to separate isomers. Some isomers have such small differences in structure that hydrophobic changes do not have the capacity to induce isomeric separation in RPLC. 13 While there are possible solutions to increase separation efficiency of RPLC, the proposed solutions are often time-consuming and laborious. 13 RPLC is a robust separational technique, but other LC modes are preferable in separating glycan isomers.

Porous graphitic carbon (PGC) is a powerful LC in separating isomeric glycans. Separation mechanism in PGC is a combination of hydrophobicity influence from the analytes and the polar retention effect of the graphitic carbon. The first application of PGC in glycan analysis was the characterization of high mannose native glycans released from Ribonuclease B. PGC has successfully achieved isomeric separation of Man8, Man7, and Man6, paving a way to utilize PGC in differentiating complex isomers. More recent applications of PGC have been done with permethylated or reducing-end derivatized glycans. Linkage isomers such as $\alpha 2-3/\alpha 2-6$ sialylated glycans were successfully separated, indicating the resolving power of PGC for glycan analysis. PGC has been demonstrated as a powerful LC mode in separating isomeric species, but the lack of reproducibility for retention time 121 has limited the application of this LC mode.

HILIC is a popular liquid chromatography mode that complements MS greatly in glycomics study.^{10, 13} HILIC was first introduced by Alpert in 1990 as a derivative of the normal phase.¹²² Separation mechanism in HILIC relies on partition mechanism (hydrogen bonding), ionic, and dipole-dipole interaction. Analytes partition between the organic mobile phase and

semi-immobilized layer of mobile phase enriched with water is formed in the stationary phase of HILIC. This partition mechanism was suggested as a crucial mechanism in the retention of carbohydrates in HILIC. There are different packing material available for HILIC column such as Zwitterionic (ZIC R^{\odot}) functional group, amide/amine group, and hydroxyl group. The unique hydrophilic interaction between the stationary phase and the analytes enables effectively separation of glycan isomers. HILIC combined with MS has successfully characterize challenging profiles of N-glycans. HILIC has been demonstrated as a power LC mode in resolving complex isomers such as $\alpha 1$ -3/ $\alpha 1$ -6 A2G1F¹⁴ or $\alpha 2$ -3/ $\alpha 2$ -6 sialylated glycan. HILIC not only provide excellent resolving power in isomeric separation but also produce reproducible and predictable retention time, which makes HILIC an ideal LC mode in glycan study.

Ion mobility Spectrometry (IMS) is emerging as a powerful separational technique for carbohydrates. Ions are moved in gases under the influence of electric field and differentiated based on mass, charge and shape. A small and compact ions travel faster than a large and bulky ions in an electric field. IMS measures the mobility of ions in the unit of time, but most studies convert ion mobility arrival time into collision cross section (CCS). CCS is a universal unit and transferable across instruments. Drift tube IMS can produce arrival time that can be directly converted into CCS using Mason-Schamp equation. Other platforms such as traveling wave IMS must use calibrant to establish a calibration curve and convert arrival time into CCS. IMS was initially employed to differentiate small carbohydrate isomers. More studies started to utilize IMS for high throughput applications due to the ability in separating analytes within milliseconds. A development of a high resolving power IMS platform called structures for lossless ion manipulations (SLIM) has been proposed as a powerful tool to

differentiate challenging isomers. SLIM is a travelling-wave based IMS that separates ions through using a unique 13 m path length. Some applications of SLIM in N-glycan isomer separation have successfully distinguish challenging positional isomers such as $(\alpha 3/\alpha 6)$ on A2G1 and A2G1F, suggesting the ability of SLIM in isomeric separation.

N-glycan database

N-glycan database is developed as an assistant tool in analysis. The study of N-glycans involves multiple steps starting from sample preparation to data analysis for final identification. Studies with information on different glycans are valuable assets. N-glycan database was established to help store and manage characterized data of N-glycan, 135 which can be used as a search tool to increase accuracy and efficiency in future data analysis. The development of N-glycan database dated back in 1980s with the first database established called Complex Carbohydrate Structural Database (CCSD). 136 Complex Carbohydrate Structural Database (CCSD) includes thousands of different glycans reported with their biological activities/applications. The emergence of new analytical techniques has led to the development of different databases including a variety of data such as NMR spectra, 137 MS spectra, LC retention time, 35 and ion mobility CCS, 36 Research in development of N-glycan database is currently in progress to help expand the coverage of available glycan data.

Orthogonality

Orthogonality is a common metric to evaluate the separation efficiency of multidimensional systems. The application of multidimensional systems has been demonstrated as a powerful approach to increase separation efficiency of an analytical technique. 41, 139 140, 141 An iconic example of multidimensional system is Multidimensional Protein Identification Technology (MudPIT) that employs an orthogonal two-dimensional liquid chromatography to

detect more than 1000 proteins in a complex proteome profile. ¹⁴² However, not all analytical techniques can result in effective resolving power and provide useful data when paired together. Orthogonal study examines the uncorrelation between data collected from the participating technique. High uncorrelation of collected data indicates each participating dimension result in unique datapoint with minimal overlap. ^{143, 144} Orthogonality metric can be calculated by evaluating the geometric coverage of the datapoint in a specific two-dimensional space. The geometric calculation of orthogonality was first introduced by Gillar et al in 2005. ¹⁴⁵ The study also showed evaluation of orthogonal metric of 7 different two-dimensional LC systems. Many following studies have applied this geometric approach to calculate the orthogonality of different two-dimensional LC systems. ^{143, 144, 146}

CHAPTER 3

N-LINKED GLYCAN QUANTITATION, IS RELATIVE QUANTITATION ALTERED BY LABEL CHOICE?

Thai, H., Orlando, R. To be submitted to Journal of Biomolecular Techniques

Abstract

Glyco-biomarker study often utilizes the quantification of glycosylated IgGs for biomarker diagnosis. Liquid chromatography (LC) paired with mass spectrometry (MS) is a common platform for the characterization and quantification of N-glycans. Derivatization of released N-glycans is highly recommended prior to LC-MS analysis. One of the most common derivative approaches is labeling the unreduced N-acetylglucosamine (GlcNAc) terminus with an amine tag. Labeling the terminus of glycans helps to increase MS signal and improve chromatographic characteristics. Different tags can be chosen for quantitative experiments as it is expected that samples labeled with different tags still yield the same ratio of glycans. Herein, an evaluation to this assumption was conducted by using three popular tags: Procainamide (ProA), 2-aminobenzamide (2AB) and 2-aminobenzoic acid (2AA) for the relative quantification of N-glycans released from IgG samples. The result reveals that the difference in chemical properties from each tag leads to dissimilarities in quantitative results.

Introduction

N-linked glycosylation is one of the most common post translational modifications that impact stability and other cellular functions of proteins. 43, 44 The alterations of N-glycosylation were found to be associated with numerous human diseases, particularly in cancer. 4 Research in biotherapeutics provided many insights into discovery on the connection between N-glycan patterns to common cancer diseases such as pancreatic, prostate, ovarian, stomach, and lung cancer. The study of changes in N-glycosylation is proposed as a potential biomarker tool for clinical diagnosis. One of the popular successful studies in glyco-biomarker is the FDA-approved case called fucosylated alpha-fetoprotein (AFP-L3) for the early detection of hepatocellular carcinoma (HCC) amongst liver cancer patients. 1,5

Biotherapeutic studies often employ Liquid Chromatography (LC) – Mass Spectrometry (MS) for N-glycan quantification. 117, 147-150 While MS is a highly sensitive technique that simultaneously detect and quantify the ratio of N-glycans, LC complements MS via assisting to differentiate some isomers that MS alone struggles to detect. Some common LC modes in glycomics includes reversed phase liquid chromatography (RPLC), porous graphitic carbon (PGC), and hydrophilic interaction liquid chromatography (HILIC). 13 The separation mechanism of HILIC utilizes hydrophilic interaction to effectively resolve challenging hydrophilic analytes such as glycan isomers. 10, 13 With great potential power in isomeric separation for carbohydrates and can produce reproducibility retention time, HILIC is a popular choice for isomeric N-glycan analysis and quantification. 10, 117, 151, 152 The quantification of N-glycan using HILIC-MS benefits from both the high sensitivity of MS and high resolution of HILIC, which helps avoid misidentification and increase accuracy in quantification.

The analysis of N-glycans starts with releasing N-glycans from the peptide backbone using PNGaseF enzyme followed by clean-up steps and optional derivatizations. Reduction and derivatization are recommended for the study of N-glycans using LC-MS method. When N-glycans are released, the terminus N-acetylglucosamine (GlcNAc) is left unreduced and produces anomeric isomers that complicate the analysis of LC profile. Reduction helps convert the unreduced GlcNAc into sugar alditols to guarantee the production of single chromatographic peaks and avoid complication in data analysis. ²¹ The structure of glycan is fragile and can be easily broken-down in the electrospray ionization (ESI) of MS. Research has found that derivatization helps to prevent in-source fragmentation and improve ionization efficiency. ²²⁻²⁵ One of the most common N-glycan derivatizations in HILIC-MS experiments is reductive animation. ²² A primary amine group is chosen for the reaction to react with the aldehyde group of the glycan through a condensation reaction. The resulted imine or Schift base is then reduced to a secondary amine using reducing agent such as NaBH₄ or Na[BH₃CN]. ²²

Various labels were chosen for the quantification of N-glycans.²² Each chosen tag has a unique chemical properties and can impact on the ionization efficiency of N-glycans in MS differently, which can cause dissimilarity in quantitative results. This study evaluates the relative quantitation results of N-glycans released from multiple IgG samples and labeled with three different tags: Procainamide (ProA), 2-aminobenzamide (2AB), and 2-aminobenzoic acid (2AA). N-glycans were released from Frankenmab (IgG2), Natalizumab (IgG4), and Human Serum IgG then labeled with the chosen tags. The released glycans were run on HILIC-MS/MS system for N-glycan profile characterization. Relative quantitation of N-glycans was calculated based on the characterized glycan profiles.

Material and Methods

Materials

Human Serum, DL-DTT (DL-Dithiothreitol), iodoacetamide (IDA), ammonium bicarbonate, Procainamide, 2-AB, 2-AA, ammonium formate, formic acid, and trypsin (tosyl phenylalanyl chloromethyl ketone treated), were purchased from Sigma-Aldrich (St. Louis, MO, USA). IgG2 ('Frankenmab') and IgG4 (Natalizumab) were provided by GlycoScientific (Athen, GA). PNGase F (5000000 U/mL) was purchased from New England BioLabs (Ipswich, MA, USA). Acetonitrile (ACN; HPLC grade and LCMS graded) and C18 SPE were purchased from Thermo Fisher Scientific (Waltham, MA, USA). Mini Trap G-10 size exclusion column and Hi-Trap™ protein G HP column was purchase from Cytiva (Marlborough, Massachusetts, USA). *N-glycans release and derivatization*

Human IgGs were purified from human serum using a Hi-TrapTM protein G HP column prior to analysis. 1 mg of IgG2 (Frankenmab), 1 mg of IgG4 (Natalizumab), and 1 mg of human serum IgGs were subjected to reduction with 200 mM DL-DTT (4 μL) in 65°C for 1 hour. The samples were then alkylated using 4 μL of 1 M iodoacetamide (IDA) in an hour, and the remaining IDA was neutralized with approximately 16 μL 200 mM DL-DTT for another hour in 65°C. TPCK treated trypsin was added (50:1, protein/trypsin) for incubation overnight at 37°C. Digested sample were dried via speedvac prior to releasing N-glycans using approximately 2-4 μL PNGaseF. The samples were left overnight at 37°C. The released glycans were cleaned from residue peptides/proteins using C₁₈ SPE column. N-glycans were labeled and reduced overnight at 37°C with either 108 mg/mL Procainamide-HCl, 54 mg/mL 2-AA, or 54 mg/mL 2-AB, along with 63 mg/mL sodium cyanoborohydride in DMSO/acetic acid (7:3 by volume). The labeled glycans were desalted using a Mini Trap G-10 size exclusion column then dried via speedvac. *HILIC-MS/MS Settings and Instrumentations*

The samples were run on an HP1100 Agilent – Synapt G2 using Halo Penta-HILIC column (Advanced Material Technology, 2.1 mm x 15 cm, 2.7 µm particle size, Wilmington, DE). The separation was done at a flowrate 0.2 mL/min at 60°C with mobile phase A and B consisting of 100% ACN/0.1% formic acid and 50 mM ammonium formate in water with 0.1% formic acid, respectively. The gradient started at 80% ACN and ramped down to 40% ACN over 40 minutes. The mass spectrometer acquired data using data dependent acquisition where the 5 most intense ions from each full mass spectrum were chosen for fragmentation using collision-induced dissociation (CID). The data collected was analyzed via Masslynx and Skyline.

Results and Discussion

Identification of released N-glycan with different labels

The characterization of N-glycans was done using HILIC-MS/MS. There were minimal differences in the detected N-glycans released from IgG2 (Frankenmab) and IgG4 (Natalizumab) when labeled with different tags. However, significant differences in the glycan profiles were observed for the detected N-glycans release from human serum IgG (Figure 3.1C). While sample labeled with Procainamide (ProA) have 25 glycans detected, sample labeled with 2-aminobenzoic acid (2AA) or 2-aminobenzamide (2AB) only have 15 glycans observed (Figure 3.1C). Glycans tagged with 2-AA or 2-AB have an overall lower signal intensity compared to those labeled with ProA. This resulted in the inability to detect low abundance N-glycans on samples derivatized with 2-AA or 2-AB. The carboxyl group in 2-AA structure tends to lose proton and 2-AB is a neutral aromatic amide that lacks strongly ionizable group, which leads to low ionization efficiency for specied labeled with 2-AA/2-AB in ESI positive mode. The structure of ProA benefits from the tertiary amide group that allows better protonation and higher detection abilities for low abundance species. The reduction of signals impacts the number of

glycans being detected and can cause different results in N-glycan quantitation. The more complicated the sample such as human serum IgG, the greater the impact.

The impact of charged state selection on N-glycan quantitation using Mass Spectrometry Doubly charged state

Doubly charged state was initially chosen as the main charged state for relative quantification of N-glycans. The relative quantitation for samples labeled with different tags were calculated by using equation 3.1. The relative ratio (%) in Figure 3.2 shows that ProA-labeled samples tend to produce more neutral glycans with significantly high relative ratios detected. However, charged glycans have a higher relative ratio in the samples labeled with 2AB and 2AA. Differences in chemical structure of each tag can lead to changes in ion efficiency, which suggested the favoritism in producing different charged state species for each tag. The lack of inclusion for variety charged states in quantification can result in the observed dissimilarities in N-glycan relative ratios. This has led to additional evaluation of species other than doubly protonated ions.

Multiple charged state

Multiple protonated charged states were chosen including M+H, M+2H and M+3H. It is crucial to note that some singly charged glycans with mass larger than 2000Da were not scanned due to the setting of the experiments, which can impact the relative ratio (%) for larger N-glycans. Despite limitation in data acquisition, the sum of multiple charged states has helped to decrease the differences in relative ratio on different labels (Figure 3.3). A big shift was detected in the relative quantitation of glycans labeled with 2-AA/2-AB (Figure 3.3), indicating the favoritism in different charged state for each tag. The structures of both 2-AA and 2-AB lack proton affinity and can struggle to consistently uptake two protons during ionization, therefore,

considering one charged state for quantitation led to inaccurate quantitative results. A high abundance of sodium adduct was observed and could potentially affect the results. This led to additional examinations on the impact of sodium adducts in glycan quantification.

Sum of multiple charged state and sodium adducts

The carboxyl group of 2-AA and the tertiary amine group in ProA are prone to take up sodium during ionization and expected to have high tendency in producing sodium adducts. While M+H+Na species were detected for all tags, ProA-tagged glycans were found to also produce M+H+2Na and M+2H+Na species. Sodium adducts were considered for the quantitation includes M+H+Na, M+H+2Na, and M+2H+Na. Improvement of relative ratios (%) was detected by using the sum of peak areas from multiple charge states and sodium adducts, but differences in glycan ratio were still observed amongst samples with different labels. This indicates biased quantitative results can happen when different labels are used for the quantification of N-glycan in LC-MS.

Conclusion

Different factors in quantitation of N-glycans in LC-MS were evaluated and found that quantitative results of glycans are driven by the chosen labels. Three popular fluorescent tags were chosen to examine whether the quantification of N-glycans in MS can be significantly impacted when using different tags. Each fluorescent tag has distinct chemical properties and can affect the ionization efficiency in mass spectrometry, which essentially changes the limit of detection. The differences amongst the detected glycans were observed to be larger when the analyzed sample is complicated and has a large pool of low abundance N-glycans. Another factor that also affects the quantitative result is the charged state selection for quantitation. The favoritism in charged state production is varied amongst different tags as they are tied to the

ability of the tag to uptake proton during ESI positive mode collection. The study has found that multiple charged species as well as adduct ions should be considered during quantitation to help provide a more accurate result.

Equation 3.1 Calculation of Relative Quantitation

Relative ratio (%) =
$$\frac{Peak\ area\ [target\ glycan]}{Peak\ area\ [all\ glycans]} \times 100\%$$

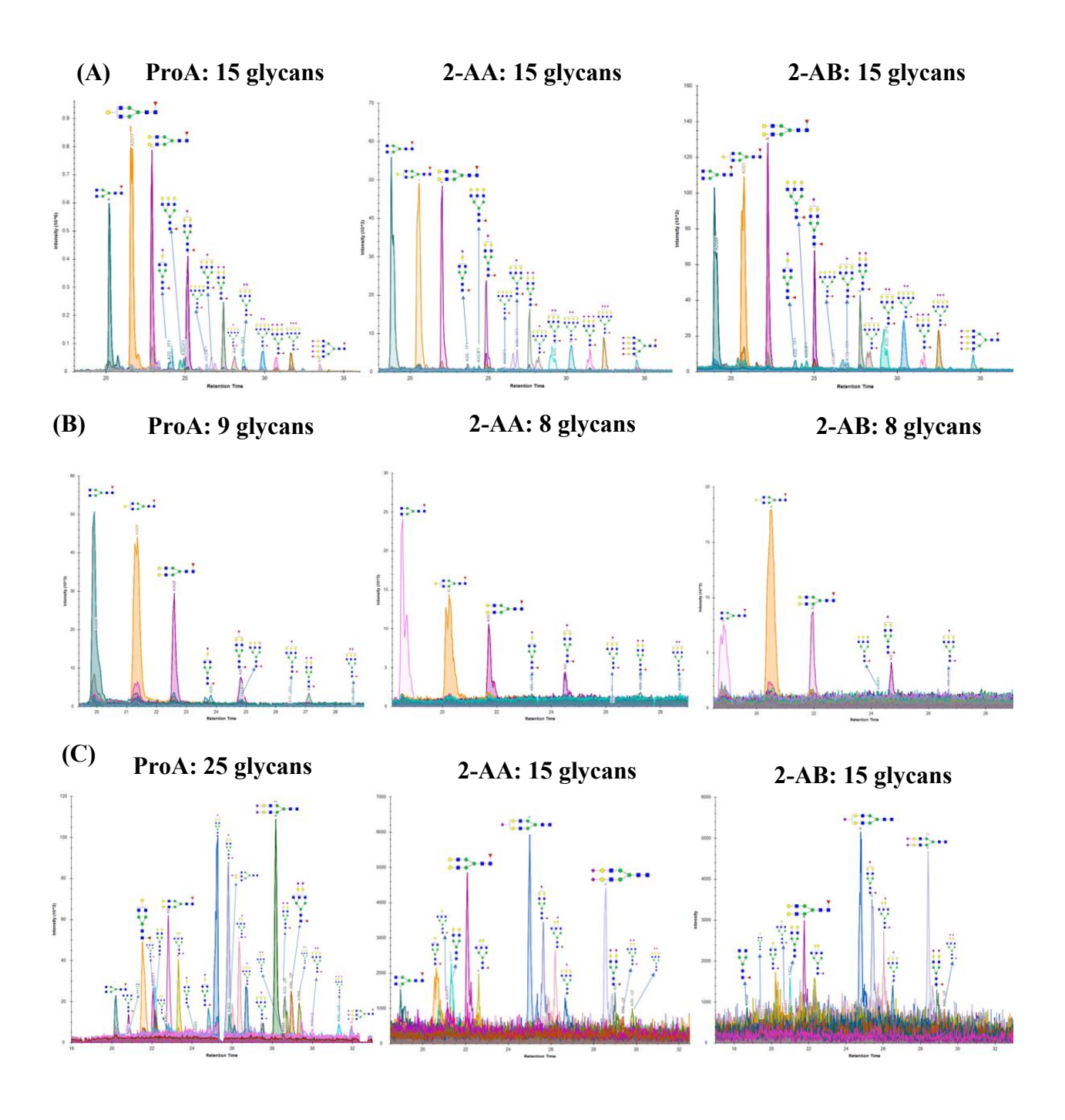


Figure 3.1 HILIC analysis of N-glycans released from (A) IgG2 (Frankenmab), (B) IgG4 (Natalizumab), and Human Serum IgG (C) when labeled with ProA, 2-AA, and 2-AB.

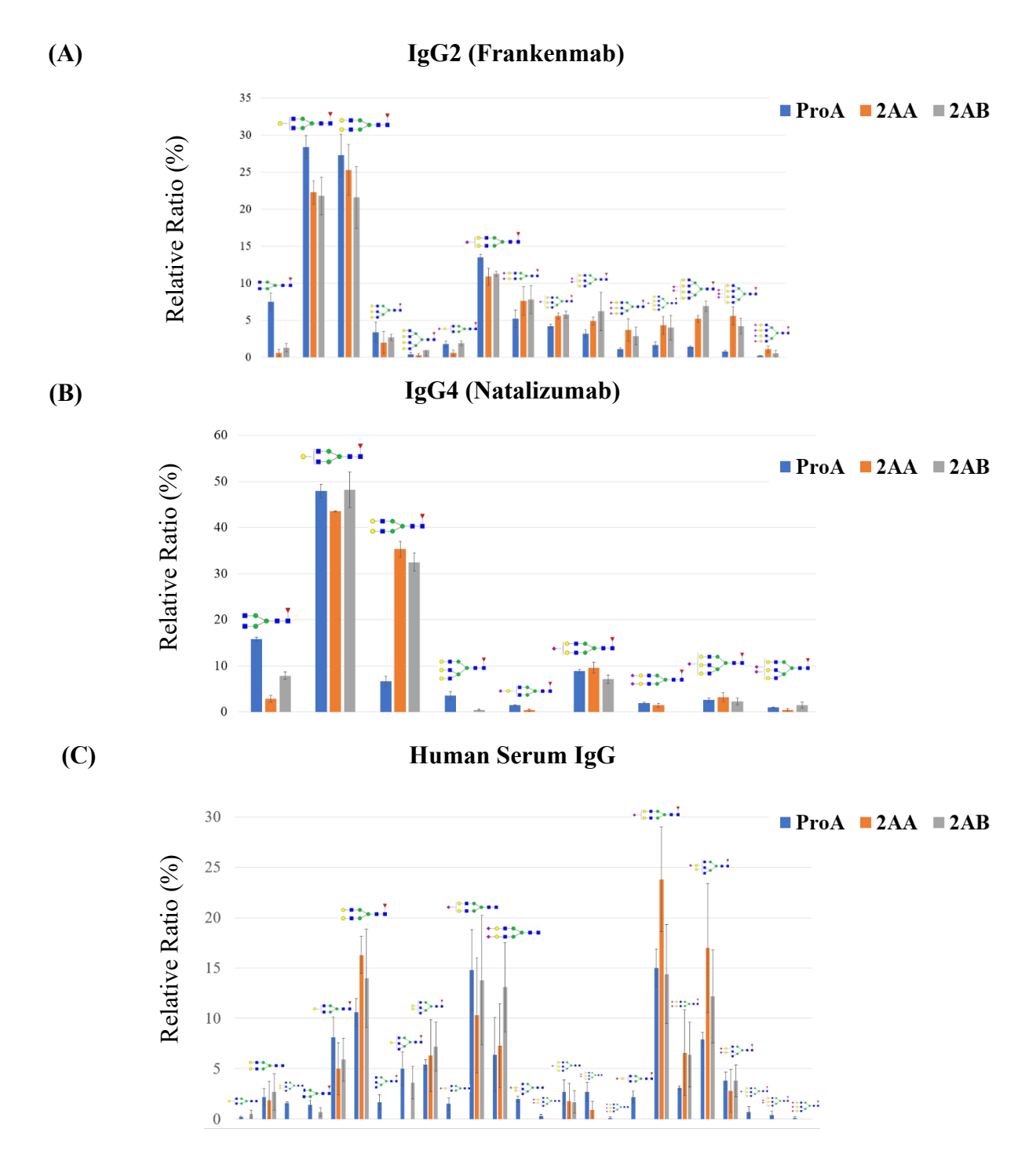


Figure 3.2 The relative quantitation of doubly protonated glycans. The results demonstrate the differences in relative ratio (%) of N-glycans detected in (A) IgG2 (Frankenmab), (B) IgG4 (Natalizumab), and Human Serum IgG (C) when labeled with ProA, 2-AA, and 2-AB.

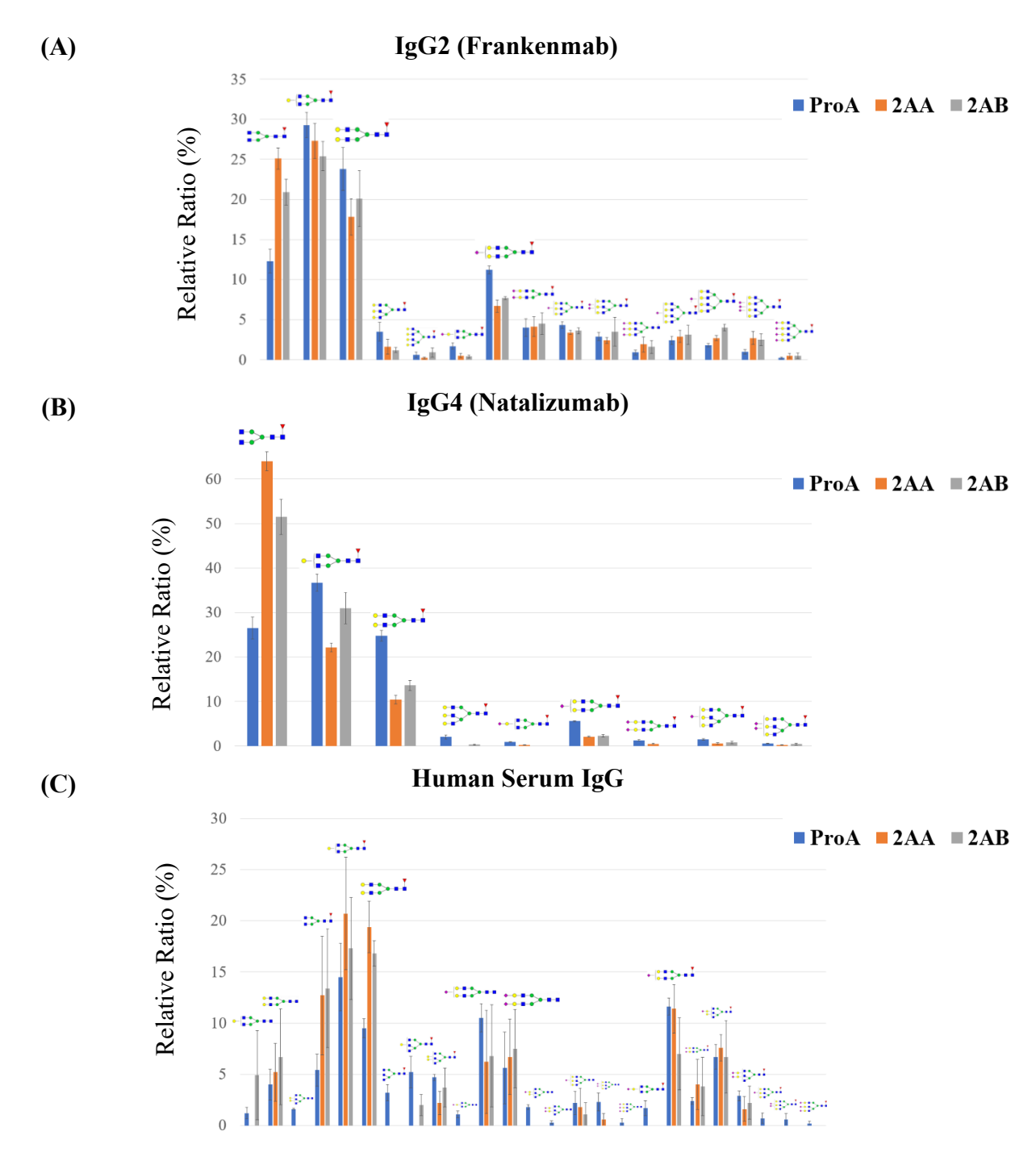


Figure 3.3. The relative quantitation of multiple protonated species, including M+H, M+2H, and M+3H. The variation in the relative ratios (%) of N-glycans with different labels detected in (A) IgG2 (Frankenmab), (B) IgG4 (Natalizumab), and (C) human serum IgG was reduced when multiple charge states were included in the calculation.

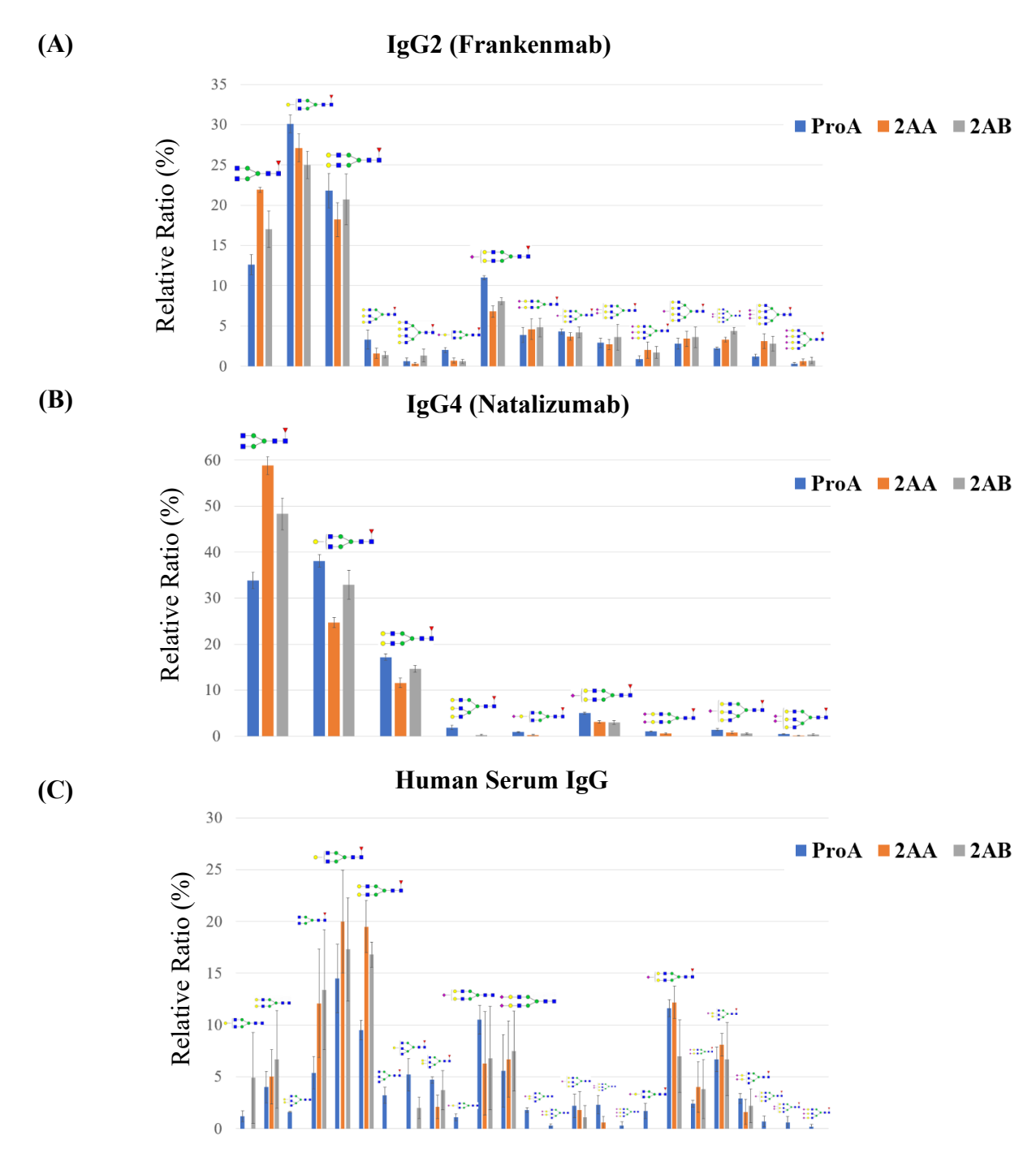


Figure 3.4. The relative quantitation of glycans calculated via the peak area of multiple protonated species and sodium adducts, including M+H+Na, M+2H+Na, and M+H+2Na. The variation in the relative ratios (%) of N-glycans with different labels detected in (A) IgG2 (Frankenmab), (B) IgG4 (Natalizumab), and (C) human serum IgG did not change significantly.

CHAPTER 4

SEPARATION OF N-GLYCAN ISOMERS VIA HILIC, ION MOBILITY AND MASS ${\tt SPECTROMETRY}$

Thai, H., Orlando, R. To be submitted to Springer Nature

Abstract

N-glycans have different types of isomers where they only differ by their linkage, anomeric, or stereochemical. Some of these isomers are difficult to differentiate using only mass spectrometry approaches. The use of additional analytical techniques is necessary to provide a more complete picture of complex N-glycan samples. Hydrophilic interaction liquid chromatography (HILIC) is a popular technique in glycan study that can effectively separate isomers such as α -2,6-sialylated from α -2,3-sialylated glycans, which are known as challenging linkage isomeric group for mass spectrometers. This study demonstrates the ability of HILIC-MS/MS in identifying different groups of glycan isomers. Separations were achieved between Neu5Ac-(α2-3/6)-Gal glycans, Neu5Ac-(α2-6)-GlcNAc glycans, and Neu5Gc-(α2-3/6)-Gal glycans, indicating the power of HILIC in differentiating complex linkage isomers. Study also found that HILIC can distinguish triantennary N-glycan from its positional isomer consisting of a bi-antennary glycan with a Gal-(β1-4)-GlcNAc extension on one of the antennae (polyLacNAc glycan). The observation of new separations implies HILIC is a great complementary dimension for mass spectrometry in isomeric separation. The resolving power of HILIC-MS was further improved by the addition of Ion mobility spectrometry (IMS). The separation of IMS provided additional resolution of possible unresolved isomers that complement the performance of HILIC-MS. Unique fingerprints were collected from IMS for each glycan species, suggesting an additional dataset that can be paired with retention time from HILIC, and m/z data from MS to increase efficiency and accuracy in identifying complex isomers. In the future, studies can be done on HILIC-IMS-MS system to explore its full potential in the analysis of complex N-glycan isomers.

Introduction

Changes in N-glycan isomers are known to be involved in numerous diseases. Sialic acids are typically connected at the non-reducing end of a glycan, which exposes the intact sialic acid to the surrounding environment and promotes their participation in biological processes including cancerogenesis. 52,53 N-acetylneuraminic acid (Neu5Ac) is the most abundance sialic acid found in mammals. 153 Abnormal increase in abundancy of α2,6-linkages Neu5Ac N-glycan was found in cancerous cells and was proposed as a potential biomarker for tumor progression diagnosis. ^{26, 27} N-glycolylneuraminic acid (Neu5Gc) is also a common sialic acid in animals but human lacks the ability to make Neu5Gc due to the absence of cytidine-5'-monophospho-Nacetylneuraminic acid (CMP-Neu5Ac) hydroxylase enzyme. 154 Research in biotherapeutics suggests that Neu5Gc is a potential immunogenic species to humans. 52, 57, 155 Another case of Nglycan involve in human diseases was found in the overexpression of the poly-Nacetyllactosamine (polyLacNAc) modifications.^{28, 29} Poly-N-acetyllactosamine (polyLacNAc) describes the repetition of a disaccharides unit composed of Gal-(\beta 1-4)-GlcNAc on a glycan antenna.⁵⁴ Overexpression of polyLacNAc is associated with the progression of cancer tumors and plays a crucial role in enabling tumor cells to evade immune host response.²⁹ The relevant of N-glycan isomers in many diseases has made the analysis of N-glycan isomers become an important task in the biotherapeutic industry.

Hydrophilic Interactions Liquid Chromatography (HILIC) is a popular technique that complements mass spectrometry (MS) in glycomics study. ^{151, 156, 157} HILIC was introduced by Alpert in 1990¹²² as a variant of normal phase where the separation mechanism involves partition mechanism (hydrogen bonding), ionic and dipole-dipole interaction. Alpert suggested that the partition mechanism plays a significant role in the retention of carbohydrates such as N-glycan in

HILIC.¹²² The stationary phase of HILIC retains a semi-immobilized layer of mobile phase enriched with water. The retention of carbohydrates is described to partition between the semi-immobilized layer and the organic mobile phase.¹²² The separation of N-glycans on HILIC is referred as "size fractionation" indicating the larger the glycan, the later it elutes.¹⁰ N-glycan studies have demonstrated the ability of HILIC in resolving challenging linkage isomers such as Neu5Ac-(α2,3)-Gal and Neu5Ac-(α2,6)-Gal.¹⁵¹ HILIC completements MS and improves the identification of N-glycans released from different complex matrices such as human serum^{151,157} and monoclonal antibodies.^{158,159} This study combines HILIC with tandem mass spectrometry (MS/MS) for the analysis of released N-glycan from fetuin bovine and Chinese Hamster Ovary (CHO) cell pellets. Exciting glycan isomeric resolutions were observed for the first time, indicating the resolving power of HILIC in isomeric separation.

Multidimensional systems have gained significant attention due to the ability in enabling high efficiency and resolution in glycans analysis. ^{160, 161} While HILIC is a powerful method that complements mass spectrometry in the glycan study, the use of one separational dimension limits the identification of some complex isomers that require a higher resolving power system. Ion Mobility Spectrometry (IMS) is a gas-phase separational technique that separates analytes via their movement in gases under the influence of electric field. ^{123, 162} The separation in IMS happens on a millisecond timescale, which can be readily paired with LC-MS system without compromising time efficiency. Some common IMS platforms include drift tube ion mobility spectrometry (DTIMS), traveling wave ion mobility spectrometry (TWIMS), Trapped Ion Mobility Spectrometry (TIMS), Field asymmetric waveform ion mobility spectrometry (FAIMS), and differential mobility spectrometry (DMS). ¹²³ A high-resolution cyclic travellingwave ion mobility using structures for lossless ion manipulations (SLIM) has been introduced

where it employs a 13m path length with traveling wave to induce movement and separate ions. $^{131,\,133,\,163}$ The extra-long path is one of the unique features of SLIM that enables high resolving power to separate complex isomers. Glycan studies utilized SLIM to separate positional isomers such as A2G1(α 1-6)/A2G1(α 1-3) 131 or A1G0(α 1-6)/A1G0(α 1-3), 163 demonstrating the resolving potential of high resolution ion mobility in differentiating complex glycan isomers. Herein, SLIM was combined with HILIC-MS to evaluate the ability of IMS in N-glycan analysis.

Materials and method

Materials

CHO cell pellets were obtained from GlycoScientific (Athens, GA, USA). Fetuin bovine, procainamide hydrochloride, dextran, acetic acid, and dimethyl sulfoxide (DMSO) were purchased from Sigma. Sodium cyanoborohydride was purchased from Acros Organics.

PNGaseF was purchased from Lectenz Bio. Denaturing buffer and NP40 were purchased from New England Biolabs (Ipswich, MA, USA). PD MiniTrap G10 was purchased from Cytiva. HyperSepTM C18 Cartridge was purchased from ThermoFisher. Ammonium bicarbonate, ammonium formate and formic acid were purchased from Fluka. Acetonitrile (LCMS graded) was purchased from Honeywell Buldrick and Jackson and Sigma-Aldrich.

N-glycan released from protein/antibodies

1 mg of fetuin were resuspended in 50 mM ammonium bicarbonate. Sample were denatured with 4 μ L of denature buffer (40 mM DTT, 0.5% SDS) at 100°C in 12 minutes. The denatured proteins were put in the freezer for 5 minutes and 4 μ L of 1% NP-40 was added to avoid deactivation of PNGaseF from residue heat and inhibitory effect of SDS. Then, 4 μ L of

PNGaseF was added to the sample and incubated at 37°C. After 16-20 hours, the sample was collected and lyophilized to dryness.

N-glycan released from cell pellets

100-10 million CHO cells were homogenized in 50 mM ammonium bicarbonate by passing through pipet tips. Samples were then sonicated in an ice bath by a probe sonicator for 15 seconds (sonicator power of 3 units) with 4 time repeat and a break time of 15 sec in between each sonication. 2 μ L of dissolved cell pellet were taken out for A280 nanodrop. After determination of protein concentration, the samples were denatured at 100°C for 12 minutes using 8-10 μ L of denature buffer (40 mM DTT, 0.5% SDS). The denatured samples were chilled in the freezer for 5 minutes followed by the addition of 4-6 μ L 1% NP-40 and 4-6 μ L of PNGaseF. Samples were then left in the incubator at 37°C for 16-20 hours to release N-glycan from peptide backbone. After incubation, the samples were lyophilized to dryness.

N-glycan purification and Procainamide (ProA) label

To clean up peptides and undigested proteins, the N-glycan released samples were resuspended in 200 μL 5% acetic acid and ran through C18 SPE column (conditioned with 6mL 100% methanol and calibrated with 5% acetic acid). The hydrophobic peptide and protein remained in the C18 SPE column. Hydrophilic N-glycans eluted to the collection tube. The purified N-glycans were lyophilized to dryness. The labeling solution was prepared with 216 mg/mL procainamide-hydrochloride and 126 mg/mL sodium cyanoborohydride in 7:3 (DMSO/acetic acid) solution. Approximately 200 μL labeling solution was added to fetuin sample and 400-600μL was added to CHO cell sample. The mixtures were incubated at 37°C overnight. After reduction and labeling, 100 μL Acetone was added to each sample to quench the reaction at 65°C for 30-60 minutes. The samples were dried down and resuspended in 140-200

 μ L 5% acetic acid. Excess labeling reagents were cleaned up via size exclusion PD Mini trap G10 column. The collected fractions were lyophilized and stored in freezer ready for LC-MS or LC-IMS-MS analysis.

HILIC-MS/MS Settings and Instrumentations

The samples were run on an HP1100 Agilent – Synapt G2 using Halo Penta-HILIC column (Advanced Material Technology, 2.1 mm x 15 cm, 2.7 µm particle size, Wilmington, DE). The separation was done at a flowrate of 0.2 mL/min at 60°C with mobile phase A and B consisting of 100% ACN with 0.1% formic acid and 50 mM ammonium formate in water with 0.1% formic acid, respectively. The gradient started at 80% ACN and ramped down to 40% ACN over 40 minutes. The mass spectrometer acquired data using data dependent acquisition where the 5 most intense ions from each full mass spectrum were chosen for fragmentation using collision-induced dissociation (CID). The data collected was analyzed via Masslynx and Skyline. *HILIC-IMS-MS Settings and Instrumentations*

The samples were run on an Agilent 1290 Infinity II with Agilent 6546 Q-TOF using 2.1 mm x 15 cm, 2.7 μm particle size Halo Penta-HILIC column. Mobile phase and gradient of HILIC was kept similar to the HP1100 Agilent LC condition to guarantee consistency in separations. After HILIC separation, the analytes were introduced into the IMS-MS system where ions were generated by the Dual AJS ESI provided by Agilent (Santa Clara, CA) with the recommended settings for N-glycan ionization. He upon entering the SLIM module, the ions were filled in storage section and then released into a single-pass path length of 13 m. He Travelling Wave (TW) potentials were generated between electrodes on two parallel printed circuit boards to propel the ions through N₂ drift gas. He settings for the TW potentials were based on the recommended parameter from the provider (MOBILion Systems Inc., Chadds

Ford, PA) with minimal optimization. The mass spectra were obtained using MS (seq) acquisition settings in the Agilent 6546 Q-TOF (Agilent, Santa Clara, CA).

The collected data was processed via HRIM Data Processor prior to analysis using Agilent MassHunter IM-MS Browser, and Skyline. Dextran was used as the external calibrant for collision cross section (CCS) calculation and the drift tube CCS of procainamide labeled dextran was extracted from reference data of Manz et al. ¹⁶⁵ The CCS calculation was based on the method described by Li et al. ¹⁶⁶

The naming of N-glycans mentioned in this study follows a notation system where Ax is the number of antennae, Gy is number of Galactoses attached to antenna GlcNAc, and Fz is number of Fucoses linked to the core GlcNAc. Sialylated glycans are denoted with (Neu5Ac)m or (Neu5Gc)n where m/n represents the number of Neu5Ac/Neu5Gc linked to either antenna Gal (α 2-3/ α 2-6) or antenna GlcNAc (α 2-6-GlcNAc or α 2-3-GlcNAc). Poly-N-acetyllactosamine glycans is describe by (Lac)t where t represents every Gal-(β 1-4)-GlcNAc disaccharides repeated.

Results and Discussion

The need for a secondary dimension in N-glycan analysis using MS

Glycans exist in isomeric mixture that have identical mass and generate similar fragment ions patterns, making it difficult to identify these species using only mass spectrometry. N-glycans with Neu5Ac-(α 2,3)-Gal and Neu5Ac-(α 2,6)-Gal linkage have identical mass and often produce similar fragment ion patterns. The tandem mass spectrum of A3G3(Neu5Ac)1 released from fetuin bovine (Figure 4.1) was collected with the attempt to differentiate α 2,3- and α 2,6-Neu5Ac glycans through unique fragment ions. The result showed that most of the fragment ions were similar between two mass spectrums, and it was impossible to identify α 2,3- and α 2,6-

sialylated species. This signifies the need for a secondary dimension to assist in the analysis process.

Neu5Ac-linked N-glycan Isomers Identification via HILIC-MS/MS

Glycoforms of fetuin is well-known for the variety of Neu5Ac-(α 2-3/6)-Gal N-glycans in bi- and tri-antennary structures. Besides the known existence of Neu5Ac-(α 2-3/6)-Gal N-glycans, a study from Townsend et al in 1989³⁰ reported the existence of glycan containing Neu5Ac-(α 2-6)-GlcNAc linkage in fetuin and successfully resolved these sialylated glycans via high pH anion exchange chromatogram (HPAC). HPAC is incomparable to mass spectrometry due to high salt concentration in mobile phase, which limited its usage in modern study. While the separations between Neu5Ac-(α 2-3)-Gal and Neu5Ac-(α 2-6)-Gal glycans were achieved in different liquid chromatography modes paired with mass spectrometry, there is no report on the resolution of glycans containing Neu5Ac-(α 2-6)-GlcNAc linkage.

A study was conducted to resolve both Neu5Ac-(α 2-3/6)-Gal glycans and Neu5Ac-(α 2-6)-GlcNAc glycans using a fuse-core penta-HILIC column from Advanced Materials

Technology (AMT). N-glycans were released from fetuin and tagged with Procainamide (ProA) prior to HILIC-MS/MS experiments. The extracted ion chromatogram (EIC) of A3G3(Neu5Ac)3 showed a total of seven chromatographic peaks (Figure 4.2A.). Using previously published data¹⁵¹ and confirming with tandem mass spectrum, chromatographic peak at 30.70 min, 31.38 min , 31.94 min, and 32.70 min was giving rise toNeu5Ac-(3 α 2-3)-Gal, Neu5Ac-(2 α 2-3, 1 α 2-6)-Gal, Neu5Ac-(1 α 2-3, 2 α 2-6)-Gal, and Neu5Ac-(3 α 2-6)-Gal species, respectively. A unique fragment ion of Neu5Ac-Gal-GlcNAc-Neu5Ac (m/z = 948) was detected in the tandem mass spectrum at peak 31.06 min, and 31.56 min (Figure 4.3), suggesting the existence of Neu5Ac - (α 2-6)-GlcNAc glycans. The identity of the species giving species to peak 31.06 min, 31.56 min,

and 32.08 min were identified based to the reported data of Townsend et el³⁰, HILIC elution rules, and fragment ions detected in tandem mass spectrometry. The fully assigned EIC of the seven chromatographic peaks of A3G3(Neu5Ac)3 in Figure 4.2B is one of the first evidence that HILIC can resolve simultaneously both Neu5Ac-(α 2-3/6)-Gal species and Neu5Ac-(α 2-6)-GlcNAc species in one experimental run, indicating the power of HILIC in the study of N-glycan isomers.

Neu5Gc-linked N-glycan Isomers Separation via HILIC-MS/MS

The detection of Neu5Gc species in fetuin was performed using HILIC-MS/MS. HILIC was demonstrated to successfully distinguish ($\alpha 2$ -3/ $\alpha 2$ -6) Neu5Gc species from ($\alpha 2$ -3/ $\alpha 2$ -6) Neu5Ac glycan (Figure 4.4). A HILIC retention time model was previously built, where the HILIC retention rules of Neu5Ac and Neu5Gc linkages are described as follow: Neu5Ac-($\alpha 2$ -3)-Gal < Neu5Ac-($\alpha 2$ -6)-Gal < Neu5Gc-($\alpha 2$ -3)-Gal < Neu5Gc-($\alpha 2$ -6)-Gal. The model suggests that glycans with combination of Neu5Gc-($\alpha 2$ -3-Gal)Neu5Ac-($\alpha 2$ -6-Gal) or (Neu5Gc- $\alpha 2$ -6-Gal)(Neu5Ac- $\alpha 2$ -3-Gal) have overlap retention time and cannot be differentiate via HILIC. He linkage identification of Neu5Gc glycans were based on the studied elution rule of Neu5Gc on HILIC (Figure 4.4A). Achieving the separation of Neu5Gc and Neu5Ac glycan indicates the power of HILIC in differentiating complex profile of sialylated glycans, which are crucial glycans in drugs development 169 and cancer diagnosis. 26, 27

PolyLacNAc N-glycan Isomer Separation via HILIC-MS/MS

Chinese Hamster Ovary (CHO) cells is a popular cell line in the production of monoclonal antibodies (mAbs) in the pharmaceutical industry.^{32, 33} The existing glycoproteins in CHO cells dictate the glycoforms pattern on the synthesized monoclonal antibodies and can impact the quality of the product line.^{32, 33} The study of glycomics in CHO cells allows better

understanding of the N-glycans patterns to help avoid potential adverse effects from unpredicted N-glycans in biotherapeutic products.

A glycan study of CHO cells was conducted via HILIC-MS/MS using the fuse-core penta-HILIC column from AMT. While the identity of most N-glycans released from CHO cells were straightforward for confirmation, the EIC of A3G3(Neu5Ac)1F unexpectedly showed two resolved chromatographic peaks (Figure 4.5A). CHO cells cannot product α2-6 sialylated glycans and the EIC of A3G3(Neu5Ac)1F(1 α 2-3-Gal) was expected to only have one resolved peak representing A3G3(Neu5Ac)1F(1 α2-3-Gal) species. ^{170, 171} Tandem mass spectrum was collected for both peaks to help confirm whether there is an additional isomer from A3G3(Neu5Ac)1F that has not been studied. The tandem mass spectrum at 25.4 min (Figure 4.5B) illustrates a normal pattern of a tri-antennary N-glycan, indicating A3G3(Neu5Ac)1F(1 α2-3-Gal) were the species giving rise to the peak at 25.4 min. A unique fragment ion of Neu5Ac-Gal-GlcNAc-Gal (1022.4 m/z) was detected in the tandem mass spectrum at 25.6 min (Figure 4.4C), which suggests the species giving rise to the peak at 25.6 min is a polyLacNAc glycan called A2G2(Lac)1(Neu5Ac)1F(1 α2-3-Gal). This indicates that HILIC can separate normal antenna glycans from their polyLacNAc isomer. The overexpression of PolyLacNAc glycans is known to be associated with tumor progression and has been suggested as a diagnostic pattern in clinical.^{28, 29} PolyLacNAc glycans are mainly detected through their abnormal large mass. The newly discovered ability of HILIC in detecting small PolyLacNAc glycans imply HILIC is a great toolbox to detect abnormal growth activity in cells in the early stage. Increasing Resolving Power with Ion Mobility: HILIC-IMS-MS

N-glycans released from CHO cells were run on HILIC-IMS-MS to evaluate the resolving power of IMS. N-glycans exist in isomeric mixtures with possible co-existence of

some positional isomers that require high resolution technique to separate. While HILIC can distinguish A2G2(LacNAc)1(Neu5Ac)1F(1 α2-3-Gal) and A3G3(Neu5Ac)1F (1 α2-3-Gal) glycan, there are possible co-existing positional isomers from these two species that were not distinguish via HILIC. An example of some possible positional tri-antenna isomers of A3G3(Neu5Ac)1F (1 α2-3-Gal) are described in Figure 4.6. The mobiligrams of both A2G2(LacNAc)1(Neu5Ac)1F and A3G3(Neu5Ac)1F (1 α2-3-Gal) species were retrieved in Figure 4.7 to evaluate whether IMS can resolve additional positional isomers. The ion mobility trace of the A3G3(Neu5Ac)1F (1 α2-3-Gal) glycan appears to have two resolved peaks at 527.2 Å² and 533.9 Å² (Figure 4.7A), suggesting the possible resolution of the positional tri-antenna isomers (Figure 4.6) and other unpredicted isomers. A distinct fingerprint was also observed from the ion mobility trace of A2G2(LacNAc)1(Neu5Ac)1F (1 α2-3-Gal) glycan with four resolved peaks at 528.9 Å², 533.5 Å², 541.3 Å², and 547.4 Å² (Figure 4.7B), indicating signs of positional isomers separation achieved by IMS. While the resolution observed reveals the ability of IMS in resolving challenging isomers that HILIC was not able to differentiate, it is also crucial to consider the possibility that the additional signals detected could be experimental artifacts. To accurately characterize the identity of the resolved peaks in IMS remains a challenging task, the unique fingerprint collected from A3G3(α 2-3)(Neu5Ac)1F (1 α 2-3-Gal) and A2G2(LacNAc)1(Neu5Ac)1F (1 α 2-3-Gal) species suggested that ion mobility traces can be used an additional identification data for N-glycan analysis. This preliminary data of HILIC-IMS-MS showed that ion mobility is a great addition to the system where researchers can benefit from the high resolving power to uncover complex glycan profiles.

Conclusion

HILIC-MS/MS system has successfully achieved resolution for challenging isomers including sialylated complex glycans and PolyLacNAc species. HILIC was demonstrated as a powerful separational dimension that complements mass spectrometry in the analysis of N-glycans. However, the resolving power of HILIC-MS is only limited to one separational dimension. High resolution ion mobility was added as a complementing dimension for HILIC-MS system. The addition of ion mobility not only resolves possible undetected isomers from HILIC analysis but also provides unique fingerprints for each species without compromising HILIC separation efficiency. Future study can be done on HILIC-IMS-MS to fully explore the potential of this multidimension system.

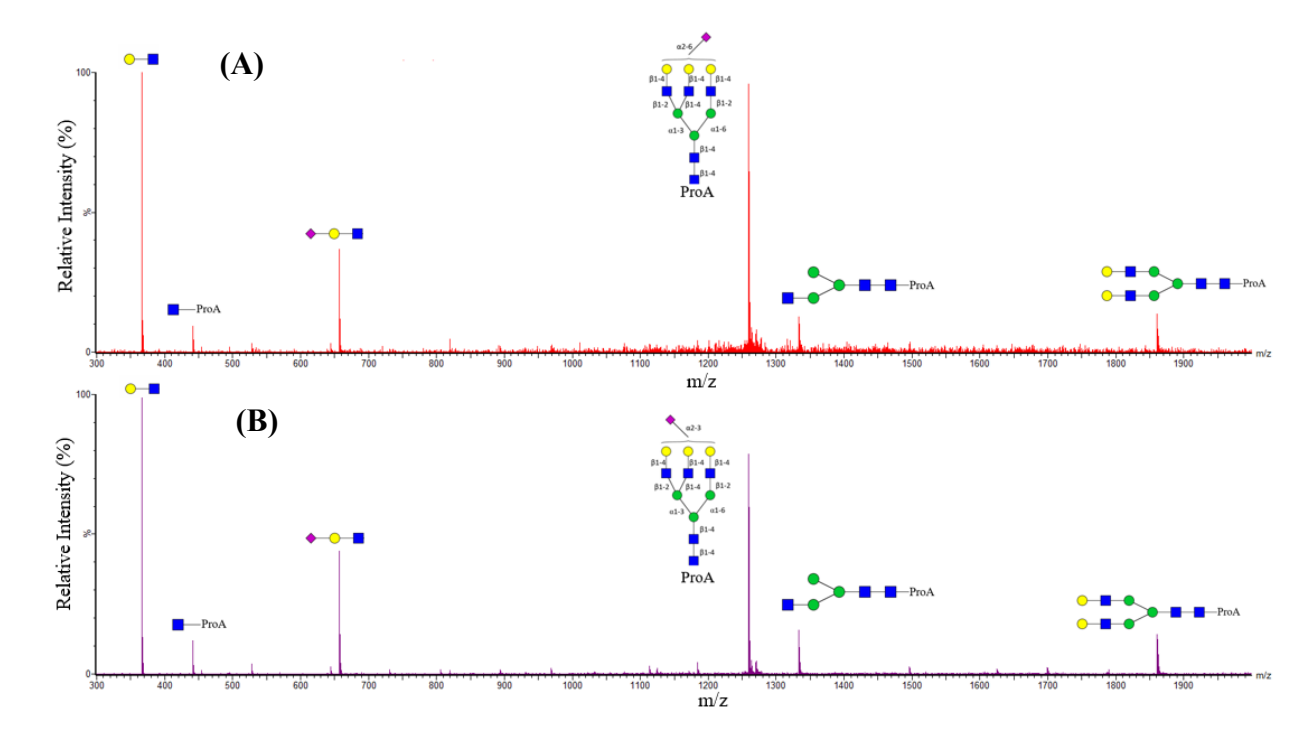


Figure 4.1 The tandem mass spectrum of (A) A3G3(Neu5Ac)1(1 α 2-6-Gal) (M+2H m/z = 1258.99) and (B) A3G3(Neu5Ac)1(1 α 2-3-Gal) (M+2H m/z = 1258.99), demonstrating the tendency to produce similar fragment ions in sialylated isomers. The similarity in fragment ion patterns makes the distinguishment between (α 2-6)- and (α 2-3) sialylated glycans difficult.

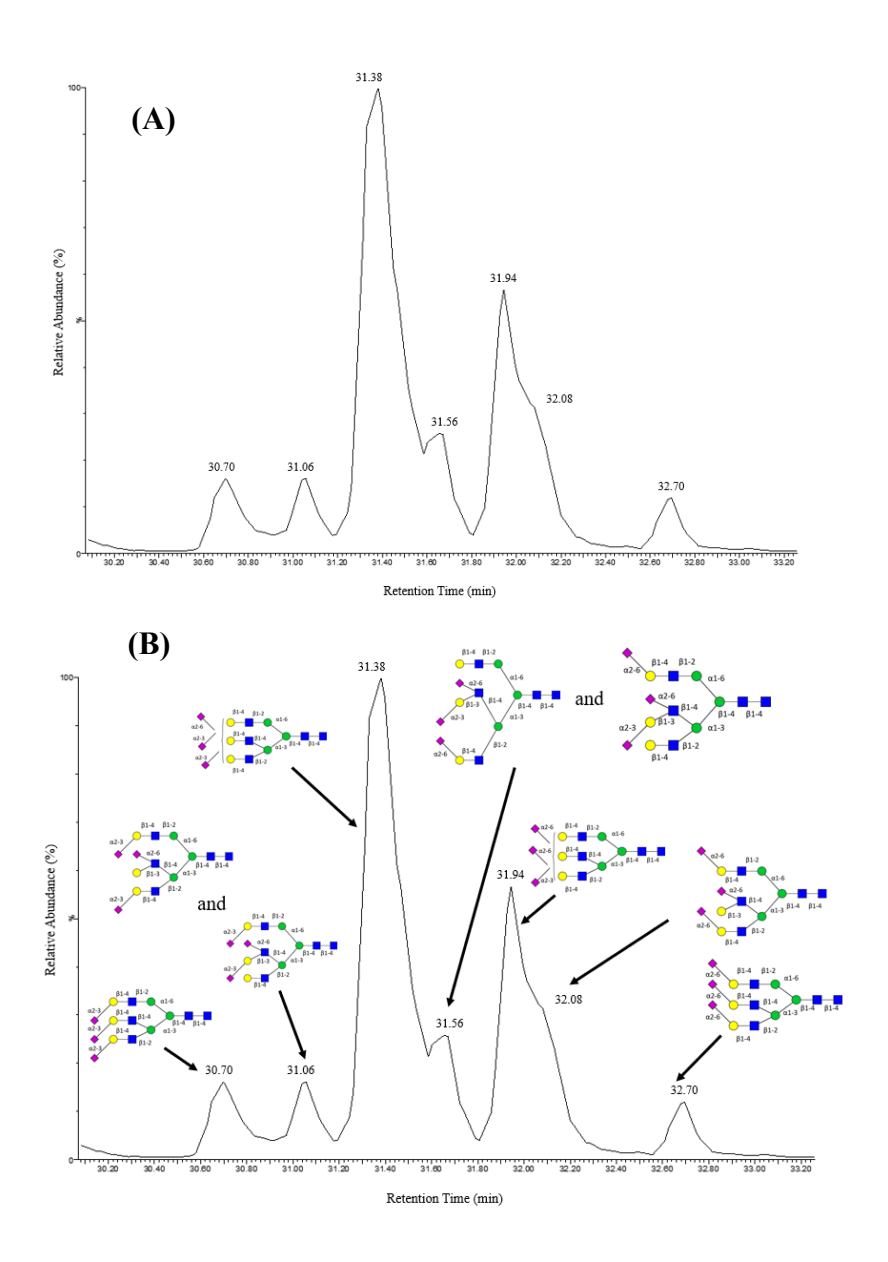


Figure 4.2 The unassigned EIC at 1550.9 (M+2H) of A3G3(Neu5Ac)3 (A) and the fully assigned EIC of A3G3(Neu5Ac)3 (B). N-glycans were identified using Townsend et al data,³⁰ HILIC retention rules, and tandem mass spectrometry. The full assigned EIC is one of the first evidences showing on the ability of HILIC to simultaneously separate Neu5Ac-(α 2-3/6)-Gal species and Neu5Ac-(α 2-6)-GlcNAc species.

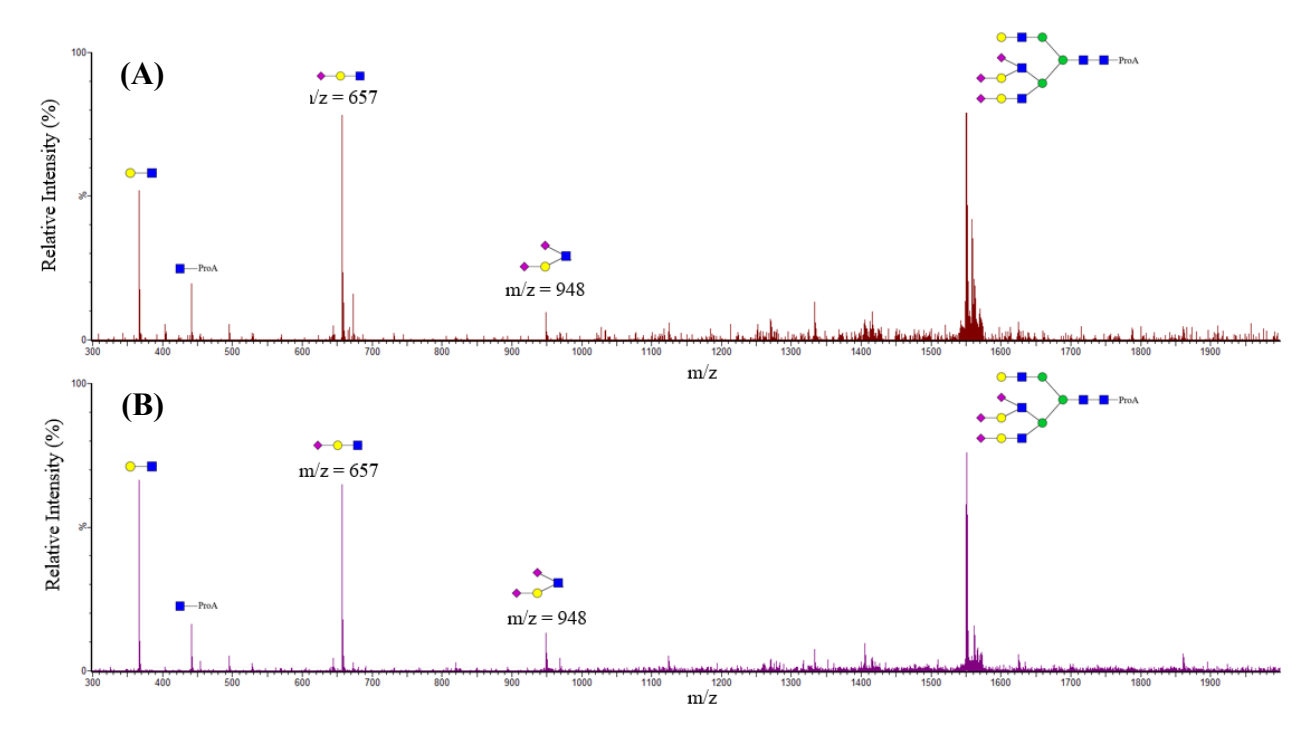


Figure 4.3 The tandem mass spectrum (A) 31.06 min and (B) 31.56 min from the EIC of A3G3(Neu5Ac)3 in figure 4.2. Besides the usual Neu5Ac-Gal-GlcNAc fragment ion (m/z = 657) found sialylated glycans, a unique fragment ion of Neu5Ac-Gal-GlcNAc-Neu5Ac (m/z = 948) were observed in both mass spectrums. This suggests the existence of Neu5Ac-(α 2-6)-GlcNAc glycans.

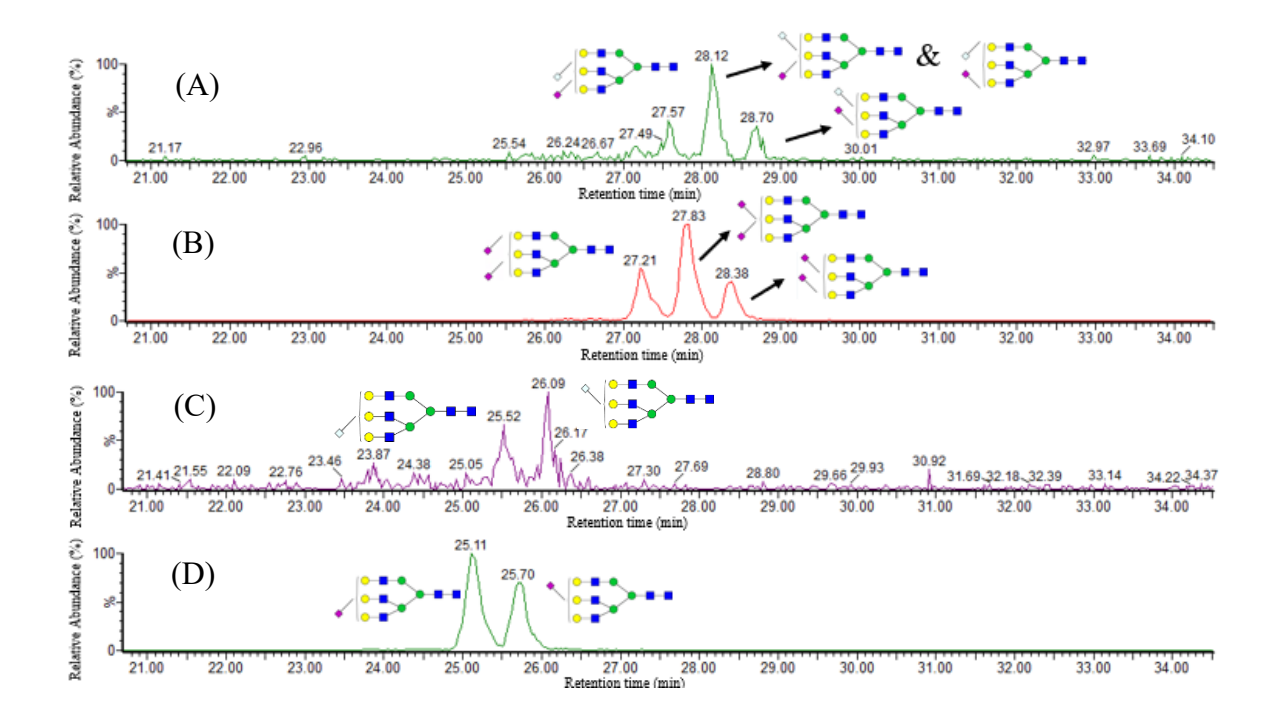


Figure 4.4 The EICs of (A) A3G3(Neu5Ac)1(Neu5Gc)1 (M+3H m/z = 942.02), (B) A3G3(Neu5Ac)2 (M+3H m/z = 936.68), (C) A3G3(Neu5Gc)1 (M+3H m/z = 844.99), and (D) A3G3(Neu5Ac)1 (M+3H m/z = 839.66). The linkage identification of Neu5Gc/Neu5Ac glycans is based on the HILIC retention behavior previously studied. The EICs show that HILIC can comfortably separate Neu5Gc and Neu5Ac glycans, but HILIC is unable to differentiate glycans with mixture of Neu5Gc-(α2-3)Neu5Ac-(α2-6) or (Neu5Gc-α2-6-Gal)(Neu5Ac-α2-3-Gal) (panel B).

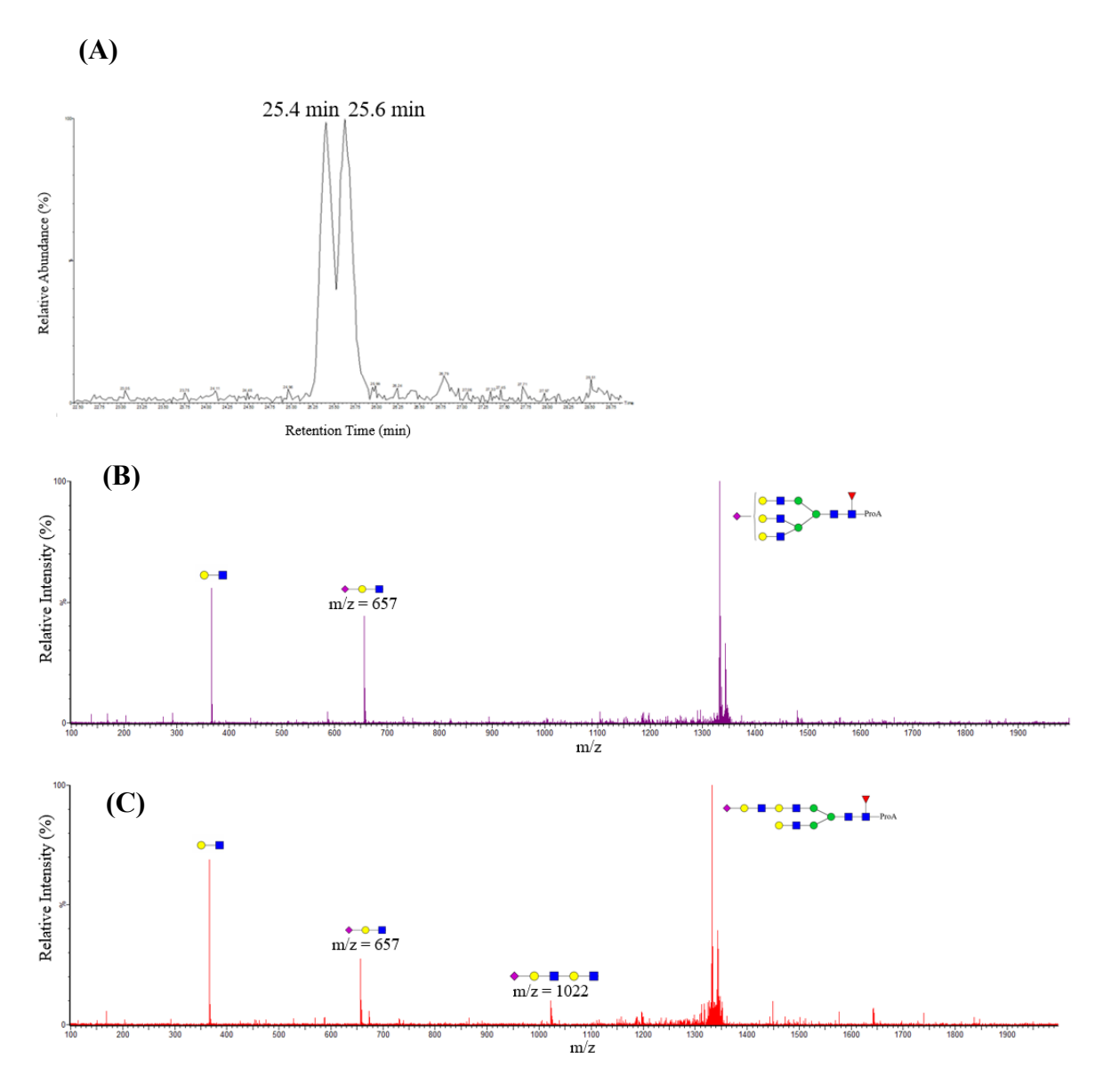


Figure 4.5 The EIC at M+2H m/z = 1332.03 of the A3G3(Neu5Ac)1F glycan and the tandem mass spectra of the two detected chromatographic peaks. The two resolved chromatographic peaks suggests an existence of an additional isomer other than the predicted A3G3(Neu5Ac)1F(1 α 2-3-Gal) species. The tandem mass spectrum of A3G3(Neu5Ac)1 at (B) 26.6 min and (C) 27.3 min were collected. While the tandem mass spectrum at (B) 26.6 min demonstrates a normal fragment ions pattern for the A3G3(Neu5Ac)1F glycan, the species giving rise to the peak at 27.3 min

generate a unique fragment ion of Neu5Ac-Gal-GlcNAc-Gal-GlcNAc indicates the existence of a polyLacNAc glycan called A2G2(Lac)1(Neu5Ac)1F.

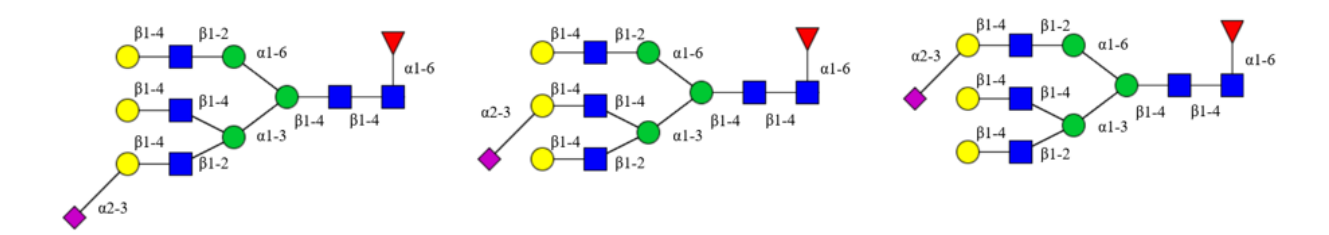


Figure 4.6. Possible positional isomers of A3G3(Ne5Ac)1F (1 α 2-3-Gal) that is not a polyLacNAc species.

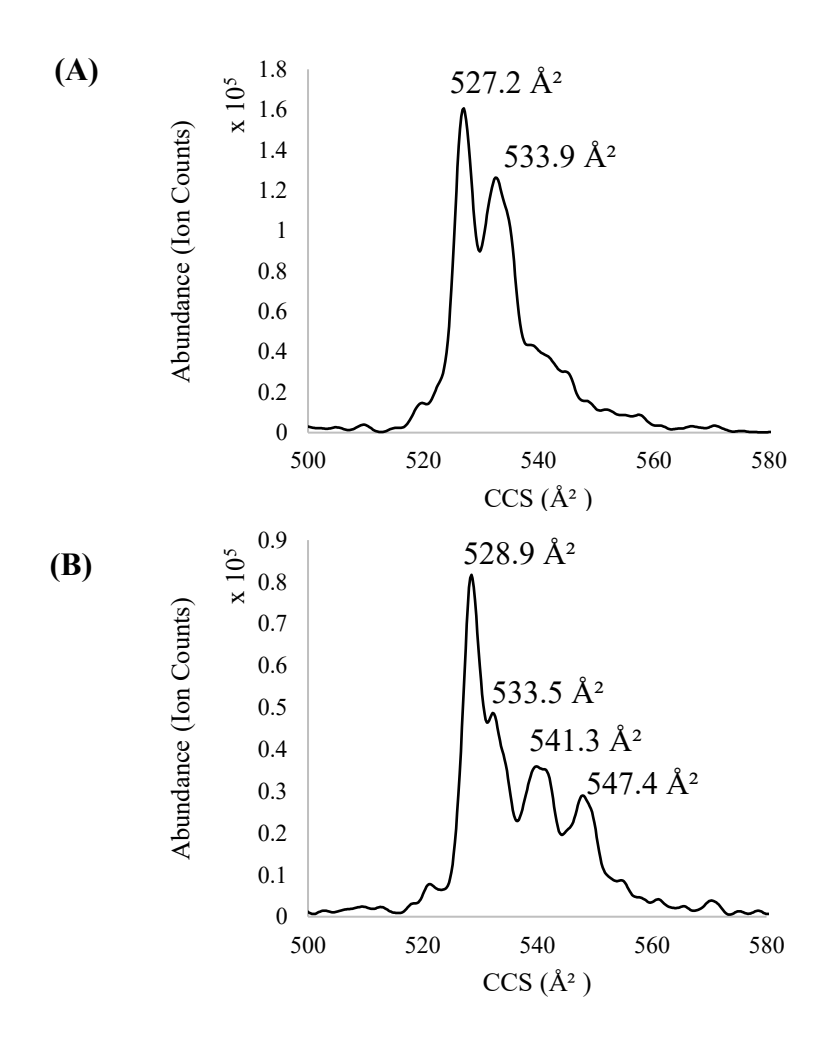


Figure 4.7 The mobiligrams of (A) A3G3(Neu5Ac)1F (1 α2-3-Gal) glycan and (B)

A2G2(LacNAc)1(Neu5Ac)1F (1 α 2-3-Gal) glycan. A unique fingerprint in IMS was detected for the mobiligram of the A3G3(Neu5Ac)1F (1 α 2-3-Gal) glycan, which has two resolved peaks at 526.6 Ų and 534.3 Ų. The two resolved peaks suggest possible resolutions from two of the positional tri-antenna isomers described in Figure 4.6. A different fingerprint with four peaks at 528.7 Ų, 533.5 Ų, 539.9 Ų, and 546.5 Ų was observed for the ion mobility trace of A2G2(LacNAc)1(Neu5Ac)1F (1 α 2-3-Gal) glycan, indicating the ability of IMS to possible resolve unpredicted isomers of this species. Two distinct ion mobility traces from panel A and B

provide unique fingerprint for each glycan species, which can be used as an identification data in glycan detection.

CHAPTER 5

USING HIGH RESOLUTION ION MOBILITY FOR THE SEPARATION OF $\alpha\text{-}GAL$ CONTAINING GLYCANS FROM THEIR NON- $\alpha\text{-}GAL$ ISOMERS

Thai, H., Orlando, R. To be submitted to Journal of Biomolecular Techniques

Abstract

Serve allergic reactions can occur from administering biotherapeutics containing the carbohydrate antigen galactose- α -1,3-galactose (α -Gal). The detection of α -Gal containing N-glycans is a challenging task due to the presence of non- α -Gal containing isomers. This study evaluates the ability of different analytical approaches to detect an α -Gal glycan in the presence of a non- α -Gal isomer. Cetuximab is known to have N-glycans containing α -Gal and was chosen for the study. N-glycans released from Cetuximab were analyzed using the HILIC-MS/MS system. HILIC-MS/MS successfully separated and identified α -Gal species when the Galactose number exceeds the antenna number. However, this system could not identify α -Gal species when the Galactose number equals the antenna number. Ion Mobility Spectrometer (IMS) was also evaluated and found to resolve isomeric a-gal/non-a-gal isomeric glycans. The study demonstrates the utility of the IMS-MS system to detect immunogenic glycans in the presence of their non- α -Gal isomers.

Introduction

Adverse consequences are observed in patients receiving biotherapeutics, such as a monoclonal antibody (mAb), possessing non-human glycans. ⁶⁻⁹An example is the administration of biotherapeutic products carrying Gal- α 1-3Gal (α -Gal) glycans, which can lead to severe allergic reactions since humans lack an enzyme to synthesize α -Gal containing glycans. The first report of α -Gal immunogenicity was a clinical study among patients who administrated Cetuximab for metastatic colorectal cancer or squamous-cell carcinoma of the head/ neck treatment. ³⁴ The study found that a novel IgE antibody (Ab) was directed against the existence of α -Gal glycans in Cetuximab and put patients at risk for hypersensitivity reactions. ³⁴

Detecting α -Gal glycans is a challenging task that requires high-resolution analytical methods. The structures of α -Gal and non- α -Gal N-glycans can be described using the following notation system: Ax represents the number of antennae, Gy is number of Galactoses attached to antenna GlcNAc, Fz is number of Fucoses linked to the core GlcNAc (Fz), and the number of existing α -Gal linkages is expressed as (α -Gal)w. An example of the N-glycan notation describing a species containing two antennae, one Galactose attached to antenna GlcNAc, one core Fucose, and one α -Gal linkage is A2G1(α -Gal)1F. Mass spectrometry (MS) is a highly sensitive tool that has been coupled with separational techniques to enhance the separation of α -Gal glycans in biotherapeutics. ^{13, 172-174} However, glycans often exist as isomeric mixtures, which makes them indistinguishable by only mass spectrometry. For example, A2G1(α -Gal)1F has an identical mass to A2G2F, one of the common N-glycans found on biotherapeutic products. Capillary electrophoresis (CE)¹⁷⁵ was paired with electrospray ionization (ESI) MS in a characterization study of α -Gal containing glycans in beef, mutton, and pork tenderloin. Although CE-MS successfully provided a profile of α -Gal species found in the tested animal

samples, the separation of isomer such as A2G1(α -Gal)1F and A2G2F was not achieved. Hydrophilic Interaction Liquid Chromatography (HILIC) is another popular separational technique in glycomics that was combined with Fluorescence Detector (FLD) and MS for glycoprofilling in Cetuximab expressed from different sources. HILIC separation provided a detailed characterization of N-glycan species in Cetuximab, but this method fails to separate α -Gal containing glycans from their non- α -Gal isomers due to the reported coelution of A2G1(α -Gal)1F with A2G2F, A3G1(α -Gal)1F with A3G2F, and A2G1(α -Gal)1F2 with A2G2F2. Developing an analytical method with high resolving powering remains a crucial need in distinguishing α -Gal glycans from their non- α -Gal isomers.

Ion mobility spectrometry (IMS) is gaining attention as a powerful tool in glycomics study. $^{127\text{-}130}$ One of the first applications of ion mobility in carbohydrate characterization demonstrated different drift times for isomers present in a series of oligosaccharides. 127 A Ion Mobility approach called Structure for Losless Ion Manipulation (SLIM) provides higher resolving power because it uses a 13m separation path, and thus, is capable of resolving components of complex isomeric mixtures that cannot be performed on ion mobility spectrometers with shorter paths. $^{178, 179}$ A separation of positional isomers (α 1-3/ α 1-6) from A2G1 and A2G1F was achieved with G1(6) arriving earlier than G1(3) via the SLIM device, 163 which suggests SLIM maybe a potential tool for separating α -Gal glycans from their non- α -Gal positional isomer.

This study evaluates the ability of different analytical methods to detect α -Gal N-glycans in biotherapeutic drugs. Cetuximab was chosen for this study due to the high abundance of α -Gal N-glycan. HILIC combined with tandem mass spectrometry (MS/MS) was initially used for the analysis of N-glycan released from Cetuximab, but HILIC-MS/MS struggled to identify

A2G1(α -Gal)1F from A2G2F. The sample was then run by HILIC-IMS-MS. IMS was demonstrated to successfully separate A2G1(α -Gal)1F from A2G2F. Exoglycosidase digestions were performed to confirm the identity of N-glycan isomers following the observed separation. These studies demonstrate the power of HILIC-IMS-MS for the analysis of complex isomeric glycan mixtures.

Materials and Method

Materials

Cetuximab was purchased from Eli Lilly (Indianapolis, IN, USA). Human Serum,

Dextran from Leuconostoc spp (Mr 6000), procainamide hydrochloride, acetic acid, dimethyl sulfoxide (DMSO), iodoacetamide and dithiothreitol (DTT) were purchased from Sigma-Aldrich (St. Louis, MO, USA). Sodium cyanoborohydride was purchased from Acros Organics (Branchbrug, NJ, USA). PNGaseF was purchased from Lectenz Bio (Athens, GA, USA).

Denaturing buffer and NP40 were purchased from New England Biolabs (Ipswich, MA, USA).

PD MiniTrap G10 and Hi-TrapTM protein G HP column were purchased from Cytiva (Marlborough, MA, USA). HyperSepTM C18 Cartridge was purchased from ThermoFisher (Waltham, MA, USA). β1-3,4 Galactosidase (cloned from bovine testis) and α1-3,4,6 Galactosidase (cloned from green coffee bean and expressed in E. coli) were purchased from New England Biolabs (Ipswich, MA, USA). Ammonium bicarbonate, ammonium formate and formic acid were purchased from Fluka (Morris Plains, NJ, USA). Acetonitrile (LCMS graded) was purchased from Honeywell Burdick and Jackson (Muskegon, MI, USA). Adalimumab was purchased from GlycoScientific (Athens, GA, USA).

N-glycans release from protein/antibody.

Human Serum IgGs were purified from human serum using a Hi-Trap™ protein G HP column prior to analysis. 1 mg of Cetuximab, 1 mg of Adalimumab (human IgG1), and 1 mg of Human Serum IgG were denatured at 100°C for 12 minutes using 4 μL of denaturing buffer (40 mM DTT, 0.5% SDS). The denatured proteins were put in the freezer for 5 minutes and 4 μL of 1% NP-40 was added to avoid deactivation of PNGaseF from residue heat and inhibitory effect of SDS. Then, 4 μL of PNGaseF was added to the sample and incubated at 37°C. After 16-20 hours, the samples were collected and lyophilized to dryness.

N-glycan purification and Procainamide (ProA) labeling.

The released N-glycans were resuspended in 200 μL of 5% acetic acid and run through C₁₈ SPE column (conditioned with 6 mL of 100% methanol and calibrated with 6 mL of 5% acetic acid) to remove residue protein(s). The purified N-glycans were collected and lyophilized to dryness. The labeling solution was prepared with 216 mg/mL procainamide-hydrochloride and 126 mg/mL sodium cyanoborohydride in 7:3 (DMSO/acetic acid) solution. Approximately 200 μL of the labeling solution was added to the purified N-glycans. The mixtures were incubated at 37°C overnight. After incubation, 100 μL Acetone was added to quench the reaction at 65°C for 30-60 minutes. The samples were dried down and resuspended in 140-200 μL of 5% acetic acid. Then, excess labeling reagents were cleaned up via size exclusion PD Mini trap G10 column. The collected fractions were lyophilized and stored in 100-150 μL of 80% ACN/H₂O at -20°C ready for analysis.

Exoglycosidase digestions

To confirm the existence of α -Gal and β -Gal linkages, 30 μ L of N-glycans solution released from Cetuximab was divided into two vials (15 μ L each) and dried down. The first vial was digested with 5 μ L of β 1-3,4 Galactosidase (8000 U/mL) and 5 μ L of GlycoBuffer (as

received) in 45 μ L nanopurewater. The second vial was digested with 5 μ L of α 1-3,4,6 Galactosidase (8000 U/mL), 5 μ L purified BSA (as received), and 5 μ L of GlycoBuffer 1 (as received) in 40 μ L nanopurewater. The digestions were incubated at 37°C overnight. After digestion, each reaction solution was lyophilized to dryness and then resuspended in 80% ACN/H₂O for analysis.

HILIC-MS/MS Settings and Instrumentations

The samples were run on HP1100 Agilent – Synapt G2 using Halo Penta-HILIC column (Advanced Material Technology, 1.5 mm x 15 cm, 2.7 µm particle size, Wilmington, DE). The separation was done at 0.1 mL/min flowrate at 60°C with mobile phase A and B consisting of 100% ACN with 0.1% formic acid and 50 mM ammonium formate in water with 0.1% formic acid, respectively. The gradient started at 80% ACN and ramped down 40% ACN over 40 minutes. The mass spectrometer acquired data using data dependent acquisition where the 5 most intense ions from each full mass spectrum were chosen for fragmentation using collision-induced dissociation (CID). The data collected was analyzed via Masslynx and Skyline.

HILIC-IMS-MS Settings and Instrumentations

The samples were run on an Agilent 1290 Infinity II LC – MOBILion SLIM - Agilent 6546 Q-TOF (MOBILion Systems Inc., Chadds Ford, PA & Agilent, Santa Clara, CA).

The HILIC separation was achieved using Halo Penta-HILIC column (Advanced Material Technology, 1.5 x 150 mm, 2.7 µm particle size, Wilmington, DE). The separation was performed at a flowrate of 0.1mL/min at 60°C with mobile phase A and B consisting of 100% ACN with 0.1% formic acid and 50mM ammonium formate in water with 0.1% formic acid, respectively. The gradient started at 80% ACN and ramped down to 40% ACN over 40 minutes.

The analytes were introduced into the IMS-MS system after HILIC separation. Ions were generated by the Dual AJS ESI provided by Agilent (Santa Clara, CA) with the recommended settings for N-glycan ionization. ¹⁶⁴ Upon entering the SLIM module, the ions were filled in storage section and then released into a single-pass path length of 13 m. ¹³¹⁻¹³³ The Travelling Wave (TW) potentials were generated between electrodes on two parallel printed circuit boards to propel the ions through N₂ drift gas. ¹³¹⁻¹³³ The settings for the TW potentials were based on the recommended parameter from the provider (MOBILion Systems Inc., Chadds Ford, PA) with minimal optimization. The mass spectra were obtained using MS (seq) acquisition settings in the Agilent 6546 Q-TOF (Agilent, Santa Clara, CA).

The collected data was processed via HRIM Data Processor prior to analysis using Agilent MassHunter IM-MS Browser, and Skyline. Dextran was used as the external calibrant for CCS calculation and the drift tube CCS of procainamide labeled dextran was extracted from reference data of Manz et al. ¹⁶⁵ The CCS calculation was based on the method described by Li et al. ¹⁶⁶

Results & Discussion

Challenges in Detecting α -Gal Containing N-Glycans

The characterization of α -Gal containing glycans plays a crucial role to ensure safety in drug development, but the analysis becomes challenging in the present of non- α -Gal isomers. Cetuximab is known to contain a variety of α -Gal glycans such as A2G2(α -Gal)1F or A2G1(α -Gal)1F and was used as the positive control for this study. Human Serum IgG and Adalimumab (IgG1) do not contain α -Gal glycans and were chosen as negative controls. The detection of α -Gal glycans can be easily achieved using HILIC-MS when the Galactose number is greater than the antenna number i.e., A2G2(α -Gal)1F, A2G2(α -Gal)2F, A3G3(α -Gal)1F, A3G3(α -Gal)2F,

A3G3(α -Gal)3F (Figure 5.1). However, the detection becomes significantly challenging when the number of Galactose is equal or less than the antenna number, i.e., A2G1(α -Gal)1F vs A2G2F. The HILIC-MS analysis shows that HILIC is unable to resolve A2G1(α -Gal)1F and A2G2F (Figure 5.2).

The behavior of α -Gal glycans via tandem mass spectrometry was studied. Human serum IgG is a non- α -Gal source and was chosen as one of the negative controls for the study. The abundance of (HexNac)₁(Hexose)₂ (m/z 528) fragment ion was noticeably high in the MS/MS spectrum of 1003.9 m/z (A2G2F/A2G2(α -Gal)1F) Cetuximab (Figure 5.3A). The m/z 528 fragment ion could be indicated as either GalGalGlcNAc or ManGlcNAcGal, hence, the non- α -Gal species can produce a fragment ion at this m/z value (Figure 5.3B). The abundance of the 528 m/z fragment ion is expected to vary depending on the ratio of the α -Gal to non- α -Gal species thus limiting the dynamic range for detection of the α -Gal species in the presence of its non- α -Gal isomer.

Analysis via HILIC- IMS-MS

HILIC-MS/MS failed to detect A2G1(α -Gal)1F in the presence of A2G2F, which is one of the most common non- α -Gal N-glycans found in antibodies. The addition of another separation dimension (High Resolution Ion Mobility) increases the resolving power of the system and enables the identification of α -Gal N-glycans in the presence of their non- α -Gal isomers.

Ion mobility traces of 1003.9 m/z (A2G2F) from Human Serum IgG and Adalimumab (IgG1) samples have a single peak with the collision cross section (CCS) value of 434.5 $\text{Å}^2 \pm 0.8$ Å^2 (Figure 5.4A and 5.4B). The mobiligram at 1003.9 m/z from Cetuximab sample (Figure 5.4C) was collected and two distinct peaks were observed with CCS value of 434.5 Å^2 and 444.6 $\text{Å}^2 \pm$

 0.8 Å^2 , respectively. The peak at 434.5 Ų from Cetuximab mobiligram (Figure 5.4C) has similar shape and identical CCS value as the peak found in both Human Serum IgG and IgG1 mobiligrams, suggesting that the 434.5 Ų peak results from the A2G2F species. The presence of the second peak at 444.6 Ų suggests that an isomer has coelutes with the A2G2F species. The coeluted peak at 444.6 Ų is hypothesized to be A2G1(α -Gal)1F since this was observed in the positive control (Cetuximab) but not in the negative sources that lacks α -gal glycans.

Exoglycosidase Digestions

A series of exoglycosidase digestions were conducted to confirm the identity of the species with CCS values of 434.5 Ų and 444.6 Å in 1003.9 m/z mobiligram of Cetuximab (Figure 5.5A). N-glycans released from Cetuximab were treated with β 1-3,4 Galactosidase. The disappearance of the peak at 434.5 Ų (Figure 5.5B) after β 1-3,4 Galactosidase digestion indicates that both Gal in this glycan are attached by β -linkages. Hence, this species corresponds to the expected A2G2F structure. The peak at 444.6 Ų was not affected after the β 1-3,4 Galactosidase digestion, suggesting the existing of an α -Gal linkage that block the cleavage of β -linkage. A second experiment was conducted with α 1-3,4,6 Galactosidase to confirm the presence of α -Gal species with a CCS value of 444.6 Ų. The disappearance of this large peak after α -galactosidase digestion (Figure 5.5C) confirms the presence of an α -Gal linkage and identifies this as the A2G1(α -Gal)1F species. The exoglysidase digestions confirmed that IMS can separate α -Gal glycans from their non- α -Gal isomers. The exoglysidase digestions revealed the ability of IMS to separate α -Gal glycans from their non- α -Gal isomers.

Conclusion

This study reveals that IMS can separate α -Gal glycans and its non α -Gal isomer, which remains a challenging task in the biopharmaceutical industry. CE and LC are popular

separational methods that have been applied to analyze glycans, $^{10, 175}$ but these traditional systems are incapable of resolving these isomers.. $^{176, 177}$ The ion mobility traces from non- α -Gal controls were compared to positive α -Gal control and confirmed the existence of an unknown glycan species that HILIC could not separate. Exoglycosidase digestions were performed and found the existence of an α -Gal containing glycan at the second peak at 444.6 Ų which was identified as the A2G1(α -Gal)1F. The HILIC-IMS-MS method used in this paper not only allows achievement of α -Gal isomeric separation but also provides three-dimensional data for detailed analysis of complex N-glycans from antibody. Future study utilizing HILIC-IMS-MS can significantly benefit from both the HILIC retention time data and Ion Mobility data to enable high efficiency and accuracy in data analysis.

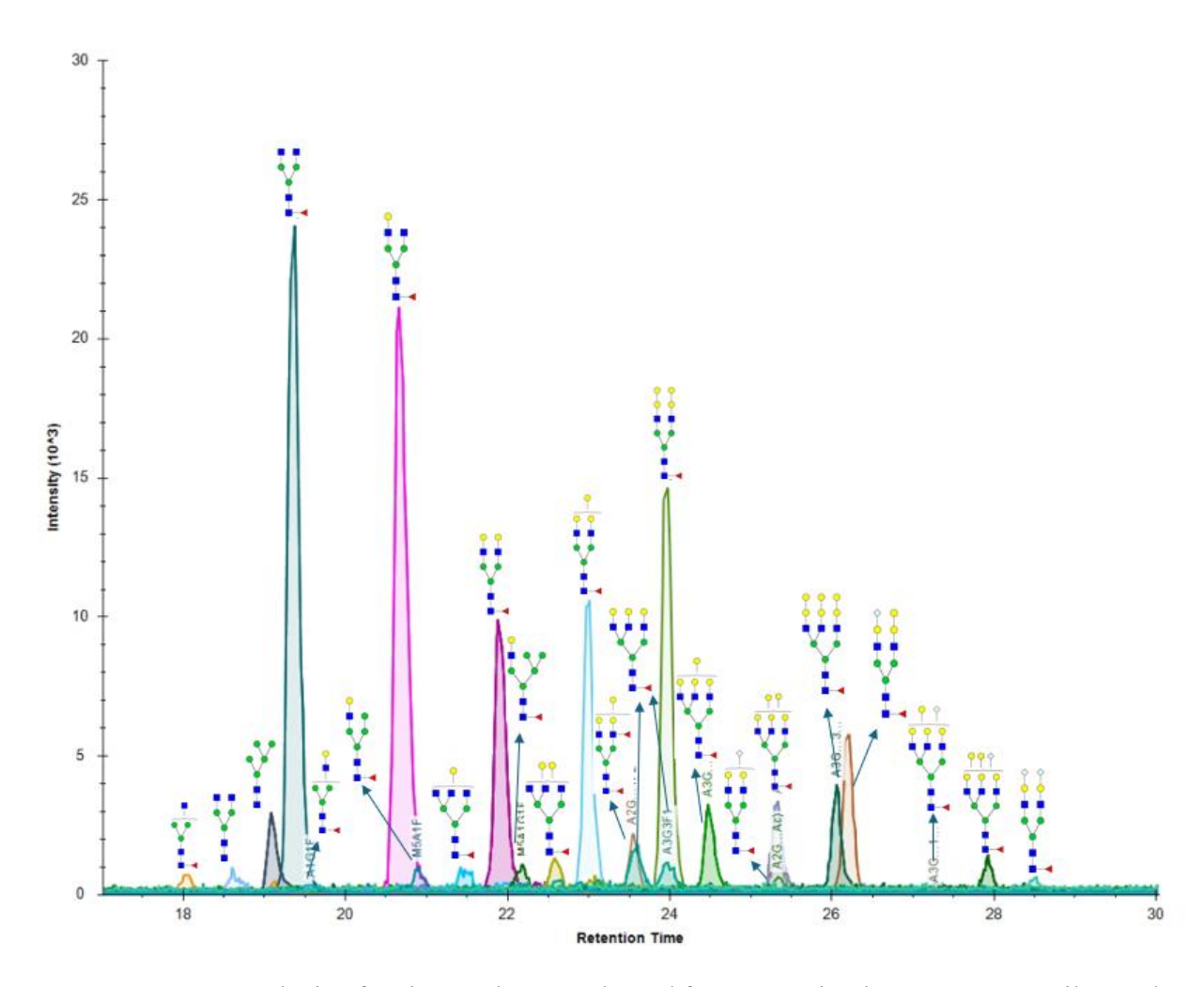


Figure 5.1 HILIC analysis of major N-glycans released from Cetuximab. HILIC can easily resolve α -Gal glycans that have a greater Galactose number than the antenna number such as A2G2(α -Gal)1F, A2G2(α -Gal)2F, A3G3(α -Gal)1F, A3G3(α -Gal)2F, A3G3(α -Gal)3F.

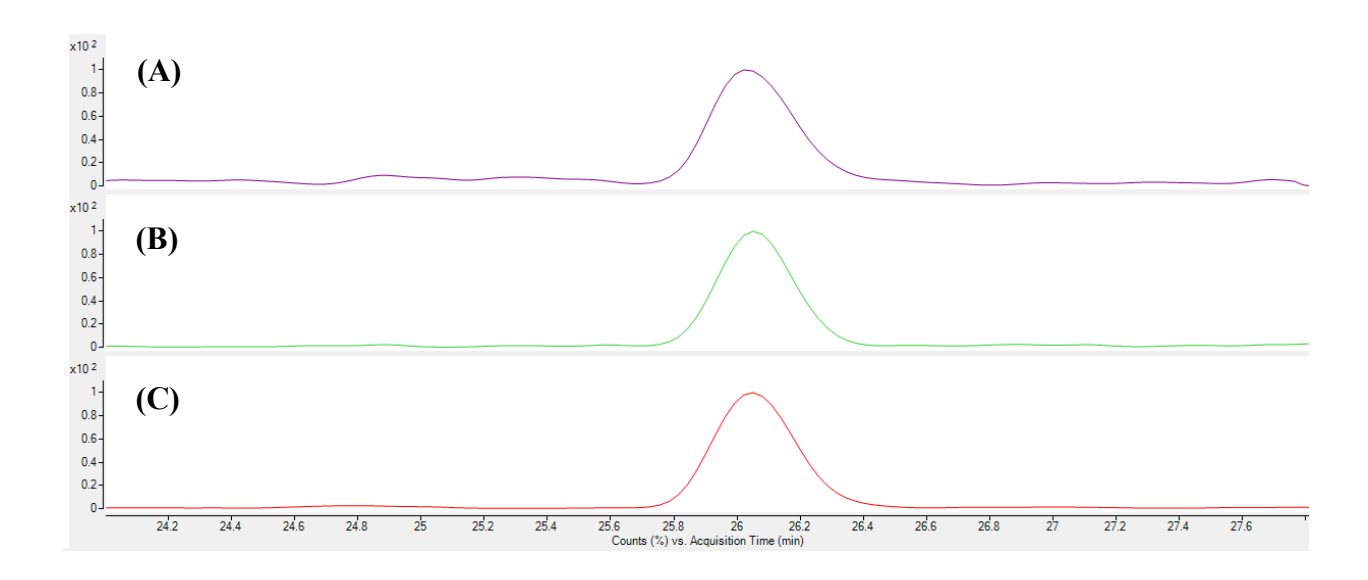


Figure 5.2 Extracted ion chromatograms (EICs) of m/z = 1003.9 from the β1-3,4 Galactosidase digested Cetuximab (A), the α 1-3,4,6 Galactosidase digested Cetuximab (B), and the control Cetuximab (C). The m/z = 1003.9 is the doubly protonated mass to charge of procainamide labeled A2G2F2 or A2G2(α -Gal)1F. The similarity in retention time of these EICs has shown that HILIC-MS is unable to resolve A2G2(α -Gal)1F and A2G2F.

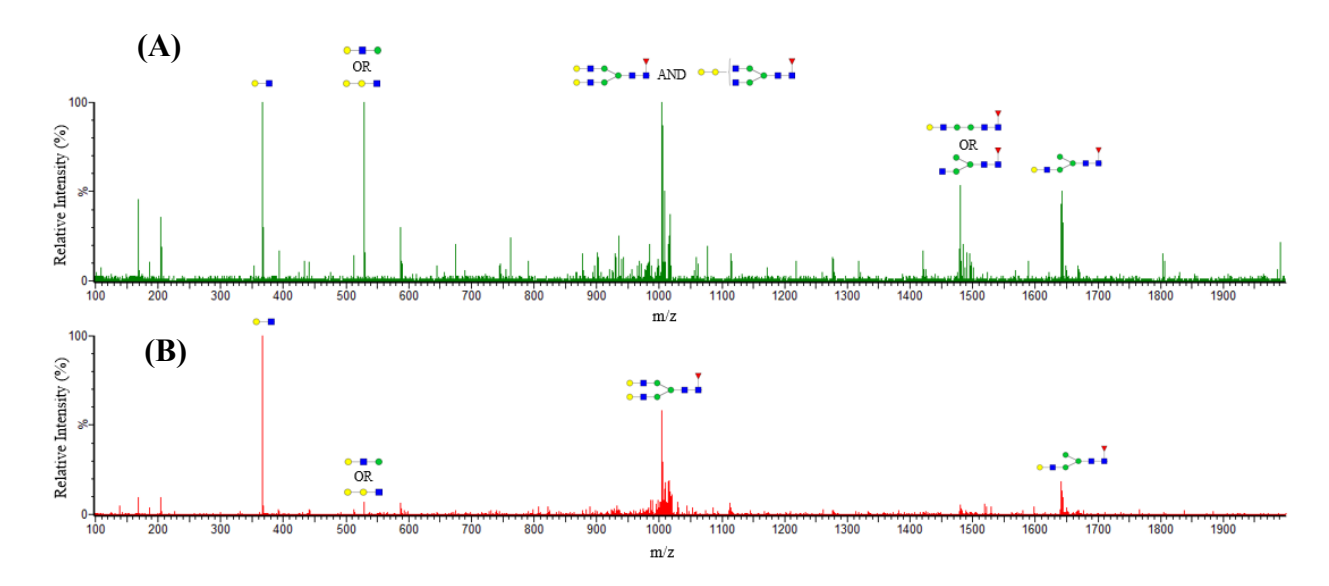


Figure 5.3 The tandem mass spectrum of the precursor ion at m/z = 1003.9 from Cetuximab (A) and human serum IgGs (B). It is worth noting that the abundance of fragment ion at 528 m/z is significantly higher in (A).

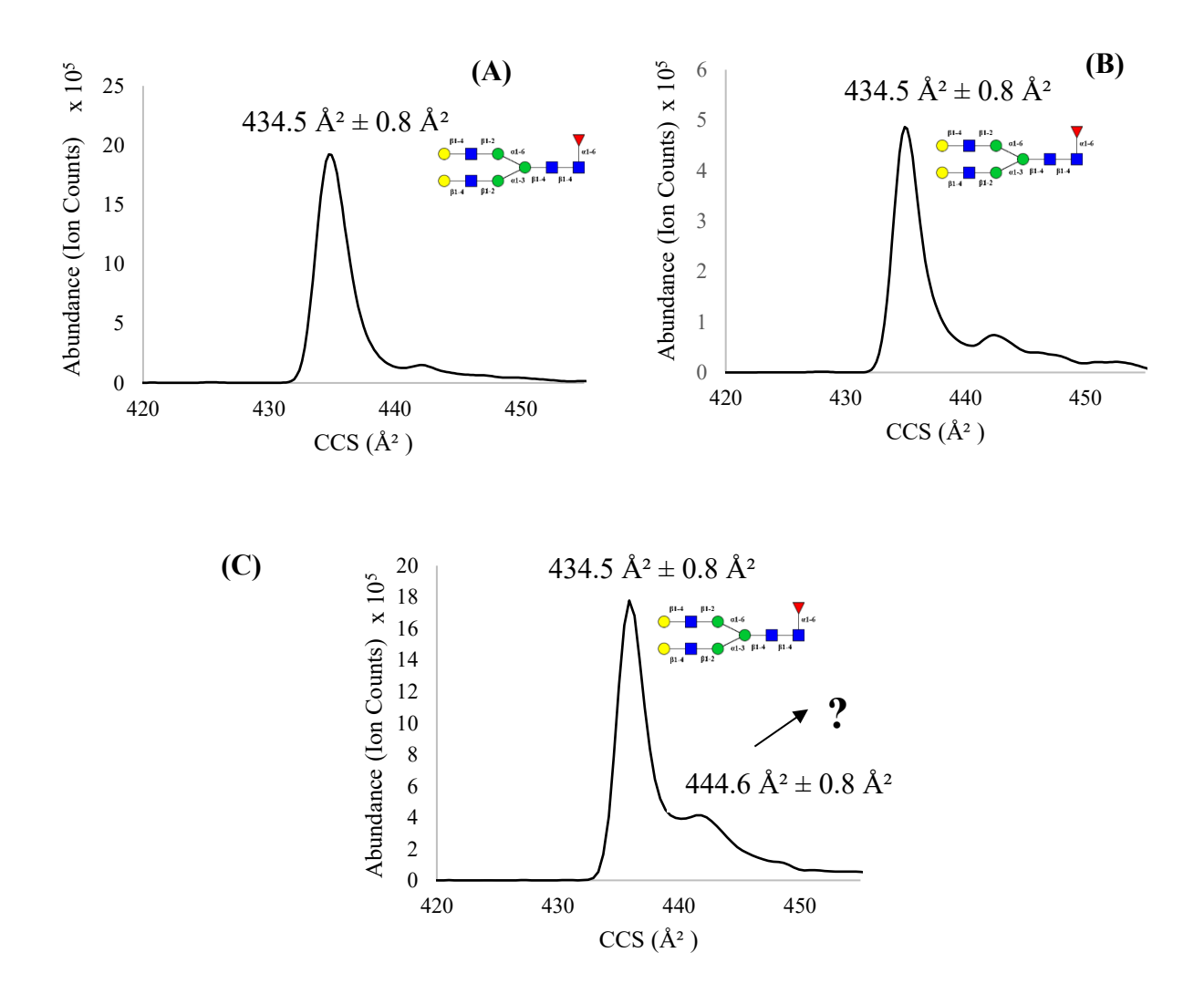


Figure 5.4 The mobiligrams of m/z = 1003.9 from (A) Adalimumab (IgG1) and (B) human serum IgGs, and Cetuximab (C). The m/z = 1003.9 (M+2H) is the mass to charge of procainamide labeled A2G2F2 or A2G2(α-Gal)1F. Both mobiligrams collected from negative controls (IgG1 and human serum IgG) have a similar single peak at 434.5 Ų showed up which confirms A2G2F has a mobiligram trace with one single dominant peak with CCS value of 434.5 Ų. An additional peak at 444.6 Ų was detected in the mobiligram of Cetuximab (C), indicating possible sign of the α-Gal isomer separation.

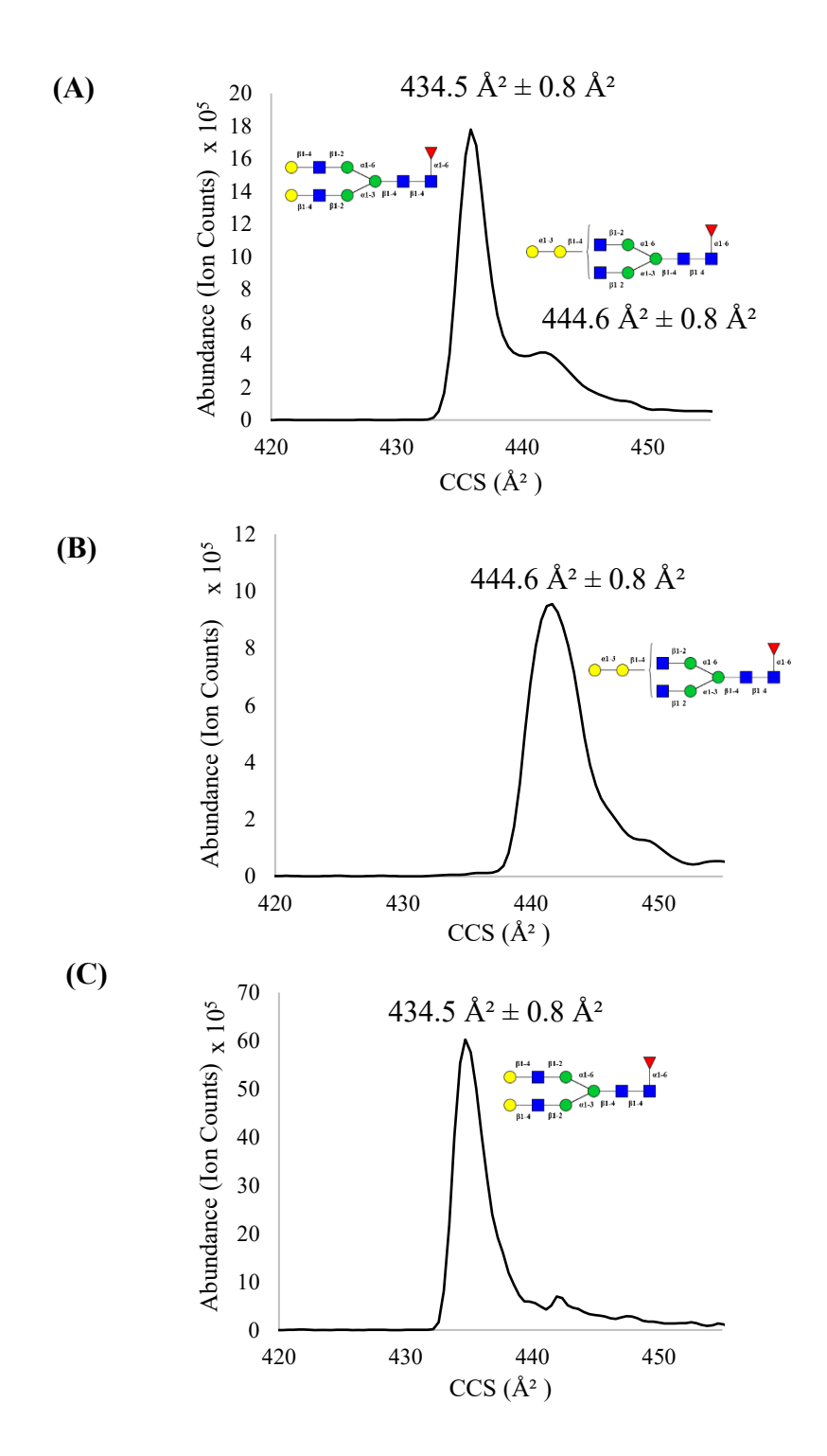


Figure 5.5 HILIC-IMS-MS results showing the ion mobility traces of the ion at 1003.9 m/z units from Cetuximab, obtained before digestion (A), after β 1-3,4 Galactosidase digestion (B), and after α 1-3,4,6 Galactosidase digestion (C). The disappearance of the peak at 434.5 Å² after β 1-

3,4 Galactosidase digestion demonstrates that both of the Gal residues are attached via a B-linkage, while the disappearance of the peak at 444.6 Å² after α 1-3,4,6 Galactosidase digestion demonstrates that this species has a single Gal terminus which is attached via an alpha linkage.

CHAPTER 6

A THREE-DIMENSIONAL DATABASE OF N-GLYCANS INCLUDES HILIC RETENTION

TIME, ION MOBILITY COLLISION CROSS SECTION, AND MASS TO CHARGE FROM

MASS SPECTROMETRY

Thai, H., Orlando, R. To be submitted to Journal of Biomolecular Techniques

Abstract

Hydrophilic interaction liquid chromatography (HILIC) – ion mobility spectrometry (IMS) – mass spectrometry (MS) is a high resolving power system in N-glycan analysis. This study developed a three-dimensional database that includes HILIC retention time, ion mobility collision cross section, and mass to charge (m/z) data of 205 Procainamide labeled N-glycans. The database is curated with non-immunogenic and immunogenic N-glycans detected in glycoproteins, cell pellets, and monoclonal antibody. The developed N-glycan database enables accurate identification of N-glycans including branched or linkage isomers and acts as a useful tool for data analysis of unknown samples.

Introduction

N-linked glycosylation regulates the stability and activity of biotherapeutic products. ¹⁸⁰⁻¹⁸² The control of glycosylation during drug development is an essential step to guarantee safety and efficacy in biotherapeutics. ^{169, 183, 184} N-glycans produced from glycosylation are chains of monosaccharide sugars that connect via different glycosylic linkages. ⁴⁷ The variety in glycosylic linkage creates different glycan structures and isomers. Characterizing glycan often needs high resolution analytical system due to the complexity of N-glycan structure and isomers.

A high throughput analytical method with high sensitivity and selectivity is desired for the study of N-glycans in biotherapeutics. Mass spectrometry (MS) is a common platform for the analysis of N-glycans. 84, 85, 185 The development of tandem mass spectrometry (MS/MS) has enabled structural identification of complex N-glycan structures via the production of fragment ions, $^{84, 85, 185}$ but this method can struggle to identify some glycan isomers such as $\alpha 2-3/\alpha 2-6$ sialylated glycans.³¹ The addition of separation techniques is necessary to increase the accuracy and efficiency for glycan profiling. Liquid chromatography (LC) combined with MS is a widely used technique in glycomics where analytes are separated prior to mass detection in MS.¹³ Hydrophilic interaction liquid chromatography (HILIC) is a popular LC mode that separates challenging isomeric groups and complements the identification process of MS. 10 HILIC-MS has been demonstrated as a powerful tool in the analysis of glycans. 10-13 Recent advancement in the analytical field has shown that the resolving power of HILIC-MS can be significantly improved through the addition of a robust separational technique called ion mobility spectrometry (IMS). 186, 187 IMS is a rapid gas-phase separation that differentiates ions based on their shape, charge and mass within milliseconds. 123 Applications of HILIC-IMS-MS revealed the ability of this multidimensional system in analyzing and resolving complex glycan isomers that cannot be

achieved via traditional two-dimensional systems. ^{188, 189} HIIC-IMS-MS is an ideal high throughput analytical system for the characterization of N-glycans.

The development of glycan databases is necessary to facilitate accuracy when using high resolution analytical systems for analysis. Complex Carbohydrate Structural Database (CCSD) is one of the first glycan databases published in 1980s that gather thousands of glycans along with their biological activities/applications. ^{135, 136} The emergence of LC-MS, IMS-MS, and LC-IMS-MS created demands for glycan databases with more complex information such as LC retention time or IMS collision cross section (CCS). Glycostore was developed in 2018 as a unique database that provides retention time of 850 unique glycans in different separational platforms including HILIC, reversed phase (RP), porous graphitic carbon (PGC), and capillary electrophoresis (CE). ³⁵ Glycomob is a more recent database that published over 900 CCS values of native glycans. ³⁶ The dataset from Glycomob can be accessed via larger glycan database platforms including UniCarbKB or UniCarbDB to help minimize scatter of glycan information. ³⁶ Efforts are being made in the glycoinformatic field to expand the glycan database for high throughput applications.

The establishment of derivatized N-glycan dataset is an essential step for the usage of glycan databases. N-glycans are typically derivatized before analysis in most MS-based technique to help increase ionization efficiency. ^{22, 24} Reductive animation is one of the common derivatization methods where primary amide fluorescence labels are chosen to react with the unreduced GlcNAc. ²² Some fluorescent tags such as Procainamide (ProA), 2-aminobenzamide (2AB), 2-aminobenzoic acid (2AA), and 2-aminopyridine (2-PA) were utilized in many studies of N-glycan profiling. ²⁴ A database of N-glycan labeled with 2-PA was published with information on LC retention time and ion mobility CCS data. ¹⁹⁰ This study developed a database

of N-glycan labeled with Procainamide, contributing to the expansion of derivatized N-glycan database. The developed database includes HILIC retention time, CCS, and m/z data of 205 glycans.

Materials and Method

Materials

Ribonuclease B (RNaseB), fetuin bovine, dextran from Leuconostoc spp (Mr 6000), procainamide hydrochloride, acetic acid, dimethyl sulfoxide (DMSO), and acetone were purchased from Sigma-Aldrich (St. Louis, MO, USA). Cetuximab was purchased from Eli Lilly (Indianapolis, IN, USA). Chinese Hamster Ovary (CHO) cell pellets and Human Embryonic Kidney (HEK) cell pellets were provided by Glycoscientific (Athens, GA, USA). Sodium cyanoborohydride was purchased from Acros Organics (Branchbrug, NJ, USA). PNGaseF were purchased from Lectenz Bio (Athens, GA, USA). Denaturing buffer and NP-40 were purchased from New England Biolabs (Ipswich, MA, USA). PD MiniTrap G10 was purchased from Cytiva (Marlborough, MA, USA). HyperSepTM C18 Cartridge was purchased from ThermoFisher (Waltham, MA, USA). Ammonium bicarbonate, ammonium formate and formic acid were purchased from Fluka (Morris Plains, NJ, USA). Acetonitrile (LCMS graded) was purchased from Honeywell Burdick and Jackson (Muskegon, MI, USA).

N-glycans release from protein/antibody using PNGaseF

1 mg of Ribonuclease B, 1 mg of fetuin bovine, and 1 mg of Cetuximab were each denatured at 100°C for 12 minutes using 4 μ L of denaturing buffer (40 mM DTT in 0.5% SDS). The samples were then cooled down in the freezer for 5 minutes followed by the addition of 2-4 μ L of 1% NP-40 to help avoid the loss of PNGaseF enzymatic activity. To the denatured

samples, 2-4 μ L of PNGaseF was added to release N-glycans overnight at 37°C. After 16-20 hours, the samples were collected and lyophilized to dryness.

N-glycans released from cell pellets using PNGaseF

About 100-10 million CHO cells or HEK cells were homogenized in 50 mM ammonium bicarbonate by passing through pipet tips. Samples were then sonicated in an ice bath by a probe sonicator in 15 seconds (sonicator power of 3 units) and were repeated 4 times with a break time of 15 seconds in between each sonication. 2 μL of dissolved cell pellet were taken out for A280 nanodrop. After determination of protein concentration, the samples were denatured at 100°C for 12 minutes using 10-15 μL of denaturing buffer (40 mM DTT in 0.5% SDS). The denatured samples were chilled in the freezer for 5 minutes followed by the addition of 4-6 μL of 1% NP-40 to help avoid the loss of PNGaseF enzymatic activity. Then, 4-6 μL of PNGaseF were added to release N-glycans. Samples were then left in the incubator at 37°C for 16-20 hours to release N-glycan from peptide backbone. After incubation, the samples were lyophilized to dryness. *N-glycans purification and Procainamide (ProA) labeling*.

The released N-glycans were resuspended in 200 μL of 5% acetic acid and ran through C₁₈ SPE column (conditioned with 6 mL of 100% methanol and calibrated with 6 mL of 5% acetic acid) to clean up residue protein(s). The purified N-glycans were lyophilized to dryness then resuspended in approximately 20 μL of water. The labeling solution was prepared with 216 mg/mL procainamide-hydrochloride and 126 mg/mL sodium cyanoborohydride in 7:3 (DMSO/acetic acid) solution. Approximately 200 μL labeling solution was added to antibody/glycoprotein samples and 400-600 μL was added to the cell pellet samples. The mixtures were incubated at 37°C overnight. After incubation, 100 μL of acetone was added to quench the reaction at 65°C for 30-60 minutes. The samples were dried down and resuspended in

140-200 μ L of 5% acetic acid. Then, excess labeling reagents were cleaned up via size exclusion PD Mini trap G10 column. The collected fractions were lyophilized and resuspended in approximately 100-150 μ L of water (1/3 the starting amount of the glycoprotein). The released and labeled N-glycans were stored in the freezer ready for analysis.

HILIC-IMS-MS Settings and Instrumentations

The samples were run on Agilent 1290 Infinity II LC – MOBILion Structures for Lossless Ion Manipulations (SLIM) IMS - Agilent 6546 Q-TOF (MOBILion Systems Inc., Chadds Ford, PA & Agilent, Santa Clara, CA).

The HILIC separation was achieved using Halo Penta-HILIC column (Advanced Material Technology, 1.5 x 150 mm, 2.7 µm particle size, Wilmington, DE). The separation was performed at a flowrate of 0.1 mL/min at 60°C with mobile phase A and B consisting of 100% ACN with 0.1% formic acid and 50 mM ammonium formate in water with 0.1% formic acid, respectively. The gradient used for N-glycan analysis started at 80% ACN and ramped down to 40% ACN over 40 minutes.

After HILIC separation, the analytes were introduced into the IMS-MS system where ions were generated by the Dual AJS ESI provided by Agilent (Santa Clara, CA) with the recommended settings for N-glycan ionization. ¹⁶⁴. Upon entering the SLIM module, the ions were filled in storage section and then released into a single-pass path length of 13 m. ¹³¹⁻¹³³ The Travelling Wave (TW) potentials are generated between electrodes on two parallel printed circuit boards to propel the ions through N₂ drift gas. ¹³¹⁻¹³³ The settings for the TW potentials were based on the recommended parameter from the provider (MOBILion Systems Inc., Chadds Ford, PA) with minimal optimization. The mass spectra were obtained using MS (seq) acquisition settings in the Agilent 6546 Q-TOF (Agilent, Santa Clara, CA).

The collected data was processed via HRIM Data Processor prior to analysis using Agilent MassHunter IM-MS Browser, Agilent Qualitative Analysis and Skyline.

Results and Discussion

Conversion of HILIC Retention Time into Glucose Unit

Retention time reported in minutes can be varied across LC instruments. Glucose unit (GU) is a "universal" metric in chromatographic measurement that normalizes retention time to avoid variation in recorded data. ¹⁹¹⁻¹⁹³ The study used dextran ladder as the external calibrant for unit conversion. The calibration curved were plotted as dextran glucose unit and their retention time. Logarithmic equation of the form y = aln(x) + b was fitted to the plotted curve. HILIC retention time of glycan in minutes was converted into glucose unit (GU) using the fitted logarithmic equation (Figure 6.1).

Calculation of collision cross section (CCS)

The arrival time of traveling wave-base ion mobility cannot be directly converted into CCS using the Mason–Schamp equation. The traveling-wave CCS can be calculated via a calibration curve fitted between the arrive time of a chosen set of calibrants and the reduced drift tube CCS values. Dextran ladder was proposed as an ideal calibrant for the calculation of glycan CCS due to its unique sequential α -1,6-linked glucose oligomers. This study utilized dextran as the external calibrant for CCS calculation and the calculation was based on the method used by Li et al for the SLIM system. The reduced CCS were calculated using equation 6.1, where the drift tube CCS values of Procainamide labeled dextran were extracted from reference data of Manz et al. The calibration curve is plotted as the reduced drift tube CCS of dextran oligosaccharides (y-axis) and the arrival time collected from traveling-wave IMS (x-axis). A calibration curve was initially fitted using conventional quadratic function (y = ax² +

bx + c), but this calibration curve resulted in relatively high CCS error (Figure 6.2). A logarithmic equation was employed as a different function for the calibration curve and found small deviations in the calculated CCS value compared to standard drift tube CCS data (Figure 6.2). The logarithmic calibration curve was used to calculate all reported CCS values in the database.

Database of HILIC retention time, ion mobility CCS, and m/z value of 205 procainamide labeled glycans

The study focusses on collecting information of N-glycans that are commonly found in biotherapeutic products. Two standard cell pellets in drug development, including CHO cells 196 and HEK cells, ¹⁹⁷ were chosen as one of the main glycoprotein sources for data collection. Nglycans released from RNaseB and fetuin bovine were also included as they contain a variety of high mannose glycans as well as high complex sialylated glycans that would benefit the dataset. The identification of immunogenic glycans is crucial during drug discovery, thus developing a database with immunogenic glycan information is a practical approach toward enhancing the utility of glycan databases. Glycans containing α -Gal (galactose- α -1,3-galactose) or Neu5Gc¹⁹⁹ are well-known immunogenic species that can lead to negative impact upon administration into the human body. The chosen list of standard glycoproteins provides Neu5Gcspecies information from the glycoforms of fetuin³¹, but still lacks information on α -Gal species. Cetuximab is a monoclonal antibody with high abundance of glycans containing α-Gal, ¹⁹⁸ which makes cetuximab an ideal candidate to fill in the missing information on α -Gal species. Nglycans released from Cetuximab were therefore added to the database. The database overall includes N-glycans released from CHO cells, HEK cells, RNaseB, fetuin bovine, and Cetuximab. The developed database covers an array N-glycans including non-fucosylated/fucosylyated glycans, α2-3/α2-6-Neu5Ac-glycans, α2-3/α2-6-Neu5Gc-glycans, Gal-(α1-3)-Gal containing glycans, Poly-N-acetyllactosamine (poly-LacNAc) glycans with repeated Gal-(β1-4)-GlcNAc disaccharides on one antenna, high mannose glycans, and hybrid glycans (Table 6.1). A three-dimensional plot of all data reported in Table 6.1 was graphed in Figure 6.3 to demonstrate an overall picture of the database. Most glycans were reported as doubly charged species except for some larger glycans (tetra- and penta-antenna) due to their high abundance in triply charged form. Each entry of data comprises of the glycoprotein source of which the N-glycan was released, the naming notation of glycan, charge state (z), mass to charge (m/z), HILIC retention time in glucose unit (GU), and ion mobility CCS value (Table 6.1). Some observed signals of N-glycan isomer cannot be confidently identified and are denoted numerically (-1, -2, -3, etc.) in the reported database. Each data reported was recorded in three replicates to ensure accuracy in data filing.

Application of the N-glycan database

An in-house analytical workflow (Figure 6.4) is described as an example to demonstrate the application of glycan database in data analysis process. Data is first analyzed in a pre-built skyline library covers composition of fucosylated/non-fucosylated glycans from A0G0 to A5G5(Neu5Ac)5, high mannose glycans (Man9-Man5), α-Gal glycans found in Cetuximab, and Neu5Gc glycans detected in fetuin. Software such as IMS Browser is then used for mass spectrum and mobiligram analysis. HILIC retention time and CCS information from the glycan database is employed to provide an additional layer of confirmation in identifying isomers.

The HILIC retention time, CCS and m/z database help to reveal more accurate details about the structure of N-glycan. Using only mass to charge (m/z) data for identification can only

identify the composition of the glycan. One composition of glycan proposed by m/z can have multiple isomeric species. The addition of HILIC retention time helps distinguish isomers including $\alpha 2$ -3/ $\alpha 2$ -6 sialylated glycans or poly-LacNAc species, which provides more accurate structural information. Ion mobility CCS acts as the third dimension to resolve species that HILIC cannot separate. A2G2F is a common glycan that can have a positional isomer containing a Gal-($\alpha 1$ -3)-Gal (α -Gal) linkage. Table 6.1 shows that A2G2F and its α -Gal containing isomer has identical HILIC retention time and m/z, but these two species were successfully resolved using IMS with two distinct CCS values reported. The data provided from the third dimension (IMS) allows high accuracy in glycan characterization. The glycan database can be used as a toolbox to simplify data analysis process and acts as an ideal tool to characterize complex glycan profiles.

Conclusion

This study developed Procainamide labeled N-glycan database involves HILIC retention time, ion mobility CCS, and m/z data of MS. An appropriate list of glycoproteins was carefully chosen to obtain information of commonly found N-glycans in biotherapeutic products. N-glycans listed in the database were released from CHO cells, HEK cells, RNaseB, fetuin bovine, and Cetuximab. HILIC retention time was converted into GU and ion mobility data was reported as CCS to allow application across different platforms. The development of procainamide labeled N-glycan database is an effort to bring the bridge of glyco-bioinformation application closer to biotherapeutic analysis. Future studies can utilize the developed database as an assistance tool for high throughput applications.

Equation 6.1

$$\Omega' = \frac{\Omega}{z \times \sqrt{\frac{1}{\mu}}}$$

Where Ω ' is reduced CCS, Ω is the known drift tube CCS, z is charge of the ion, and μ is the reduced mass

Equation 6.2

$$\mu = \frac{m_{ion} \times m_{gas}}{m_{ion} + m_{gas}}$$

Where m $_{\text{ion}}$ is mass of the ion, and m $_{\text{gas}}$ is mass of the inert gas

Table 6.1

Procainamide-labeled N-glycans database with m/z, HILIC retention time in GU, and ion mobility traveling-wave CCS information. The structure of N-glycans is described using the following naming system: Ax represents the number of antennae, Gy is number of Galactoses attached to antenna GlcNAc, and Fz is number of Fucoses linked to the core GlcNAc. Sialylated glycans are denoted with (Neu5Ac)m where m represents the number of Neu5Ac linked to either antenna Gal (α 2-3/ α 2-6) or antenna GlcNAc (α 2-6-GlcNAc or α 2-3-GlcNAc). N-glycans with Neu5Gc attached are described with (Neu5Gc)n notation where n is the number of Neu5Gc linked to antenna Gal via α 2-3/ α 2-6 linkage. Poly-LacNAc glycans, which have repeated Gal α 1-4GlcNAc disaccharides on one antenna, is describe by (Lac)t where t represents every one Gal α 1-4GlcNAc disaccharides repeated. The existing α -Gal linkages are expressed as (α -Gal)w.

| Glycoprotein | | | | | |
|--------------|-----------------|---|--------|--------|-------|
| Source | N-glycan Naming | z | m/z | RT(GU) | CCS |
| RNaseB | Man5 | 2 | 727.79 | 6.2 | 364.7 |
| RNaseB | Man5 with α1-2 | 2 | 727.79 | 6.2 | 384 |
| RNaseB | Man6 | 2 | 808.82 | 7.2 | 398.1 |
| RNaseB | Man7 | 2 | 889.85 | 8.1 | 419.2 |
| RNaseB | Man7 | 2 | 889.85 | 8.2 | 421.7 |
| RNaseB | Man7 | 2 | 889.85 | 8.2 | 427.4 |
| RNaseB | Man8 | 2 | 970.87 | 9.2 | 445.6 |
| RNaseB | Man8 | 2 | 970.87 | 9.3 | 454.3 |
| RNaseB | Man9 | 2 | 1051.9 | 10 | 470.2 |
| Fetuin | A2G2 | 2 | 930.87 | 7.7 | 431.6 |

| Fetuin | A2G2(Neu5Ac)1(α2-3)-1 | 2 | 1076.43 | 9.7 | 460.9 |
|--------|--|---|---------|------|-------|
| Fetuin | A2G2(Neu5Ac)1(α2-3)-2 | 2 | 1076.43 | 9.4 | 465.9 |
| Fetuin | A2G2(Neu5Ac)1(α2-6)-1 | 2 | 1076.43 | 10.4 | 471.4 |
| Fetuin | A2G2(Neu5Ac)1(α2-6)-2 | 2 | 1076.43 | 10.4 | 478.3 |
| Fetuin | A2G2(Neu5Ac)2 (2α2-3)-1 | 2 | 1221.99 | 12.2 | 507.6 |
| Fetuin | A2G2(Neu5Ac)2 (1α 2-3 + 1α 2-6) | 2 | 1221.99 | 13 | 516.3 |
| Fetuin | A2G2(Neu5Ac)2 (2 α2-6) | 2 | 1221.99 | 13.9 | 523.1 |
| Fetuin | A3G3 | 2 | 1113.46 | 9.1 | 470.2 |
| Fetuin | A3G3(Neu5Ac)1(α2-3)-1 | 2 | 1259 | 11.2 | 504.3 |
| Fetuin | A3G3(Neu5Ac)1(α2-3)-2 | 2 | 1259 | 11.2 | 515.7 |
| Fetuin | A3G3(Neu5Ac)1(α2-6)-1 | 2 | 1259 | 11.9 | 506.4 |
| Fetuin | A3G3(Neu5Ac)1(α2-6)-2 | 2 | 1259 | 11.9 | 517.1 |
| Fetuin | A3G3(Neu5Ac)2 (2α2-3) - 1 | 2 | 1404.55 | 13.8 | 547.7 |
| Fetuin | A3G3(Neu5Ac)2 (1α2-3, 1α2-6-GlcNAc)-1 | 2 | 1404.55 | 14 | 551.2 |
| Fetuin | A3G3(Neu5Ac)2 (1α2-3, 1α2-6-GlcNAc)-2 | 2 | 1404.55 | 14 | 536.4 |
| Fetuin | A3G3(Neu5Ac)2 $(1\alpha 2-3 + 1\alpha 2-6)-1$ | 2 | 1404.55 | 14.5 | 546.4 |
| Fetuin | A3G3(Neu5Ac)2 $(1\alpha 2-3 + 1\alpha 2-6)-2$ | 2 | 1404.55 | 14.5 | 552.7 |
| Fetuin | A3G3(Neu5Ac)2 (2α2-6)-1 | 2 | 1404.55 | 15.5 | 547.2 |
| Fetuin | A3G3(Neu5Ac)2 (2α2-6)-2 | 2 | 1404.55 | 15.5 | 521.3 |
| Fetuin | A3G3(Neu5Ac)3 (3 α2-3)-1 | 2 | 1550.1 | 16.9 | 583.2 |
| Fetuin | A3G3(Neu5Ac)3 (3 α2-3)-2 | 2 | 1550.1 | 16.9 | 599.7 |
| Fetuin | A3G3(Neu5Ac)3 (2α2-3, 1 α2-6-GlcNAc)-1 | 2 | 1550.1 | 17.3 | 569.5 |
| Fetuin | A3G3(Neu5Ac)3 (2α2-3, 1 α2-6-GlcNAc)-2 | 2 | 1550.1 | 17.3 | 581.1 |

| Fetuin | A3G3(Neu5Ac)3 (1 α2-6, 2 α2-3) | 2 | 1550.1 | 17.9 | 580.7 |
|--------|---|---|---------|------|-------|
| | A3G3(Neu5Ac)3 (1α2-3, 1 α2-6, 1 α2-6– | | | | |
| Fetuin | GlcNAc)-1 | 2 | 1550.1 | 18.2 | 581.9 |
| | A3G3(Neu5Ac)3 (1α2-3, 1 α2-6, 1 α2-6– | | | | |
| Fetuin | GlcNAc)-2 | 2 | 1550.1 | 18.2 | 586.5 |
| Fetuin | A3G3(Neu5Ac)3 (2 α2-6, 1 α2-3)-1 | 2 | 1550.1 | 18.8 | 578.8 |
| Fetuin | A3G3(Neu5Ac)3 (2 α2-6, 1 α2-3)-2 | 2 | 1550.1 | 18.8 | 570.3 |
| Fetuin | A3G3(Neu5Ac)3 (2 α2-6, 1 α2-6 – GlcNAc) | 2 | 1550.1 | 19.1 | 579.7 |
| Fetuin | A3G3(Neu5Ac)3(3 α2-6)-1 | 2 | 1550.1 | 19.8 | 577.4 |
| Fetuin | A3G3(Neu5Ac)3 (3 α2-6) - 2 | 2 | 1550.1 | 19.8 | 581 |
| Fetuin | A3G3(Neu5Ac)4 - 1 | 3 | 1130.75 | 21.1 | 636 |
| | A3G3(Neu5Ac)4 (1 α2-6, 1 α2-3, 2 α2-6 – | | | | |
| Fetuin | GlcNAc) | 3 | 1130.75 | 21.8 | 652.9 |
| | A3G3(Neu5Ac)4 (1 α2-6, 2 α2-3, 1 α2-6 – | | | | |
| Fetuin | GlcNAc) | 3 | 1130.75 | 22.3 | 638.4 |
| | A3G3(Neu5Ac)4 (2 α2-6, 1 α2-3, 1α2-6 – | | | | |
| Fetuin | GlcNAc) | 3 | 1130.75 | 23.5 | 655.5 |
| Fetuin | A2G2(Neu5Gc)1(1 α2-3) | 2 | 1084.44 | 10.1 | 462.8 |
| Fetuin | A2G2(Neu5Gc)1(1 α2-6) | 2 | 1084.44 | 10.8 | 473.6 |
| Fetuin | A2G2(Neu5Gc)1(Neu5Ac)1 (2 α2-6) | 2 | 1229.98 | 14.7 | 523.2 |
| Fetuin | A3G3(Neu5Gc)1(1 α2-3)-1 | 2 | 1267 | 11.7 | 505.8 |
| Fetuin | A3G3(Neu5Gc)1(1 α2-3)-2 | 2 | 1267 | 11.7 | 515.4 |
| Fetuin | A3G3(Neu5Gc)1(1 α2-3)-3 | 2 | 1267 | 11.7 | 525.6 |

| Fetuin | A3G3(Neu5Gc)1 (1 α2-6)-1 | 2 | 1267 | 12.3 | 508 |
|-----------|-----------------------------------|---|---------|------|-------|
| Fetuin | A3G3(Neu5Gc)1 (1α2-6)-2 | 2 | 1267 | 12.3 | 517 |
| Fetuin | A3G3(Neu5Gc)1 (1α2-6)-3 | 2 | 1267 | 12.3 | 523.5 |
| Fetuin | A3G3(Neu5Gc)1(Neu5Ac)1 (2 α2-3) | 2 | 1412.55 | 14.4 | 547.6 |
| Fetuin | A3G3(Neu5Gc)1(Neu5Ac)1 (2 α2-6)-1 | 2 | 1412.55 | 16.2 | 523.9 |
| Fetuin | A3G3(Neu5Gc)1(Neu5Ac)1 (2 α2-6)-2 | 2 | 1412.55 | 16.2 | 547.9 |
| Fetuin | A3G3(Neu5Gc)1(Neu5Ac)1 (2 α2-6)-3 | 2 | 1412.55 | 16.2 | 571 |
| CHO cells | M9 - Glc2-1 | 2 | 1213.97 | 11.5 | 511.9 |
| CHO cells | M9 - Glc2-2 | 2 | 1213.97 | 11.5 | 516.7 |
| CHO cells | M9 - Glc1 | 2 | 1132.94 | 10.8 | 486.5 |
| CHO cells | A2G2(Lac)1 | 2 | 1113.46 | 9.3 | 490.1 |
| CHO cells | A2G0 | 2 | 768.84 | 5.9 | 379.1 |
| CHO cells | A2G1-1 | 2 | 849.86 | 6.8 | 413.9 |
| CHO cells | A2G1-2 | 2 | 849.86 | 7 | 392.8 |
| CHO cells | A3G2 OR A2G2B-1 | 2 | 1032.85 | 8.4 | 456.7 |
| CHO cells | A3G2 OR A2G2B-2 | 2 | 1032.85 | 8.4 | 461.1 |
| CHO cells | A3G2 OR A2G2B-3 | 2 | 1032.85 | 8.4 | 467.9 |
| CHO cells | A3G2 OR A2G2B-4 | 2 | 1032.85 | 8.4 | 473.9 |
| CHO cells | A4G4-1 | 2 | 1296.02 | 10.8 | 510.6 |
| CHO cells | A4G4-2 | 2 | 1296.02 | 10.8 | 517.8 |
| CHO cells | A4G4-3 | 2 | 1296.02 | 10.8 | 524.7 |
| CHO cells | A4G4-3 | 2 | 1296.02 | 10.8 | 532.6 |
| CHO cells | A1G1(Neu5Ac) (1 α2-3-GlcNAc)-1 | 2 | 893.87 | 7.9 | 409.4 |

| CHO cells | A1G1(Neu5Ac) (1 α2-3-GlcNAc)-2 | 2 | 893.87 | 7.9 | 442.7 |
|-----------|---------------------------------|---|---------|------|-------|
| CHO cells | A1G1(Neu5Ac)1 (1 α2-3)-1 | 2 | 893.87 | 8.2 | 422.8 |
| CHO cells | A1G1(Neu5Ac)1 (1 α2-3)-2 | 2 | 893.87 | 8.2 | 428.5 |
| CHO cells | A1G1(Neu5Ac)1 (1 α2-3)-3 | 2 | 893.87 | 8.2 | 443 |
| CHO cells | A2G2(Neu5Ac)1 (2α2-3)-2 | 2 | 1221.99 | 12 | 500.9 |
| CHO cells | A2G2(Neu5Ac)1(1 α2-3) (Lac)1 -1 | 2 | 1259 | 11.4 | 512.2 |
| CHO cells | A2G2(Neu5Ac)1(1 α2-3) (Lac)1 -2 | 2 | 1259 | 11.4 | 521.9 |
| CHO cells | A3G3(Neu5Ac)1(1 α2-3) - 3 | 2 | 1259 | 11.1 | 521.1 |
| CHO cells | A3G3(Neu5Ac)1(1 α2-3) - 4 | 2 | 1259 | 11.1 | 525.5 |
| CHO cells | A3G3(Neu5Ac)1 (2α2-3)-2 | 2 | 1404.55 | 13.7 | 545.2 |
| CHO cells | A3G3(Neu5Ac)2 (2α2-3)-3 | 2 | 1404.55 | 13.7 | 552 |
| CHO cells | A4G4(Neu5Ac)1(1 α2-3)-1 | 2 | 1441.57 | 12.8 | 549.7 |
| CHO cells | A4G4(Neu5Ac)1(1 α2-3)-2 | 2 | 1441.57 | 12.8 | 554.6 |
| CHO cells | A4G4(Neu5Ac)1(1 α2-3)-3 | 2 | 1441.57 | 12.8 | 561.7 |
| CHO cells | A4G4(Neu5Ac)1(1 α2-3)-4 | 2 | 1441.57 | 12.8 | 566.3 |
| CHO cells | A4G4(Neu5Ac)2 (2 α2-3)-1 | 2 | 1587.12 | 15.3 | 576.3 |
| CHO cells | A4G4(Neu5Ac)2 (2 α2-3)-2 | 2 | 1587.12 | 15.3 | 588.2 |
| CHO cells | A4G4(Neu5Ac)2 (2 α2-3)-3 | 2 | 1587.12 | 15.3 | 596.2 |
| CHO cells | A0G0F-1 | 2 | 638.79 | 4.8 | 350.2 |
| CHO cells | A0G0F-2 | 2 | 638.79 | 4.8 | 373 |
| CHO cells | A2G0F-1 | 2 | 841.87 | 6.4 | 401.5 |
| CHO cells | A2G0F-2 | 2 | 841.87 | 6.4 | 419.6 |
| CHO cells | A2G1F-1 | 2 | 922.89 | 7.3 | 431 |

| CHO cells | A2G1F-2 | 2 | 922.89 | 7.3 | 433.9 |
|-----------|---------------------------|---|---------|------|-------|
| CHO cells | A2G2F | 2 | 1003.92 | 8.1 | 434.5 |
| CHO cells | A3G0F-2 | 2 | 943.41 | 7.2 | 435.2 |
| CHO cells | A3G2F | 2 | 1105.46 | 8.9 | 478.5 |
| CHO cells | A3G3F | 2 | 1186.49 | 9.5 | 484 |
| CHO cells | A2G2(Lac)1F -1 | 2 | 1186.49 | 9.8 | 495.3 |
| CHO cells | A2G2(Lac)1F -2 | 2 | 1186.49 | 9.8 | 510 |
| CHO cells | A4G0F | 2 | 1044.95 | 7.7 | 478.6 |
| CHO cells | A4G3F-1 | 2 | 1288.02 | 10.3 | 504.8 |
| CHO cells | A4G3F-2 | 2 | 1288.02 | 10.3 | 518 |
| CHO cells | A4G3F-3 | 2 | 1288.02 | 10.3 | 528.5 |
| CHO cells | A4G4F | 2 | 1369.05 | 11.1 | 532.2 |
| CHO cells | A5G5F-1 | 2 | 1551.62 | 12.5 | 569.5 |
| CHO cells | A5G5F-2 | 2 | 1551.62 | 12.5 | 575.7 |
| CHO cells | A1G1(Neu5Ac)1F (1 α2-3)-1 | 2 | 1068.44 | 9 | 475.1 |
| CHO cells | A1G1(Neu5Ac)1F (1 α2-3)-2 | 2 | 1068.44 | 9.2 | 467 |
| CHO cells | A1G1(Neu5Ac)1F (1 α2-3)-3 | 2 | 1068.44 | 9.2 | 471.2 |
| CHO cells | A2G2(Neu5Ac)1F (1 α2-3)-1 | 2 | 1149.47 | 10.1 | 484.5 |
| CHO cells | A2G2(Neu5Ac)1F (1 α2-3)-1 | 2 | 1149.47 | 10.1 | 489 |
| CHO cells | A2G2(Neu5Ac)1F (1 α2-3)-1 | 2 | 1149.47 | 10.1 | 493.4 |
| CHO cells | A2G2(Neu5Ac)2F (2 α2-3)-1 | 2 | 1295.01 | 12.6 | 528.8 |
| CHO cells | A2G2(Neu5Ac)2F (2 α2-3)-2 | 2 | 1295.01 | 12.6 | 531.2 |
| CHO cells | A3G2(Neu5Ac)1F (1 α2-3)-1 | 2 | 1251 | 10.7 | 509.8 |

| CHO cells | A3G2(Neu5Ac)1F (1 α2-3)-2 | 2 | 1251 | 10.7 | 524.6 |
|-----------|---------------------------------|---|---------|------|-------|
| CHO cells | A3G2(Neu5Ac)1F (1 α2-3)-3 | 2 | 1251 | 11 | 501.4 |
| CHO cells | A3G2(Neu5Ac)1F (1 α2-3)-4 | 2 | 1251 | 11 | 509.8 |
| CHO cells | A3G2(Neu5Ac)1F (1 α2-3)-5 | 2 | 1251 | 11 | 521.1 |
| CHO cells | A3G2(Neu5Ac)1F (1 α2-3)-6 | 2 | 1251 | 11 | 526.7 |
| CHO cells | A3G3(Neu5Ac)1F (1 α2-3)-1 | 2 | 1332.03 | 11.5 | 527.2 |
| CHO cells | A3G3(Neu5Ac)1F (1 α2-3)-2 | 2 | 1332.03 | 11.5 | 533.9 |
| CHO cells | A2G1(Neu5Ac)1(Lac)1F (1 α2-3)-1 | 2 | 1332.03 | 11.8 | 528.9 |
| CHO cells | A2G1(Neu5Ac)1(Lac)1F (1 α2-3)-2 | 2 | 1332.03 | 11.8 | 533.5 |
| CHO cells | A2G1(Neu5Ac)1(Lac)1F (1 α2-3)-3 | 2 | 1332.03 | 11.8 | 541.3 |
| CHO cells | A2G1(Neu5Ac)1(Lac)1F (1 α2-3)-4 | 2 | 1332.03 | 11.8 | 547.4 |
| CHO cells | A3G3(Neu5Ac)2F (2 α2-3)-1 | 2 | 1477.58 | 14.2 | 564.2 |
| CHO cells | A3G3(Neu5Ac)2F (2 α2-3)-2 | 2 | 1477.58 | 14.2 | 568.8 |
| CHO cells | A3G3(Neu5Ac)2F (2 α2-3)-3 | 2 | 1477.58 | 14.2 | 573.9 |
| CHO cells | A3G3(Neu5Ac)3F (3 α2-3)-1 | 2 | 1623.13 | 17.3 | 598.2 |
| CHO cells | A3G3(Neu5Ac)3F (3 α2-3)-2 | 2 | 1623.13 | 17.3 | 605.4 |
| CHO cells | A3G3(Neu5Ac)3F (3 α2-3)-3 | 2 | 1623.13 | 17.3 | 614.9 |
| CHO cells | A4G4(Neu5Ac)1F (1 α2-3)-1 | 2 | 1514.6 | 13.2 | 562.1 |
| CHO cells | A4G4(Neu5Ac)1F (1 α2-3)-2 | 2 | 1514.6 | 13.2 | 569.6 |
| CHO cells | A4G4(Neu5Ac)1F (1 α2-3)-3 | 2 | 1514.6 | 13.2 | 574.3 |
| CHO cells | A4G4(Neu5Ac)1F (1 α2-3)-4 | 2 | 1514.6 | 13.2 | 576.9 |
| CHO cells | A4G4(Neu5Ac)1F (1 α2-3)-5 | 2 | 1514.6 | 13.2 | 580.7 |
| CHO cells | A4G4(Neu5Ac)2F (2 α2-3)-1 | 2 | 1660.15 | 15.7 | 589.3 |

| CHO cells | A4G4(Neu5Ac)2F (2 α2-3)-2 | 2 | 1660.15 | 15.7 | 599.3 |
|-----------|---------------------------|---|---------|------|-------|
| CHO cells | A4G4(Neu5Ac)2F (2 α2-3)-3 | 2 | 1660.15 | 15.7 | 602.1 |
| CHO cells | A4G4(Neu5Ac)2F (2 α2-3)-4 | 2 | 1660.15 | 15.7 | 604.1 |
| CHO cells | A4G4(Neu5Ac)2F (2 α2-3)-5 | 2 | 1660.15 | 15.7 | 610.1 |
| CHO cells | A4G4(Neu5Ac)3F (3 α2-3)-1 | 3 | 1204.13 | 18.9 | 609 |
| CHO cells | A4G4(Neu5Ac)3F (3 α2-3)-2 | 3 | 1204.13 | 18.9 | 647.2 |
| CHO cells | A4G4(Neu5Ac)3F (3 α2-3)-3 | 3 | 1204.13 | 18.9 | 662 |
| CHO cells | A4G4(Neu5Ac)3F (3 α2-3)-4 | 3 | 1204.13 | 18.9 | 670.8 |
| CHO cells | A4G4(Neu5Ac)3F (3 α2-3)-5 | 3 | 1204.13 | 18.9 | 688.5 |
| CHO cells | A4G4(Neu5Ac)4F (4 α2-3)-1 | 3 | 1301.16 | 22.8 | 652.3 |
| CHO cells | A4G4(Neu5Ac)4F (4 α2-3)-2 | 3 | 1301.16 | 22.8 | 667.6 |
| CHO cells | A4G4(Neu5Ac)4F (4 α2-3)-3 | 3 | 1301.16 | 22.8 | 687.1 |
| CHO cells | A5G5(Neu5Ac)1F (1 α2-3)-1 | 3 | 1131.78 | 14.7 | 614.9 |
| CHO cells | A5G5(Neu5Ac)1F (1 α2-3)-2 | 3 | 1131.78 | 14.7 | 644.1 |
| CHO cells | A5G5(Neu5Ac)2F (2 α2-3)-1 | 3 | 1228.81 | 17.2 | 648 |
| CHO cells | A5G5(Neu5Ac)2F (2 α2-3)-2 | 3 | 1228.81 | 17.2 | 668 |
| CHO cells | A5G5(Neu5Ac)2F (2 α2-3)-3 | 3 | 1228.81 | 17.2 | 689.7 |
| CHO cells | A5G5(Neu5Ac)2F (2 α2-3)-4 | 3 | 1228.81 | 17.2 | 706.2 |
| CHO cells | A5G5(Neu5Ac)3F (3 α2-3)-1 | 3 | 1325.84 | 20.2 | 685.2 |
| CHO cells | A5G5(Neu5Ac)3F (3 α2-3)-2 | 3 | 1325.84 | 20.2 | 707.2 |
| CHO cells | A5G5(Neu5Ac)3F (3 α2-3)-3 | 3 | 1325.84 | 20.2 | 723.4 |
| CHO cells | A5G5(Neu5Ac)3F (3 α2-3)-4 | 3 | 1325.84 | 20.2 | 737.8 |
| HEK cells | A5G4F-1 | 3 | 980.73 | 11.4 | 595.1 |

| HEK cells | A5G4F-2 | 3 | 980.73 | 11.4 | 622.7 |
|-----------|------------------------------------|---|---------|------|-------|
| HEK cells | A2G1(Neu5Ac)1F (1 α2-6) | 2 | 1068.44 | 9.9 | 465.4 |
| HEK cells | A2G2(Neu5Ac)1F (1 α2-6) | 2 | 1149.47 | 10.8 | 491.6 |
| HEK cells | A2G2(Neu5Ac)2F (1 α2-3, 1 α2-6) | 2 | 1295.01 | 13.4 | 535.9 |
| HEK cells | A2G2(Neu5Ac)2F (2 α2-6) | 2 | 1295.01 | 14.2 | 531.5 |
| HEK cells | A3G2(Neu5Ac)1F (1 α2-6) | 2 | 1251 | 11.4 | 520.9 |
| HEK cells | A3G3(Neu5Ac)2F (1 α2-3, 1 α2-6) | 2 | 1477.58 | 14.8 | 566.1 |
| HEK cells | A4G4(Neu5Ac)1F (1 α2-6) | 2 | 1514.6 | 13.8 | 569.6 |
| HEK cells | A4G4 (Neu5Ac)2F (1 α2-3, 1 α2-6)-1 | 2 | 1660.15 | 16.5 | 600.1 |
| HEK cells | A4G4 (Neu5Ac)2F (1 α2-3, 1 α2-6)-2 | 2 | 1660.15 | 16.5 | 608.3 |
| HEK cells | A5G4 (Neu5Ac)1F (1 α2-3)-1 | 3 | 1077.76 | 13.5 | 608.2 |
| HEK cells | A5G4(Neu5Ac)1F (1 α2-3)-2 | 3 | 1077.76 | 13.5 | 624.8 |
| HEK cells | A5G4 (Neu5Ac)1F (1 α2-3)-3 | 3 | 1077.76 | 13.5 | 635.5 |
| HEK cells | A5G4 (Neu5Ac)1F (1 α2-6)-1 | 3 | 1077.76 | 14.4 | 649.1 |
| HEK cells | A5G4 (Neu5Ac)1F (1 α2-6)-2 | 3 | 1077.76 | 14.4 | 664.1 |
| Cetuximab | A2G2(α-Gal)1F-1 | 2 | 1084.95 | 8.8 | 460 |
| Cetuximab | A2G2(α-Gal)1F-2 | 2 | 1084.95 | 8.8 | 465 |
| Cetuximab | A2G2(α-Gal)2F | 2 | 1165.97 | 9.8 | 486.7 |
| Cetuximab | A3G3(α-Gal)1F-1 | 2 | 1267.51 | 10.2 | 509.1 |
| Cetuximab | A3G3(α-Gal)1F-2 | 2 | 1267.51 | 10.2 | 513.3 |
| Cetuximab | A3G3(α-Gal)2F-1 | 2 | 1348.54 | 11.1 | 519.8 |
| Cetuximab | A3G3(α-Gal)2F-2 | 2 | 1348.54 | 11.1 | 531.6 |
| Cetuximab | A3G3(α-Gal)2F-3 | 2 | 1348.54 | 11.1 | 542.7 |

| Cetuximab | A3G3(α-Gal)3F-1 | 2 | 1429.56 | 11.9 | 550.4 |
|-----------|--------------------------|---|---------|------|-------|
| Cetuximab | A3G3(α-Gal)3F-2 | 2 | 1429.56 | 11.9 | 560.6 |
| Cetuximab | A2G2(α-Gal)1F2-1 | 2 | 1157.97 | 9.4 | 490.6 |
| Cetuximab | A2G2(α-Gal)1F2-2 | 2 | 1157.97 | 9.4 | 496.2 |
| Cetuximab | A2G2(α-Gal)1(Neu5Gc)1F-1 | 2 | 1238.49 | 12.3 | 507.4 |
| Cetuximab | A2G2(α-Gal)1(Neu5Gc)1F-2 | 2 | 1238.49 | 12.3 | 518.3 |
| Cetuximab | A3G3(α-Gal)1(Neu5Gc)1F | 2 | 1421.06 | 13.8 | 548.5 |
| Cetuximab | A3G3(α-Gal)2(Neu5Gc)1F-1 | 2 | 1502.08 | 14.6 | 562.3 |
| Cetuximab | A3G3(α-Gal)2(Neu5Gc)1F-3 | 2 | 1502.08 | 14.6 | 572.5 |
| Cetuximab | A2G1(α-Gal)1F | 2 | 1003.9 | 7.9 | 444.6 |
| Cetuximab | A2G2(Neu5Gc)1F-1 | 2 | 1157.46 | 11.2 | 493 |
| Cetuximab | A2G2(Neu5Gc)1F-2 | 2 | 1157.46 | 11.2 | 504.3 |
| Cetuximab | A2G2(Neu5Gc)2F | 2 | 1311 | 15.6 | 532.4 |
| Cetuximab | M5G1F | 2 | 902.36 | 7.2 | 424.6 |
| Cetuximab | M5A1G1F-1 | 2 | 983.39 | 8.3 | 439.7 |
| Cetuximab | M5A1G1F-2 | 2 | 983.39 | 8.3 | 451.5 |

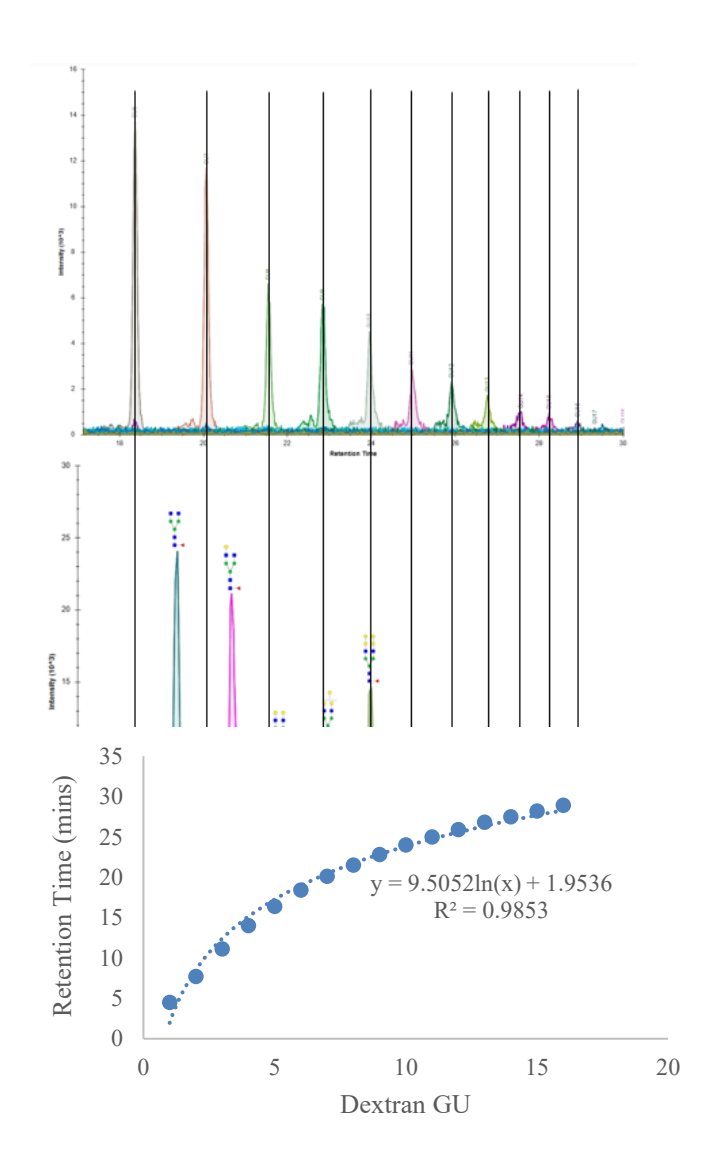


Figure 6.1 Procainamide-labeled dextran is used as an external calibrant to convert retention time in minutes into glucose unit (GU). Dextran ladder elutes as in the increasing term of glucose unit (A). Released N-glycans are ran under the same experimental condition after dextran calibration (B). A logarithmic calibration curve between dextran GU and their corresponding retention time is plotted to conver minutes into GU.

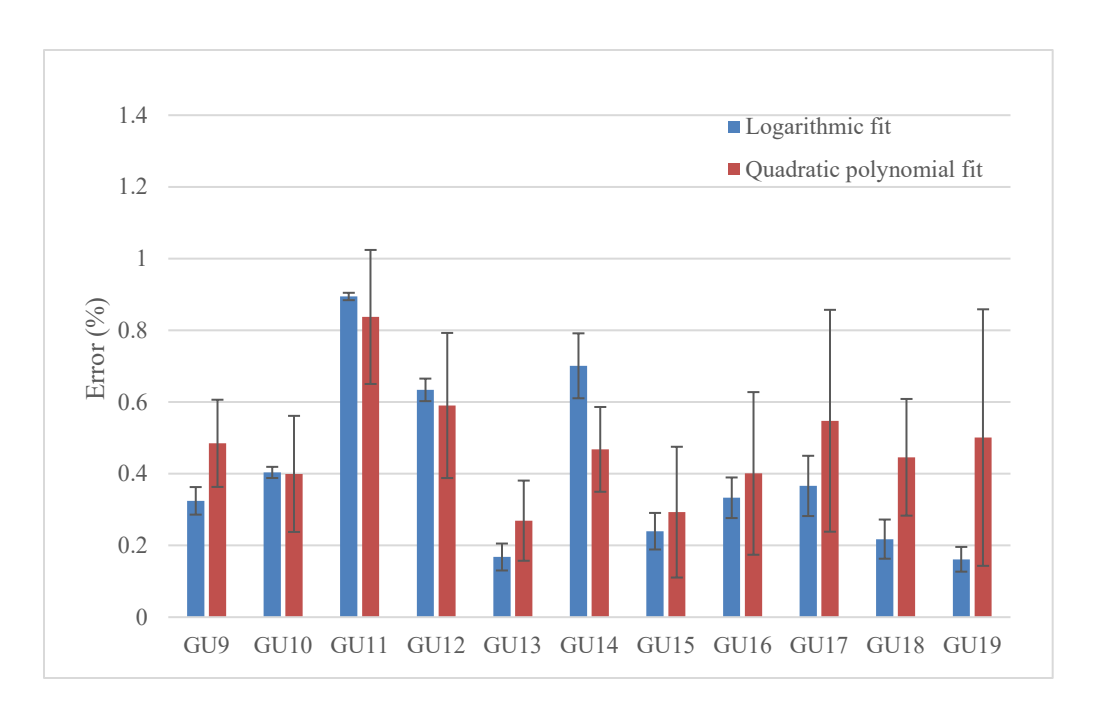


Figure 6.2 The CCS calibration errors of dextran ladder from GU9 to GU19 using two different fitting functions including: logarithmic fit and quadratic polynomial fit. The graph suggests that logarithmic fit is a more suitable equation fit with lower CCS errors.

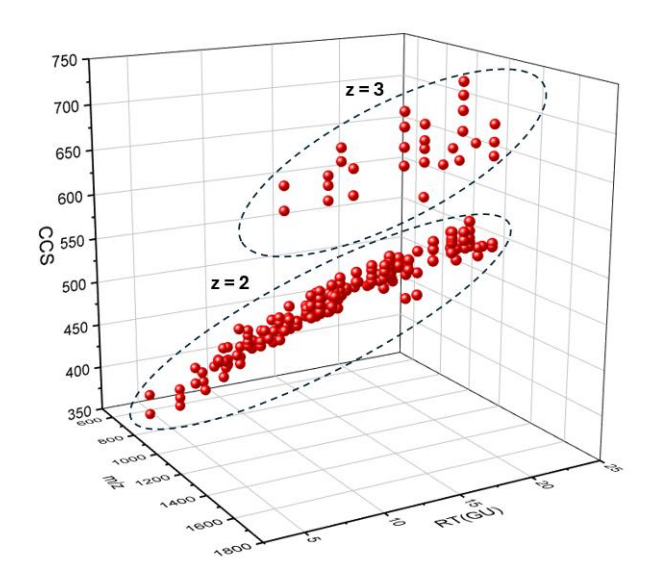


Figure 6.3 A three-dimensional plotted space of the procainamide labeled glycans database composed of HILIC retention time in GU, ion mobility values in CCS, and m/z data. The data has M+2H (z=2) and M+3H (z=3) species, which are grouped base on their charge in the dotted eclisped.

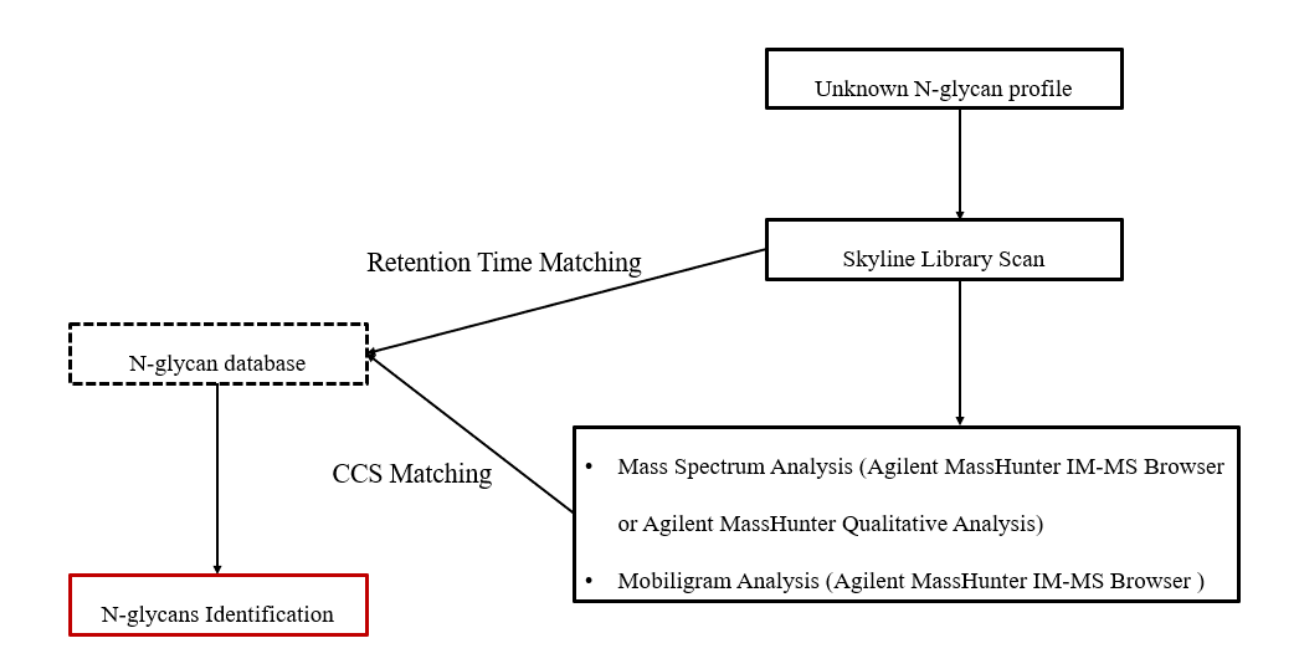


Figure 6.4 An in-house N-glycan identification protocol using the assistance of the developed N-glycan database. The unknown glycan dataset is initially imported into a pre-built skyline library for a quick scan of possible N-glycan presents in the dataset. The mass spectrum and mobiligrams are analyzed to help re-confirm the identification of the skyline-selected species. The developed N-glycan database is used to accurately verify the identity of any glycans that have linkage/branched isomers.

CHAPTER 7

Thai, H., Orlando, R. To be submitted to Journal of Biomolecular Techniques

Abstract

Optimizing peak capacity is a common approach to improve resolving power. Combining multiple separational techniques is known as one of the most effective ways to optimize peak capacity. The resolving power of a multidimensional system can be evaluated via measuring the orthogonality amongst each participating dimension. Ion mobility spectrometry (IMS) is a robust gas-phase separational method that can be paired with liquid chromatography (LC) and mass spectrometry (MS) to create a high resolving power system. The study of orthogonality for LC-IMS-MS is still underdeveloped. This study examines orthogonality of different LC modes paired with IMS-MS. Hydrophilic interaction liquid chromatography (HILIC)-IMS-MS and porous graphitic carbon (PGC)-IMS-MS were used for the analysis of N-glycans. Data collected from PGC-IMS-MS displays high dispersion of datapoints with higher orthogonality percentage compared to HILIC-IMS-MS, indicating PGC-IMS-MS has a higher resolving power in Nglycan analysis. The second part of the study involves the evaluation of HILIC-IMS-MS and reversed phase (RP)-IMS-MS in proteomics. HILIC-IMS-MS demonstrates an overall higher orthogonality compared to RP-IMS-MS, implying HILIC-IMS-MS can provide better resolution in peptide study. The orthogonality of multidimensional systems is governed by the separation mechanism between the analytes and the participating dimensions. The study of orthogonality helps identify an appropriate multidimension technique with high resolving power for the targeted biomolecules.

Introduction

Peak capacity measures the separation efficiency of analytical techniques such as liquid chromatography (LC).^{37, 38} The concept of peak capacity was first introduced by Giddings²⁰⁰ and Hovarth et al²⁰¹ as the measurement of the maximum number of resolvable peaks in a chromatographic elution. LC is a common separational technique in proteomics^{202, 203} and glycomics^{68, 204, 205}, optimizing peak capacity of LC is desired to increase resolving power. Chromatographic peak capacity can be optimized by altering different components including flowrates, gradient speeds, temperatures, and length of the column. ^{206, 207} While changes in the chromatographic conditions are proven to increase peak capacity, the use of multidimensional systems can push the boundary of peak capacity to significantly boost the separation efficiency. 141, 208-210 Peak capacity of a powerful one dimensional (1-D) chromatography is limited to the hundred range, 140, 141 but peak capacity of a multidimensional system is the product of maximum number of resolvable peaks in each dimension²¹¹ and can offer capacities in the range of thousands. ^{212, 213} The high number of peak capacities enable multidimensional systems to identify complex profiles of biomolecules that are challenging to 1-D techniques.^{214, 215} One of the widely recognized multidimensional technique is called Multidimensional Protein Identification Technology (MudPIT). MudPIT is a powerful method that utilizes the separation power of an orthogonal two-dimensional liquid chromatography to achieve identification of more than 1000 proteins in a complex proteome profile. 142 The success of two-dimensional systems in numerous studies has drawn the needs to study orthogonality of multidimensional systems, which assists researchers in choosing an appropriate high resolving power system for analysis. 145

Orthogonality is a popular metric in multidimensional chromatography that measures how uncorrelated the separations provided by each participating dimension. ^{143, 144} High uncorrelation equivalents with a better resolving power due to the unique datapoint collected from each dimension. The calculation of orthogonality can be done using a geometric approach where data are normalized and plotted into a 2-D separation space. ¹⁴⁵ The orthogonality measures the area of the 2-D separation space that covers with the plotted data. ¹⁴⁵ The geometric approach is a popular and simple method to calculate the orthogonality of different two-dimensional liquid chromatography systems. ^{145, 146} While geometric concepts have only been applied to 2-D LC systems, the calculation of this approach does not consider the properties of the dimension and only evaluate the coverage of the plotted datapoint. This means the geometric approach can be applied to evaluate the orthogonality of any 2-D systems.

The development of multidimensional system is not only limited to LC x LC but also expands to the combination of other separational techniques. 139, 141 Ion mobility spectrometry (IMS) is a gas-phase separational technique 123 that can be paired with LC-MS to create a high throughput multidimensional system with enhanced resolving power. 41, 139 The separation in IMS is achieved by the interaction between the charged analytes and the inert buffer gas. 123 Analytes in IMS are separated based on their charge, mass, and shape within milliseconds. 123 Applications of LC-IMS-MS in proteomics have accomplished attractive results with successful analysis of complex proteomics samples under high throughput conditions. 39, 139, 216 The improved resolving power of LC-IMS-MS also enables the separation of some complex isomers in glycan analysis that cannot be differentiated using one-dimensional LC-MS system. 187, 189, 217 LC-IMS-MS is emerging as a strong multidimensional technique, but there is limited study on the assessment for the orthogonality of this system.

The orthogonality of different LC mode combined with IMS-MS was examined in this study. The study involves the geometric orthogonality evaluation of different multidimensional systems for N-glycans and peptide analysis. Two systems including hydrophilic interaction liquid chromatography (HILIC) – IMS-MS and porous graphitic carbon (PGC) – IMS-MS were utilized for the analysis of N-glycans. The HILIC-IMS-MS and reversed phase (RP) -IMS-MS were used in the analysis of peptides.

Materials and Method

Materials

Ribonuclease B (bovine), Fetuin (bovine), dextran from Leuconostoc spp (Mr 6000), bovine serum albumin, human serum albumin, procainamide hydrochloride, acetic acid, dimethyl sulfoxide (DMSO), iodoacetamide, DL-Dithiothreitol (DL-DTT), and acetone were purchased from Sigma-Aldrich (St. Louis, MO, USA). Chinese Hamster Ovary cell pellets, Human Embryonic Kidney (HEK) cell pellets, and Adalimumab (IgG1) were provided by Glycoscientific (Athens, GA, USA). Sodium cyanoborohydride was purchased from Acros Organics (Branchbrug, NJ, USA). PNGaseF were purchased from Lectenz Bio (Athens, GA, USA). Sequencing Grade Modified Trypsin were purchased from Promega (Madison, WI, USA). Denaturing buffer, and NP40 were purchased from New England Biolabs (Ipswich, MA, USA). PD MiniTrap G10 was purchased from Cytiva (Marlborough, MA, USA). HyperSepTM C18 Cartridge was purchased from ThermoFisher (Waltham, MA, USA). Ammonium bicarbonate, ammonium formate and formic acid were purchased from Fluka (Morris Plains, NJ, USA). Acetonitrile (LCMS graded) was purchased from Honeywell Burdick and Jackson (Muskegon, MI, USA).

N-glycans release from protein/antibody using PNGaseF

1mg of Ribonuclease B and 1 mg of Fetuin were each denatured at 100° C for 12 minutes using 4 μ L of denaturing buffer (40 mM DTT in 0.5% SDS). The samples were then cooled down in the freezer for 5 minutes followed by the addition of 2-4 μ L of 1% NP-40 to help avoid the loss of PNGaseF enzymatic activity. To the denatured samples, 2-4 μ L of PNGaseF was added to release N-glycans overnight at 37°C. After 16-20 hours, the samples were collected and lyophilized to dryness.

N-glycans released from cell pellets using PNGaseF

About 100-10 million CHO cells or HEK cells were homogenized in 50 mM ammonium bicarbonate by passing through pipet tips. Samples were then sonicated in an ice bath by a probe sonicator in 15 seconds (sonicator power of 3 units) and were repeated 4 times with a break time of 15 seconds in between each sonication. 2 μL of dissolved cell pellet were taken out for A280 nanodrop. After determination of protein concentration, the samples were denatured at 100°C for 12 minutes using 10-15 μL of denaturing buffer (40 mM DTT in 0.5% SDS). The denatured samples were chilled in the freezer for 5 minutes followed by the addition of 4-6 μL of 1% NP-40 to help avoid the loss of PNGaseF enzymatic activity. Then, 4-6 μL of PNGaseF were added to release N-glycans. Samples were then left in the incubator at 37°C for 16-20 hours to release N-glycan from peptide backbone. After incubation, the samples were lyophilized to dryness. *N-glycans purification and Procainamide (ProA) labeling*.

The released N-glycans were resuspended in 200 μ L of 5% acetic acid and ran through C₁₈ SPE column (conditioned with 6 mL of 100% methanol and calibrated with 6 mL of 5% acetic acid) to clean up residue protein(s). The purified N-glycans were lyophilized to dryness then resuspended in approximately 20 μ L of water. The labeling solution was prepared with 216 mg/mL procainamide-hydrochloride and 126 mg/mL sodium cyanoborohydride in 7:3

(DMSO/acetic acid) solution. Approximately 200 μ L labeling solution was added to antibody/glycoprotein samples and 400-600 μ L was added to the cell pellet samples. The mixtures were incubated at 37°C overnight. After incubation, 100 μ L of acetone was added to quench the reaction at 65°C for 30-60 minutes. The samples were dried down and resuspended in 140-200 μ L of 5% acetic acid. Then, excess labeling reagents were cleaned up via size exclusion PD Mini trap G10 column. The collected fractions were lyophilized and resuspended in approximately 100-150 μ L of water (1/3 the starting amount of the glycoprotein). The released and labeled N-glycans were stored in the freezer ready for analysis.

Trypsin digestion of peptide

1mg of IgG1 (Adalimumab), 1mg of human serum albumin, and 1mg of bovine serum albumin were each subjected to reduction with 200 mM DL-DTT (4 μL) in 65°C for 1 hour. Then, the samples were alkylated via 4 μL of 1 M iodoacetamide (IDA) in an hour, and the remaining IDA was neutralized with approximately 16 μL 200 mM DL-DTT for another hour in 65°C. Sequencing grade modified trypsin was added (50:1, protein/trypsin) for incubation overnight at 37°C. Digested sample were dried via speedvac and stored in freezer ready for analysis.

LC-IMS-MS Settings and Instrumentations

The samples were run on Agilent 1290 Infinity II LC – MOBILion SLIM - Agilent 6546 Q-TOF (MOBILion Systems Inc., Chadds Ford, PA & Agilent, Santa Clara, CA).

The HILIC separation was achieved using Halo Penta-HILIC column (Advanced Material Technology, 1.5 x 150 mm, 2.7 µm particle size, Wilmington, DE). The condition was set at a flowrate of 0.1 mL/min at 60°C with mobile phase A and B consisted of 100% ACN with 0.1% formic acid and 50 mM ammonium formate in water with 0.1% formic acid, respectively.

The HILIC gradient for N-glycans analysis started at 80% ACN and ramped down to 40% ACN over 40 minutes. To optimize HILIC separation of peptide, a secondary gradient was developed where the gradient started at 90% ACN and decreased to 40% ACN over 20 minutes.

The PGC separation was achieved using Supel[™] Carbon LC column (Sigma-Aldrich, 2.1 x 100 mm, 2.7 µm particle size, St. Louis, MO). The separation was performed at a flowrate of 0.2 mL/min at 100°C with mobile phase A and B consisted of 100% ACN with 0.1% formic acid and 50 mM ammonium formate in water with 0.1% formic acid, respectively. The PGC gradient for N-glycans analysis started at 25% ACN and ramped up to 50% ACN over 25 minutes.

The separation of RP was achieved using HALO 90 Å C18 column (Advanced Material Technology, 1.5 x 150 mm, 2.7 µm particle size, Wilmington, DE). The flowrate was conditioned at 0.1 mL/min at 60°C with mobile phase A and B consisted of 100% ACN with 0.1% formic acid and 10 mM ammonium formate in water with 0.1% formic acid, respectively. The RP gradient for peptide analysis started at 5% ACN and ramped up to 70% ACN over 32.5 minutes.

The analytes were introduced into the IMS-MS system after HILIC separation. Ions were generated by the Dual AJS ESI provided by Agilent (Santa Clara, CA) with the recommended settings for N-glycan ionization. ¹⁶⁴ Upon entering the SLIM module, the ions were filled in storage section and then released into a single-pass path length of 13 m. ¹³¹⁻¹³³ The Travelling Wave (TW) potentials were generated between electrodes on two parallel printed circuit boards to propel the ions through N₂ drift gas. ¹³¹⁻¹³³ The settings for the TW potentials were based on the recommended parameter from the provider (MOBILion Systems Inc., Chadds Ford, PA) with minimal optimization. The mass spectra were obtained using MS (seq) acquisition settings in the Agilent 6546 Q-TOF (Agilent, Santa Clara, CA).

The collected data was processed via HRIM Data Processor prior to analysis using Agilent MassHunter IM-MS Browser, and Skyline. Dextran was used as the external calibrant for CCS calculation and the drift tube CCS of procainamide labeled dextran was extracted from reference data of Manz et al. ¹⁶⁵ The CCS calculation was based on the method described by Li et al. ¹⁶⁶ The N-glycan database from Chapter 6 was utilized for the orthogonality study of HILIC-IMS-MS in N-glycan analysis. The orthogonality was calculated using calculator provided by Gilar et al. ¹⁴³

Results and Discussion

Orthogonality: HILIC, IMS, and MS in N-glycan Analysis

The orthogonality of HILIC, IMS and MS in N-glycan analysis was examined. The data used for the evaluation was extracted from the database of N-glycans reported in Chapter 6 that includes HILIC retention time, IMS collision cross section (CCS), and mass to charge (m/z).

The study started with an evaluation of the relationship between MS and IMS. Mass Spectrometry (MS) is not a conventional separation technique, but the data provided from MS is unique for each N-glycans and can be treated as the third separational dimension. The orthogonal evaluation of CCS and molecular weight of molecules found a low orthogonality metric at 19% with most data point cluster along the diagonal line (Figure 7.1A). The shape of ions dictates their arrival time in an IMS experimental, but the mass of the ions also plays a critical role in the movement of ions in an IMS drift tube/path. The separation in IMS is influenced by mass, which correlates with mass-based identification mechanism in MS. The orthogonal results provide a metric measurement that suggests IMS and MS shares highly similarity in N-glycan separation mechanism.

The study continues by comparing the orthogonality between HILIC and MS. N-glycans interact with the stationary phase of HILIC mainly through their hydrophilic components such as hydroxyl group (-OH). Large N-glycans have a higher number of hydroxyl groups and elute later in a HILIC run. The separation of N-glycans in HILIC is essentially driven by the size of the molecules otherwise called mass-related. Molecules in MS are also mass-based, thus suggesting correlation in N-glycan separation mechanism between HILIC and MS. A low surface coverage was observed for the normalized graph between HILIC and molecular weight of N-glycans (Figure 7.1B) along with low orthogonality metric calculated (23%), which quantitatively agree HILIC and MS have high correlation in separating N-glycan.

The orthogonal study between IMS-MS and HILIC-MS suggests the separation of N-glycan in HILIC and IMS are mass-related. A relatively high correlation is expected for data collected from HILIC and IMS. The orthogonality metric calculated for HILIC and IMS were 29% with most datapoint align in the diagonal line. While the performance of HILIC-IMS-MS was demonstrated to surpass traditional separation method, the orthogonality between HILIC, IMS, and MS are relatively low. This led us to replace HILIC with a different LC mode to investigate the changes in orthogonality of multidimensional system in N-glycan analysis. *Orthogonality: PGC, IMS, and MS in N-glycan Analysis*

PGC has a unique retention mechanism that is believed to be the combination of polar retention effect and dispersive interactions. ¹¹⁸ The retention time produced by PGC is not reproducible, ¹²¹ thus limiting the application of this LC mode in many studies. In this study, HILIC was replaced by PGC to examine possible changes in orthogonality. The glycoprotein pool used in HILIC-IMS-MS study including RNase, Fetuin, Cetuximab, CHO cells, and HEK cells were employed for the study of PGC-IMS-MS to guarantee consistency between two

experiments. Due to limitations in sensitivity and knowledge of separation rules for N-glycans in PGC, 88 N-glycans were identified using PGC-IMS-MS.

CCS data of an analyte is a universal metric and expected to remain unchanged. This means changes in LC dimension should not impact the CCS value for a given analyte. Limitation in the data pool of PGC-IMS-MS means the datapoints between CCS and MS graphed in Figure 7.2A are subsets from the datapoints displayed in Figure 7.1A. The subset datapoints from Figure 7.2A have an orthogonality metric at 12%, which is lower compared to the orthogonality metric collected from a larger N-glycan data pool in Figure 7.1A (19%). The difference in orthogonality between a small and a large dataset implies that the geometric calculation depends heavily on the number of datapoints. A small pool of datapoints is limited in geometric coverage and can negatively impact the accuracy of the calculation.

PGC-IMS-MS has better data dispersion compared to HILIC-IMS-MS despite its limitation in datapoints. The orthogonal graph of data collected from PGC and MS shows higher uncorrelation of data with orthogonality calculated at 29% (Figure 7.2B). The PGC-IMS plot has a high spread of data with the calculated orthogonality metric yield at 31% (Figure 7.2C), which is only 1% orthogonality lower than the orthogonality metric calculated for HILIC-IMS (Figure 7.1C). While optimization of LC conditions is needed to decrease the limit of detection in PGC, future studies can take advantage of the high resolving power PGC-IMS-MS system in the application of resolving N-glycan isomers. The evaluation between two different systems including HILIC-IMS-MS and PGC-IMS-MS shows orthogonality can be used as a tool to identify the appropriate high resolving power system for analysis.

Orthogonality evaluation: RP-IMS-MS and HILIC-IMS-MS in Peptide Analysis

Peptide was chosen as the secondary analyte for the orthogonal study. Reversed phase (RP) is a popular LC mode in the analysis of peptide due to its hydrophobic separation mechanism.^{218, 219} HILIC is a less well-known LC mode in peptide analysis but has been shown to be an excellent choice in the analysis of protein post translational modifications.^{14, 220} RP and HILIC were each combined with IMS-MS to create two distinct multidimensional systems for the analysis of peptide.

The orthogonality of HILIC-IMS-MS and RP-IMS-MS were evaluated. The normalized graphs of HILIC retention time – molecular weight (MW) (Figure 7.3B) and RP retention time – MW of peptide (Figure 7.3D) display a high spread of datapoint along with high orthogonality percentage calculated, suggesting peptide separation mechanism from HILIC or RP have low correlation to the mass-based mechanism in MS. The separation mechanism of RP is mainly driven by hydrophobic interaction, which explains the uncorrelation between RP and MS. The orthogonal evaluation of N-glycans suggests that HILIC separation is mass-related in glycan separation, but the high orthogonality observed in Figure 7.3B indicates that the separation of peptide in HILIC is governed by the hydrophilic interaction between the amino acid and the stationary phase of HILIC. A larger peptide with a high number of hydrophobic amino acids can still elute earlier in a HILIC chromatogram compared to those smaller peptides but with higher hydrophilicity.²²¹ Due to the minimal influence of mass in the separation of peptide using RP or HILIC, an increase in the uncorrelation between IMS and HILIC/RP is expected. The datapoints from both normalized graphs of HILIC-IMS and RP-IMS (Figure 7.3C & E) significantly improve in dispersion with minimal data align on the diagonal line. The orthogonality metric was 49% for HILIC-IMS, which is significantly higher compared to orthogonality metric of HILIC-IMS in N-glycan analysis. The difference of orthogonality for the HILIC-IMS-MS in peptide and N-glycan analysis confirms that the change in analytes alters the separation mechanisms amongst separational dimensions and affects the separation efficiency of a multidimensional system.

Conclusion

This study investigated the orthogonality of various LC modes combining with IMS-MS. The performance of multidimensional systems that include LC, IMS, and MS gained significant attention in many research fields for their high resolving power and time efficiency compared to traditional methods. HILIC-IMS-MS was used for the analysis of peptide and N-glycans. The different separational behavior of peptide and glycans resulted in two distinct orthogonality metrics for HILIC-IMS-MS, indicating the dependence of orthogonality on the target analytes. The study of orthogonality also allows better understanding of separational mechanism within each participating separational dimension, thus permitting optimization in selecting the appropriate system for a targeted analyte. Two multidimensional systems including HILIC-IMS-MS and PGC-IMS-MS were used for N-glycan analysis. The study of orthogonality suggested PGC-IMS-MS was in fact a higher orthogonal multidimensional system compared to HILIC-IMS-MS in N-glycan analysis, proposing the use of PGC-IMS-MS in achieving challenging separation of N-glycan isomers.

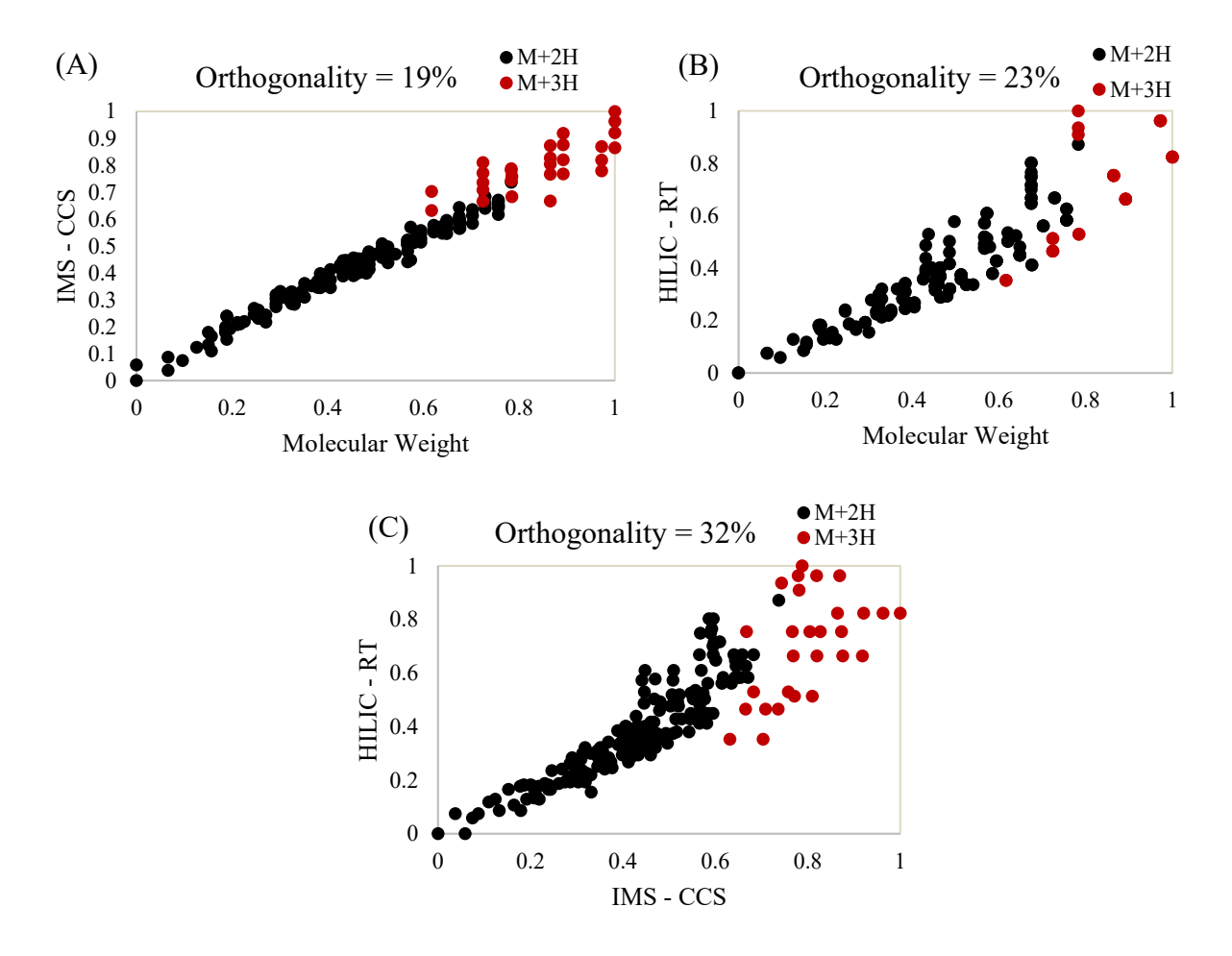


Figure 7.1 Two-dimensional plots of N-glycan data collected from HILIC-IMS-MS system. Panel A shows normalized plot between collision cross section (CCS) and molecular weight of molecules. The normalized HILIC retention time (RT) and molecular weight of molecule plot is displayed in Panel B. Panel C illustrates normalized retention time and collision cross section (CCS) plot between HILIC and IMS. The normalized plots show low dispersion of datapoints along, suggesting high correlation between data collected from HILIC, IMS and MS.

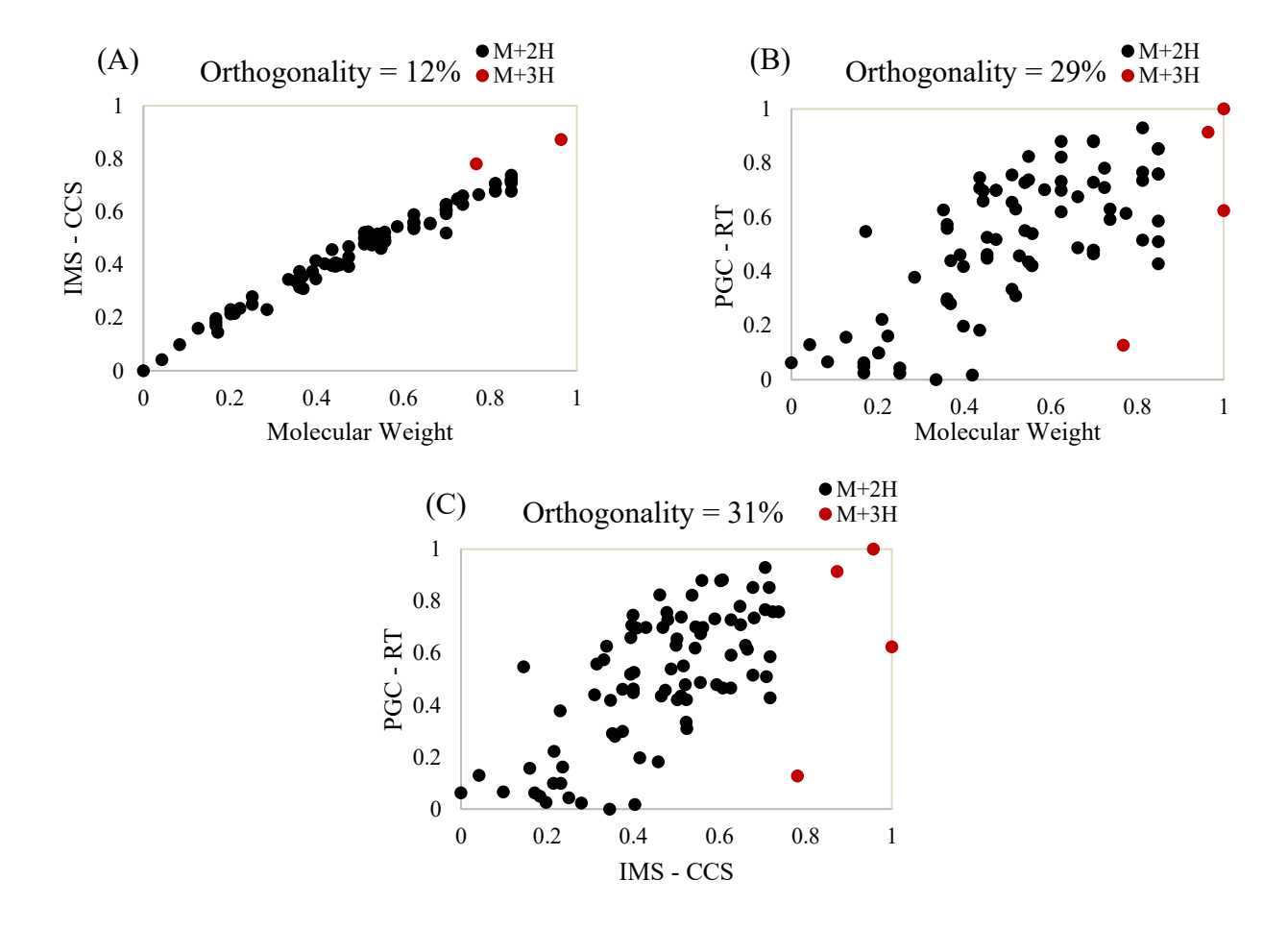
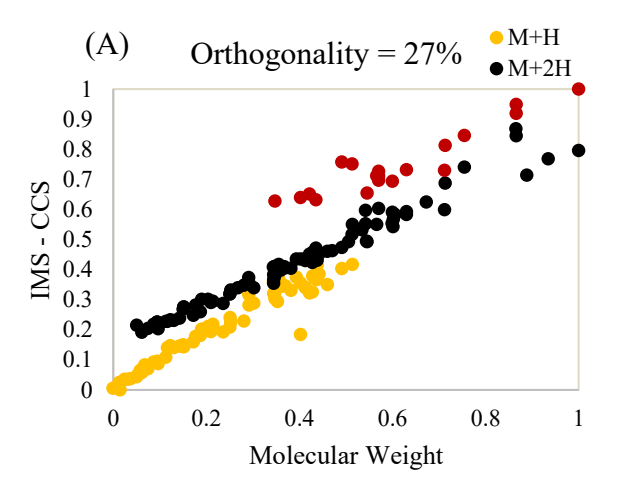


Figure 7.2 The normalized plots of N-glycan data collected from PGC-IMS-MS. Panel A represents the relationship between the molecular weight of molecules (MW) and corresponding CCS values. Panel B displays the correlation between the molecular weight of molecules and their PGC retention time. The separation relationship between PGC and IMS for N-glycan analysis is shown in Panel C. Both plots from panel B and C demonstrate low correlation with less data cluster at the diagonal, which indicates data collected from PGC has high uncorrelation to data obtained from MS and IMS.



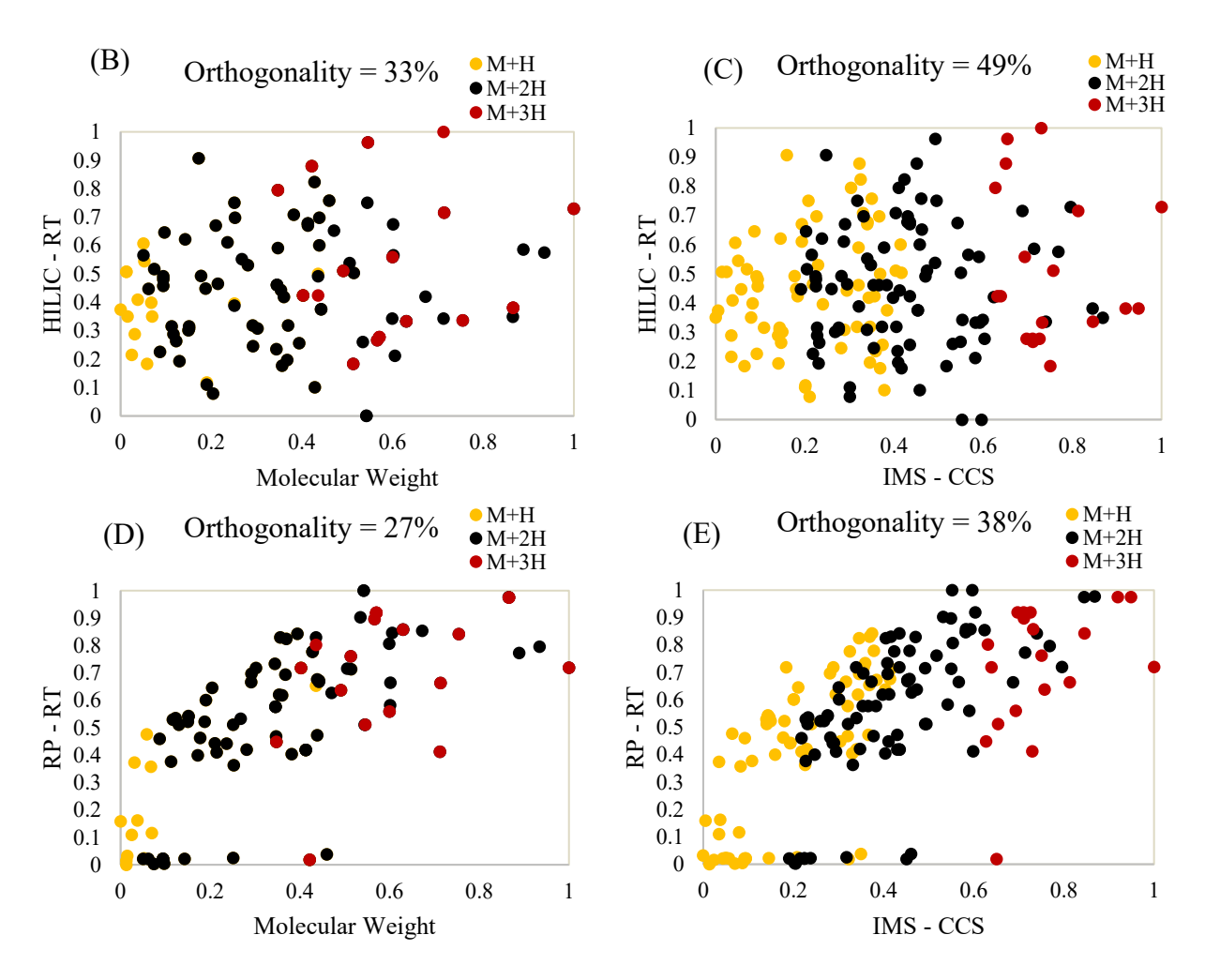


Figure 7.3 The normalized plots of peptide data obtained from HILIC-IMS-MS and RP-IMS-MS platforms. The relationship between IMS CCS – molecular weight (MW) of peptide (A),

HILIC retention time - MW (B), HILC retention time - IMS CCS (C), RP retention time - MW (D), and RP retention time - IMS CCS (E) are illustrated via two-dimensional plots. HILIC-IMS-MS has an overall higher orthogonality compared to RP-IMS-MS in peptide analysis.

CHAPTER 8

CONCLUSION

The main focus of this work is improving the analysis of N-glycan through hydrophilic interaction liquid chromatogram (HILIC), ion mobility spectrometry (IMS), and mass spectrometry (MS). The first half of this work utilized HILIC-MS to examine glycan quantification and distinguish complex glycan isomers. The second half discusses the high resolving power of HILIC-IMS-MS in glycan applications. A database was developed as a toolbox for future high throughput applications. Orthogonality of different LC-IMS-MS systems were evaluated, providing an insight into the behavior of some LC-IMS-MS systems used in proteomics and glycomics.

Chapter 3 examines relative abundance (%) of N-glycans released from the same sources but labeled with three different tags including: Procainamide (ProA), 2-aminobenzamide (2AB), and 2-aminobenzoic acid (2AA). ProA has a tertiary amide group that enables good protonation in electrospray ionization (ESI) positive mode. ProA-labeled glycans have overall high signal intensity with the high number of N-glycans detected in IgG4 (9 glycans) and human serum IgG (25 glycans). The structures of 2-AA and 2-AB lack protonation group and have low ionization efficiency in ESI positive mode. This cause increases in the limit of detection in the analysis of 2-AA and 2-AB labeled glycans, which lead to lower number of N-glycans observed compared to those derivatized with ProA. The dissimilarities in glycan profile have led to differences in quantitative results. Relative quantitation of N-glycans is determined by choosing the most abundance charge state to calculate percentage of peak areas. Each tag with distinct chemical

structure has a preferred protonated charge state. Choosing only one charge state led to inaccurate and biased quantitative results amongst different tags. Significant differences in relative abundance were observed when considering only doubly charged state, but taking account of multiple charged states and adducts dramatically decreased the dissimilarities in quantitative results. The study found that different labels have distinct ionization and favoritism in protonated charge states, which affects LC-MS quantitative outcomes.

Chapter 4 describes the ability of HILIC-MS/MS to differentiate challenging glycan isomers. Previous study has successfully resolved 4 linkage isomers of A3G3(Neu5Ac)3 in fetuin including Neu5Ac-(3 α2-3)-Gal, Neu5Ac-(2 α2-3, 1 α2-6)-Gal, Neu5Ac-(1 α2-3, 2 α2-6)-Gal, and Neu5Ac-(3 α 2-6)-Gal. ¹² The extracted ion chromatogram (EIC) of A3G3(Neu5Ac)3 collected in this study displays seven resolved peaks, indicating more than four glycans were separated. The collected tandem mass spectrum found that the additional detection peaks were giving rise to species with Neu5Ac-(α2-6)-GlcNAc linkage. The study also demonstrated the distinguishment of ($\alpha 2-3/\alpha 2-6$) Neu5Gc species from ($\alpha 2-3/\alpha 2-6$) Neu5Ac glycan using HILIC. These results indicate the power of HILIC in separating high complex glycans with sialic acid. N-glycan released from Chinese Hamster Ovary (CHO) cells were also analyzed using HILIC-MS/MS. A separation was achieved between the triantennary N-glycan and its Poly-N-acetyllactosamine (poly-LacNAc) positional isomer with repeated Gal-(β1-4)-GlcNAc extension on one of the antennae. Overexpression of poly-LacNAc glycans is known to be associated with tumorigenesis. ^{28, 29} The ability of HILIC in differentiating small PolyLacNAc glycans suggests HILIC is an ideal toolbox for application in early-stage diagnosis. HILIC-MS has been demonstrated as a powerful tool in separating linkages of isomers as well as positional isomers. The addition of IMS to HILIC-MS can significantly improve the resolving power and

completement the separation obtained in HILIC. A preliminary study was conducted and found that extra peaks were detected in IMS, indicating additional isomers were possibly resolved.

Distinct ion mobility trace was obtained for each species, which can be used as an additional identification data for the characterization of N-glycans.

Chapter 5 demonstrates the resolving power of a high-resolution ion mobility via the separation of α -Gal containing glycan from its non- α -Gal isomer. A2G2F is one of the most common N-glycans found in antibodies, but it has a positional isomer called A2G1(α -Gal)1F that contains an α -Gal linkage. HILIC-MS/MS struggled to distinguish between A2G2F and A2G1(α -Gal)1F. A high-resolution IMS was employed with the effort to distinguish this group of isomers. The mobiligram of A2G2F (m/z 1003.9) from Cetuximab depicts two resolved peaks whose collision cross section (CCS) values were 434.5 \pm 0.8 Ų and 444.6 \pm 0.8 Ų. The Gal linkages of the species giving rise to two observed peaks were identified via exoglycosidase digestions. Only β -Gal linkages were detected the peak at 434.5 Ų, indicating A2G2F gave rise the 434.5 Ų peak. The existence of a-Gal linkage was confirmed at the 444.6 Ų peak and suggested the glycan gave rise to this peak is A2G1(α -Gal)1F. IMS successfully attained the separation of α -Gal glycan from its non- α -Gal isomer. This study reveals the ability of IMS in complementing the separation of HILIC to enable challenging separation required higher resolving power.

Chapter 6 details the development of a Procainamide labeled N-glycan database involves three-dimensional data including: HILIC retention time, ion mobility CCS, and mass to charge values collected from MS. This platform covers 205 commonly found N-glycans in biotherapeutic products. Information on immunogenic glycans containing α-Gal linkage or Neu5Gc is also included. The dataset can be used as an assistance tool during analysis to help

provide accurate identification of isomers that cannot be distinguished using only one or twodimensional data analysis. The N-glycan database allows high accuracy during analysis and is suitable as a toolbox for high throughput applications.

Chapter 7 discusses the orthogonality of LC-IMS-MS systems in glycomics and proteomics. Orthogonality evaluation has been extensively done for two-dimensional LC-LC systems, 145, 146 but orthogonal study of LC-IMS-MS platforms is still underdeveloped.

Orthogonality of HILIC-IMS-MS and porous graphitic carbon (PGC)-IMS-MS was examined for N-glycans analysis. The orthogonal metric of PGC-IMS-MS was higher than orthogonal metric calculated for HILIC-IMS-MS. This suggests future studies can use PGC-IMS-MS to target challenging glycan profiles that require a high resolving power system. The orthogonal study was also conducted for HILIC-IMS-MS and reversed phase (RP)-IMS-MS in proteomics. While RP is a more common LC mode in peptide analysis, HILIC-IMS-MS resulted in an overall higher orthogonal metric compared to RP-IMS-MS. The distinct behavior of HILIC-IMS-MS when analyzing peptides and N-glycans implies that the separation mechanism between the analytes and the participating separational dimensions plays a crucial role in orthogonality evaluation. Studying the orthogonality of multidimension systems enables better understanding of the separation mechanism involved and separation efficiency.

REFERENCES

- (1) Adamczyk, B.; Tharmalingam, T.; Rudd, P. M. Glycans as cancer biomarkers. *Biochim Biophys Acta* **2012**, *1820* (9), 1347-1353. DOI: 10.1016/j.bbagen.2011.12.001 From NLM.
- (2) He, M.; Zhou, X.; Wang, X. Glycosylation: mechanisms, biological functions and clinical implications. *Signal Transduct Target Ther* **2024**, *9* (1), 194. DOI: 10.1038/s41392-024-01886-1 From NLM Medline.
- (3) Eggermont, L.; Lumen, N.; Van Praet, C.; Delanghe, J.; Rottey, S.; Vermassen, T. A comprehensive view of N-glycosylation as clinical biomarker in prostate cancer. *Biochim Biophys Acta Rev Cancer* **2025**, *1880* (1), 189239. DOI: 10.1016/j.bbcan.2024.189239 From NLM Medline.
- (4) An, H. J.; Miyamoto, S.; Lancaster, K. S.; Kirmiz, C.; Li, B.; Lam, K. S.; Leiserowitz, G. S.; Lebrilla, C. B. Profiling of glycans in serum for the discovery of potential biomarkers for ovarian cancer. *J Proteome Res* **2006**, *5* (7), 1626-1635. DOI: 10.1021/pr060010k From NLM Medline.
- (5) Taniguchi, N. Toward cancer biomarker discovery using the glycomics approach. *Proteomics* **2008**, *8* (16), 3205-3208. DOI: 10.1002/pmic.200890056 From NLM Medline.
- (6) Liu, L. Antibody glycosylation and its impact on the pharmacokinetics and pharmacodynamics of monoclonal antibodies and Fc-fusion proteins. *J Pharm Sci* **2015**, 104 (6), 1866-1884. DOI: 10.1002/jps.24444 From NLM.
- (7) Boune, S.; Hu, P.; Epstein, A. L.; Khawli, L. A. Principles of N-Linked Glycosylation Variations of IgG-Based Therapeutics: Pharmacokinetic and Functional Considerations. *Antibodies (Basel)* **2020**, *9* (2). DOI: 10.3390/antib9020022 From NLM.
- (8) Yehuda, S.; Padler-Karavani, V. Glycosylated Biotherapeutics: Immunological Effects of N-Glycolylneuraminic Acid. *Front Immunol* **2020**, *11*, 21. DOI: 10.3389/fimmu.2020.00021 From NLM Medline.
- (9) Ghaderi, D.; Taylor, R. E.; Padler-Karavani, V.; Diaz, S.; Varki, A. Implications of the presence of N-glycolylneuraminic acid in recombinant therapeutic glycoproteins. *Nat Biotechnol* **2010**, *28* (8), 863-867. DOI: 10.1038/nbt.1651 From NLM.
- (10) Wuhrer, M.; de Boer, A. R.; Deelder, A. M. Structural glycomics using hydrophilic interaction chromatography (HILIC) with mass spectrometry. *Mass Spectrom Rev* **2009**, 28 (2), 192-206. DOI: 10.1002/mas.20195 From NLM Medline.
- (11) Ahn, J.; Bones, J.; Yu, Y. Q.; Rudd, P. M.; Gilar, M. Separation of 2-aminobenzamide labeled glycans using hydrophilic interaction chromatography columns packed with 1.7μm sorbent. *Journal of Chromatography B* **2010**, 878 (3), 403-408. DOI: https://doi.org/10.1016/j.jchromb.2009.12.013.
- (12) Tao, S.; Huang, Y.; Boyes, B. E.; Orlando, R. Liquid Chromatography-Selected Reaction Monitoring (LC-SRM) Approach for the Separation and Quantitation of Sialylated N-Glycans Linkage Isomers. *Analytical Chemistry* **2014**, *86* (21), 10584-10590. DOI: 10.1021/ac5020996.

- (13) Veillon, L.; Huang, Y.; Peng, W.; Dong, X.; Cho, B. G.; Mechref, Y. Characterization of isomeric glycan structures by LC-MS/MS. *Electrophoresis* **2017**, *38* (17), 2100-2114. DOI: 10.1002/elps.201700042 From NLM.
- (14) Huang, Y.; Nie, Y.; Boyes, B.; Orlando, R. Resolving Isomeric Glycopeptide Glycoforms with Hydrophilic Interaction Chromatography (HILIC). *J Biomol Tech* **2016**, *27* (3), 98-104. DOI: 10.7171/jbt.16-2703-003 From NLM Medline.
- (15) Wang, X.; Li, W.; Li, Z.; Han, T.; Rong, J.; Fan, J.; Huang, L.; Lu, Y.; Wang, Z. Human milk whey glycoprotein N-glycans varied greatly among different maternal secretor status. *Carbohydr Polym* **2023**, *310*, 120728. DOI: 10.1016/j.carbpol.2023.120728 From NLM Medline.
- (16) van der Burgt, Y. E. M.; Siliakus, K. M.; Cobbaert, C. M.; Ruhaak, L. R. HILIC-MRM-MS for Linkage-Specific Separation of Sialylated Glycopeptides to Quantify Prostate-Specific Antigen Proteoforms. *J Proteome Res* **2020**, *19* (7), 2708-2716. DOI: 10.1021/acs.jproteome.0c00050 From NLM Medline.
- (17) Shang, T. Q.; Saati, A.; Toler, K. N.; Mo, J.; Li, H.; Matlosz, T.; Lin, X.; Schenk, J.; Ng, C. K.; Duffy, T.; et al. Development and application of a robust N-glycan profiling method for heightened characterization of monoclonal antibodies and related glycoproteins. *J Pharm Sci* **2014**, *103* (7), 1967-1978. DOI: 10.1002/jps.24004 From NLM Medline.
- (18) Shipman, J.; Sommers, C.; Keire, D. A.; Chen, K.; Zhu, H. Comprehensive N-Glycan Mapping using Parallel Reaction Monitoring LC-MS/MS. *Pharm Res* **2023**, *40* (6), 1399-1410. DOI: 10.1007/s11095-022-03453-1 From NLM Medline.
- (19) She, Y. M.; Dai, S.; Tam, R. Y. Highly sensitive characterization of non-human glycan structures of monoclonal antibody drugs utilizing tandem mass spectrometry. *Sci Rep* **2022**, *12* (1), 15109. DOI: 10.1038/s41598-022-19488-8 From NLM Medline.
- (20) Hofmann, J.; Hahm, H. S.; Seeberger, P. H.; Pagel, K. Identification of carbohydrate anomers using ion mobility–mass spectrometry. *Nature* **2015**, *526* (7572), 241-244. DOI: 10.1038/nature15388.
- (21) Jensen, P. H.; Karlsson, N. G.; Kolarich, D.; Packer, N. H. Structural analysis of N- and O-glycans released from glycoproteins. *Nat Protoc* **2012**, *7* (7), 1299-1310. DOI: 10.1038/nprot.2012.063 From NLM Medline.
- (22) Ruhaak, L. R.; Zauner, G.; Huhn, C.; Bruggink, C.; Deelder, A. M.; Wuhrer, M. Glycan labeling strategies and their use in identification and quantification. *Anal Bioanal Chem* **2010**, *397* (8), 3457-3481. DOI: 10.1007/s00216-010-3532-z From NLM Medline.
- (23) Lauber, M. A.; Yu, Y. Q.; Brousmiche, D. W.; Hua, Z.; Koza, S. M.; Magnelli, P.; Guthrie, E.; Taron, C. H.; Fountain, K. J. Rapid Preparation of Released N-Glycans for HILIC Analysis Using a Labeling Reagent that Facilitates Sensitive Fluorescence and ESI-MS Detection. *Anal Chem* **2015**, *87* (10), 5401-5409. DOI: 10.1021/acs.analchem.5b00758 From NLM Medline.
- (24) Zhou, S.; Veillon, L.; Dong, X.; Huang, Y.; Mechref, Y. Direct comparison of derivatization strategies for LC-MS/MS analysis of N-glycans. *Analyst* **2017**, *142* (23), 4446-4455. DOI: 10.1039/c7an01262d From NLM Medline.
- (25) Helali, Y.; Delporte, C. Updates of the current strategies of labeling for N-glycan analysis. *J Chromatogr B Analyt Technol Biomed Life Sci* **2024**, *1237*, 124068. DOI: 10.1016/j.jchromb.2024.124068 From NLM Medline.

- (26) Alley, W. R., Jr.; Novotny, M. V. Glycomic analysis of sialic acid linkages in glycans derived from blood serum glycoproteins. *J Proteome Res* **2010**, *9* (6), 3062-3072. DOI: 10.1021/pr901210r From NLM.
- (27) Pally, D.; Pramanik, D.; Hussain, S.; Verma, S.; Srinivas, A.; Kumar, R. V.; Everest-Dass, A.; Bhat, R. Heterogeneity in 2,6-Linked Sialic Acids Potentiates Invasion of Breast Cancer Epithelia. *ACS Central Science* **2021**, *7* (1), 110-125. DOI: 10.1021/acscentsci.0c00601.
- (28) Kinoshita, M.; Mitsui, Y.; Kakoi, N.; Yamada, K.; Hayakawa, T.; Kakehi, K. Common Glycoproteins Expressing Polylactosamine-Type Glycans on Matched Patient Primary and Metastatic Melanoma Cells Show Different Glycan Profiles. *Journal of Proteome Research* **2014**, *13* (2), 1021-1033. DOI: 10.1021/pr401015b.
- (29) Scott, D. A.; Casadonte, R.; Cardinali, B.; Spruill, L.; Mehta, A. S.; Carli, F.; Simone, N.; Kriegsmann, M.; Del Mastro, L.; Kriegsmann, J.; et al. Increases in Tumor N-Glycan Polylactosamines Associated with Advanced HER2-Positive and Triple-Negative Breast Cancer Tissues. *Proteomics Clin Appl* **2019**, *13* (1), e1800014. DOI: 10.1002/prca.201800014 From NLM.
- (30) Townsend, R. R.; Hardy, M. R.; Cumming, D. A.; Carver, J. P.; Bendiak, B. Separation of branched sialylated oligosaccharides using high-pH anion-exchange chromatography with pulsed amperometric detection. *Anal Biochem* **1989**, *182* (1), 1-8. DOI: 10.1016/0003-2697(89)90708-2 From NLM.
- (31) Nishikaze, T.; Tsumoto, H.; Sekiya, S.; Iwamoto, S.; Miura, Y.; Tanaka, K. Differentiation of Sialyl Linkage Isomers by One-Pot Sialic Acid Derivatization for Mass Spectrometry-Based Glycan Profiling. *Anal Chem* **2017**, *89* (4), 2353-2360. DOI: 10.1021/acs.analchem.6b04150 From NLM.
- (32) Wang, Q.; Yin, B.; Chung, C. Y.; Betenbaugh, M. J. Glycoengineering of CHO Cells to Improve Product Quality. *Methods Mol Biol* **2017**, *1603*, 25-44. DOI: 10.1007/978-1-4939-6972-2 2 From NLM.
- (33) Yang, G.; Hu, Y.; Sun, S.; Ouyang, C.; Yang, W.; Wang, Q.; Betenbaugh, M.; Zhang, H. Comprehensive Glycoproteomic Analysis of Chinese Hamster Ovary Cells. *Anal Chem* **2018**, *90* (24), 14294-14302. DOI: 10.1021/acs.analchem.8b03520 From NLM.
- (34) Chung, C. H.; Mirakhur, B.; Chan, E.; Le, Q. T.; Berlin, J.; Morse, M.; Murphy, B. A.; Satinover, S. M.; Hosen, J.; Mauro, D.; et al. Cetuximab-induced anaphylaxis and IgE specific for galactose-alpha-1,3-galactose. *N Engl J Med* **2008**, *358* (11), 1109-1117. DOI: 10.1056/NEJMoa074943 From NLM.
- (35) Zhao, S.; Walsh, I.; Abrahams, J. L.; Royle, L.; Nguyen-Khuong, T.; Spencer, D.; Fernandes, D. L.; Packer, N. H.; Rudd, P. M.; Campbell, M. P. GlycoStore: a database of retention properties for glycan analysis. *Bioinformatics* **2018**, *34* (18), 3231-3232. DOI: 10.1093/bioinformatics/bty319 From NLM.
- (36) Struwe, W. B.; Pagel, K.; Benesch, J. L. P.; Harvey, D. J.; Campbell, M. P. GlycoMob: an ion mobility-mass spectrometry collision cross section database for glycomics. *Glycoconjugate Journal* **2016**, *33* (3), 399-404. DOI: 10.1007/s10719-015-9613-7.
- (37) Wang, X.; Stoll, D. R.; Schellinger, A. P.; Carr, P. W. Peak capacity optimization of peptide separations in reversed-phase gradient elution chromatography: fixed column format. *Anal Chem* **2006**, 78 (10), 3406-3416. DOI: 10.1021/ac0600149 From NLM.
- (38) Neue, U. D. Theory of peak capacity in gradient elution. *Journal of Chromatography A* **2005**, *1079* (1), 153-161. DOI: https://doi.org/10.1016/j.chroma.2005.03.008.

- (39) Baker, E. S.; Livesay, E. A.; Orton, D. J.; Moore, R. J.; Danielson, W. F., 3rd; Prior, D. C.; Ibrahim, Y. M.; LaMarche, B. L.; Mayampurath, A. M.; Schepmoes, A. A.; et al. An LC-IMS-MS platform providing increased dynamic range for high-throughput proteomic studies. *J Proteome Res* **2010**, *9* (2), 997-1006. DOI: 10.1021/pr900888b From NLM.
- (40) Manz, C.; Mancera-Arteu, M.; Zappe, A.; Hanozin, E.; Polewski, L.; Giménez, E.; Sanz-Nebot, V.; Pagel, K. Determination of Sialic Acid Isomers from Released N-Glycans Using Ion Mobility Spectrometry. *Analytical Chemistry* **2022**, *94* (39), 13323-13331. DOI: 10.1021/acs.analchem.2c00783.
- (41) Rister, A. L.; Dodds, E. D. Liquid chromatography-ion mobility spectrometry-mass spectrometry analysis of multiple classes of steroid hormone isomers in a mixture. *J Chromatogr B Analyt Technol Biomed Life Sci* **2020**, *1137*, 121941. DOI: 10.1016/j.jchromb.2019.121941 From NLM.
- (42) He, M.; Zhou, X.; Wang, X. Glycosylation: mechanisms, biological functions and clinical implications. *Signal Transduction and Targeted Therapy* **2024**, *9* (1), 194. DOI: 10.1038/s41392-024-01886-1.
- (43) Esmail, S.; Manolson, M. F. Advances in understanding N-glycosylation structure, function, and regulation in health and disease. *Eur J Cell Biol* **2021**, *100* (7-8), 151186. DOI: 10.1016/j.ejcb.2021.151186 From NLM Medline.
- (44) Radovani, B.; Gudelj, I. N-Glycosylation and Inflammation; the Not-So-Sweet Relation. *Front Immunol* **2022**, *13*, 893365. DOI: 10.3389/fimmu.2022.893365 From NLM Medline.
- (45) Schjoldager, K. T.; Narimatsu, Y.; Joshi, H. J.; Clausen, H. Global view of human protein glycosylation pathways and functions. *Nature Reviews Molecular Cell Biology* **2020**, *21* (12), 729-749. DOI: 10.1038/s41580-020-00294-x.
- (46) Reily, C.; Stewart, T. J.; Renfrow, M. B.; Novak, J. Glycosylation in health and disease. *Nature Reviews Nephrology* **2019**, *15* (6), 346-366. DOI: 10.1038/s41581-019-0129-4.
- (47) Stanley, P.; Moremen, K. W.; Lewis, N. E.; Taniguchi, N.; Aebi, M. N-Glycans. In *Essentials of Glycobiology*, 4th ed.; Varki, A., Cummings, R. D., Esko, J. D., Stanley, P., Hart, G. W., Aebi, M., Mohnen, D., Kinoshita, T., Packer, N. H., Prestegard, J. H., et al. Eds.; 2022; pp 103-116.
- (48) Bieberich, E. Synthesis, Processing, and Function of N-glycans in N-glycoproteins. *Adv Neurobiol* **2014**, *9*, 47-70. DOI: 10.1007/978-1-4939-1154-7_3 From NLM PubMednot-MEDLINE.
- (49) Fiedler, K.; Simons, K. The role of N-glycans in the secretory pathway. *Cell* **1995**, *81* (3), 309-312. DOI: 10.1016/0092-8674(95)90380-1 From NLM Medline.
- (50) Rini, J.; Esko, J.; Varki, A. Glycosyltransferases and Glycan-processing Enzymes. In *Essentials of Glycobiology*, 2nd ed.; Varki, A., Cummings, R. D., Esko, J. D., Freeze, H. H., Stanley, P., Bertozzi, C. R., Hart, G. W., Etzler, M. E. Eds.; 2009.
- (51) Pang, X.; Li, H.; Guan, F.; Li, X. Multiple Roles of Glycans in Hematological Malignancies. *Front Oncol* **2018**, *8*, 364. DOI: 10.3389/fonc.2018.00364 From NLM.
- (52) Amon, R.; Reuven, E. M.; Leviatan Ben-Arye, S.; Padler-Karavani, V. Glycans in immune recognition and response. *Carbohydrate Research* **2014**, *389*, 115-122. DOI: https://doi.org/10.1016/j.carres.2014.02.004.
- (53) Dobie, C.; Skropeta, D. Insights into the role of sialylation in cancer progression and metastasis. *British Journal of Cancer* **2021**, *124* (1), 76-90. DOI: 10.1038/s41416-020-01126-7.

- (54) Stanley, P.; Cummings, R. D. Structures Common to Different Glycans. In *Essentials of Glycobiology*, 3rd ed.; Varki, A., Cummings, R. D., Esko, J. D., Stanley, P., Hart, G. W., Aebi, M., Darvill, A. G., Kinoshita, T., Packer, N. H., Prestegard, J. H., et al. Eds.; 2015; pp 161-178.
- (55) Muchmore, E. A.; Milewski, M.; Varki, A.; Diaz, S. Biosynthesis of N-glycolyneuraminic acid. The primary site of hydroxylation of N-acetylneuraminic acid is the cytosolic sugar nucleotide pool. *J Biol Chem* **1989**, *264* (34), 20216-20223. From NLM.
- (56) Chou, H. H.; Takematsu, H.; Diaz, S.; Iber, J.; Nickerson, E.; Wright, K. L.; Muchmore, E. A.; Nelson, D. L.; Warren, S. T.; Varki, A. A mutation in human CMP-sialic acid hydroxylase occurred after the Homo-Pan divergence. *Proc Natl Acad Sci U S A* **1998**, *95* (20), 11751-11756. DOI: 10.1073/pnas.95.20.11751 From NLM.
- (57) Altman, M. O.; Gagneux, P. Absence of Neu5Gc and Presence of Anti-Neu5Gc Antibodies in Humans-An Evolutionary Perspective. *Front Immunol* **2019**, *10*, 789. DOI: 10.3389/fimmu.2019.00789 From NLM.
- (58) Zhu, A.; Hurst, R. Anti-N-glycolylneuraminic acid antibodies identified in healthy human serum. *Xenotransplantation* **2002**, *9* (6), 376-381. DOI: 10.1034/j.1399-3089.2002.02138.x From NLM.
- (59) Fischler, D. A.; Orlando, R. N-linked Glycan Release Efficiency: A Quantitative Comparison between NaOCl and PNGase F Release Protocols. *J Biomol Tech* **2019**, *30* (4), 58-63. DOI: 10.7171/jbt.19-3004-001 From NLM.
- (60) Figl, R.; Altmann, F. Reductive Alkaline Release of N-Glycans Generates a Variety of Unexpected, Useful Products. *Proteomics* **2018**, *18* (3-4). DOI: 10.1002/pmic.201700330 From NLM.
- (61) Patel, T.; Bruce, J.; Merry, A.; Bigge, C.; Wormald, M.; Parekh, R.; Jaques, A. Use of hydrazine to release in intact and unreduced form both N- and O-linked oligosaccharides from glycoproteins. *Biochemistry* **1993**, *32* (2), 679-693. DOI: 10.1021/bi00053a037.
- (62) Muramatsu, H.; Tachikui, H.; Ushida, H.; Song, X.; Qiu, Y.; Yamamoto, S.; Muramatsu, T. Molecular cloning and expression of endo-beta-N-acetylglucosaminidase D, which acts on the core structure of complex type asparagine-linked oligosaccharides. *J Biochem* **2001**, *129* (6), 923-928. DOI: 10.1093/oxfordjournals.jbchem.a002938 From NLM.
- (63) Kurz, S.; Sheikh, M. O.; Lu, S.; Wells, L.; Tiemeyer, M. Separation and Identification of Permethylated Glycan Isomers by Reversed Phase NanoLC-NSI-MSn. *Molecular & Cellular Proteomics* **2021**, *20*, 100045. DOI: https://doi.org/10.1074/mcp.RA120.002266.
- (64) Zhou, S.; Dong, X.; Veillon, L.; Huang, Y.; Mechref, Y. LC-MS/MS analysis of permethylated N-glycans facilitating isomeric characterization. *Analytical and Bioanalytical Chemistry* **2017**, *409* (2), 453-466. DOI: 10.1007/s00216-016-9996-8.
- (65) Purdie, T.; Irvine, J. C. C.—The alkylation of sugars. *Journal of the Chemical Society, Transactions* **1903**, *83* (0), 1021-1037, 10.1039/CT9038301021. DOI: 10.1039/CT9038301021.
- (66) Ciucanu, I.; Kerek, F. A simple and rapid method for the permethylation of carbohydrates. *Carbohydrate Research* **1984**, *131* (2), 209-217. DOI: https://doi.org/10.1016/0008-6215(84)85242-8.
- (67) Dong, X.; Mondello, S.; Kobeissy, F.; Talih, F.; Ferri, R.; Mechref, Y. LC-MS/MS glycomics of idiopathic rapid eye movement sleep behavior disorder. *Electrophoresis* **2018**, *39* (24), 3096-3103. DOI: 10.1002/elps.201800316 From NLM.

- (68) Tsai, T.-H.; Wang, M.; Di Poto, C.; Hu, Y.; Zhou, S.; Zhao, Y.; Varghese, R. S.; Luo, Y.; Tadesse, M. G.; Ziada, D. H.; et al. LC–MS Profiling of N-Glycans Derived from Human Serum Samples for Biomarker Discovery in Hepatocellular Carcinoma. *Journal of Proteome Research* **2014**, *13* (11), 4859-4868. DOI: 10.1021/pr500460k.
- (69) Peng, W.; Goli, M.; Mirzaei, P.; Mechref, Y. Revealing the Biological Attributes of N-Glycan Isomers in Breast Cancer Brain Metastasis Using Porous Graphitic Carbon (PGC) Liquid Chromatography-Tandem Mass Spectrometry (LC-MS/MS). *Journal of Proteome Research* **2019**, *18* (10), 3731-3740. DOI: 10.1021/acs.jproteome.9b00429.
- (70) Zhou, S.; Huang, Y.; Dong, X.; Peng, W.; Veillon, L.; Kitagawa, D. A. S.; Aquino, A. J. A.; Mechref, Y. Isomeric Separation of Permethylated Glycans by Porous Graphitic Carbon (PGC)-LC-MS/MS at High Temperatures. *Analytical Chemistry* **2017**, *89* (12), 6590-6597. DOI: 10.1021/acs.analchem.7b00747.
- (71) Guillard, M.; Gloerich, J.; Wessels, H. J. C. T.; Morava, E.; Wevers, R. A.; Lefeber, D. J. Automated measurement of permethylated serum N-glycans by MALDI–linear ion trap mass spectrometry. *Carbohydrate Research* **2009**, *344* (12), 1550-1557. DOI: https://doi.org/10.1016/j.carres.2009.06.010.
- (72) Sundaram, S.; Alice, M.; Jun, Q.; Jingming, Z.; Ming-Ching, H.; Tun, L.; Richard, C.; Babita, P.; and Zhou, Q. An innovative approach for the characterization of the isoforms of a monoclonal antibody product. *mAbs* **2011**, *3* (6), 505-512. DOI: 10.4161/mabs.3.6.18090.
- (73) Stumpo, K. A.; Reinhold, V. N. The N-Glycome of Human Plasma. *Journal of Proteome Research* **2010**, *9* (9), 4823-4830. DOI: 10.1021/pr100528k.
- (74) Jennings, K. R.; Dolnikowski, G. G. [2] Mass analyzers. In *Methods in Enzymology*, Vol. 193; Academic Press, 1990; pp 37-61.
- (75) Haag, A. M. Mass Analyzers and Mass Spectrometers. In *Modern Proteomics Sample Preparation, Analysis and Practical Applications*, Mirzaei, H., Carrasco, M. Eds.; Springer International Publishing, 2016; pp 157-169.
- (76) MS Detectors. Analytical Chemistry 2005, 77 (21), 418 A-427 A. DOI: 10.1021/ac053495p.
- (77) Pabst, M.; Altmann, F. Glycan analysis by modern instrumental methods. *Proteomics* **2011**, *11* (4), 631-643. DOI: 10.1002/pmic.201000517 From NLM.
- (78) Harvey, D. J. Ionization and collision-induced fragmentation of N-linked and related carbohydrates using divalent cations. *Journal of the American Society for Mass Spectrometry* **2001**, *12* (8), 926-937. DOI: 10.1016/S1044-0305(01)00268-9.
- (79) Harvey, D. J. Collision-induced fragmentation of underivatized N-linked carbohydrates ionized by electrospray. *J Mass Spectrom* **2000**, *35* (10), 1178-1190. DOI: 10.1002/1096-9888(200010)35:10<1178::Aid-jms46>3.0.Co;2-f From NLM.
- (80) Zhao, C.; Xie, B.; Chan, S.-Y.; Costello, C. E.; O'Connor, P. B. Collisionally activated dissociation and electron capture dissociation provide complementary structural information for branched permethylated oligosaccharides. *Journal of the American Society for Mass Spectrometry* **2008**, *19* (1), 138-150. DOI: 10.1016/j.jasms.2007.10.022.
- (81) Han, L.; Costello, C. E. Electron Transfer Dissociation of Milk Oligosaccharides. *Journal of the American Society for Mass Spectrometry* **2011**, *22* (6), 997-1013. DOI: 10.1007/s13361-011-0117-9.
- (82) Kayili, H. M. Identification of bisecting N-glycans in tandem mass spectra using a procainamide labeling approach for in-depth N-glycan profiling of biological samples.

- International Journal of Mass Spectrometry **2020**, 457, 116412. DOI: https://doi.org/10.1016/j.ijms.2020.116412.
- (83) Prien, J. M.; Ashline, D. J.; Lapadula, A. J.; Zhang, H.; Reinhold, V. N. The high mannose glycans from bovine ribonuclease B isomer characterization by ion trap MS. *J Am Soc Mass Spectrom* **2009**, *20* (4), 539-556. DOI: 10.1016/j.jasms.2008.11.012 From NLM.
- (84) Han, L.; Costello, C. E. Mass spectrometry of glycans. *Biochemistry (Mosc)* **2013**, *78* (7), 710-720. DOI: 10.1134/s0006297913070031 From NLM.
- (85) Leymarie, N.; Zaia, J. Effective Use of Mass Spectrometry for Glycan and Glycopeptide Structural Analysis. *Analytical Chemistry* **2012**, *84* (7), 3040-3048. DOI: 10.1021/ac3000573.
- (86) Hosseini, S.; Martinez-Chapa, S. O. Principles and Mechanism of MALDI-ToF-MS Analysis. In *Fundamentals of MALDI-ToF-MS Analysis: Applications in Bio-diagnosis, Tissue Engineering and Drug Delivery*, Hosseini, S., Martinez-Chapa, S. O. Eds.; Springer Singapore, 2017; pp 1-19.
- (87) Reiding, K. R.; Blank, D.; Kuijper, D. M.; Deelder, A. M.; Wuhrer, M. High-Throughput Profiling of Protein N-Glycosylation by MALDI-TOF-MS Employing Linkage-Specific Sialic Acid Esterification. *Analytical Chemistry* **2014**, *86* (12), 5784-5793. DOI: 10.1021/ac500335t.
- (88) Lee, J. W.; Lee, K.; Ahn, S. H.; Son, B. H.; Ko, B. S.; Kim, H. J.; Chung, I. Y.; Kim, J.; Lee, W.; Ko, M.-S.; et al. Potential of MALDI-TOF-based serum N-glycan analysis for the diagnosis and surveillance of breast cancer. *Scientific Reports* **2020**, *10* (1), 19136. DOI: 10.1038/s41598-020-76195-y.
- (89) Vreeker, G. C. M.; Bladergroen, M. R.; Nicolardi, S.; Mesker, W. E.; Tollenaar, R. A. E. M.; van der Burgt, Y. E. M.; Wuhrer, M. Dried blood spot N-glycome analysis by MALDI mass spectrometry. *Talanta* **2019**, *205*, 120104. DOI: https://doi.org/10.1016/j.talanta.2019.06.104.
- (90) Drake, R. R.; Powers, T. W.; Jones, E. E.; Bruner, E.; Mehta, A. S.; Angel, P. M. Chapter Four MALDI Mass Spectrometry Imaging of N-Linked Glycans in Cancer Tissues. In *Advances in Cancer Research*, Drake, R. R., McDonnell, L. A. Eds.; Vol. 134; Academic Press, 2017; pp 85-116.
- (91) Duncan, M.; DeMarco, M. L. MALDI-MS: Emerging roles in pathology and laboratory medicine. *Clin Mass Spectrom* **2019**, *13*, 1-4. DOI: 10.1016/j.clinms.2019.05.003 From NLM.
- (92) Ho, C. S.; Lam, C. W.; Chan, M. H.; Cheung, R. C.; Law, L. K.; Lit, L. C.; Ng, K. F.; Suen, M. W.; Tai, H. L. Electrospray ionisation mass spectrometry: principles and clinical applications. *Clin Biochem Rev* **2003**, *24* (1), 3-12. From NLM.
- (93) Stadlmann, J.; Pabst, M.; Kolarich, D.; Kunert, R.; Altmann, F. Analysis of immunoglobulin glycosylation by LC-ESI-MS of glycopeptides and oligosaccharides. *Proteomics* **2008**, *8* (14), 2858-2871. DOI: 10.1002/pmic.200700968 From NLM.
- (94) Zhang, Y.; Zhu, J.; Yin, H.; Marrero, J.; Zhang, X.-X.; Lubman, D. M. ESI–LC–MS Method for Haptoglobin Fucosylation Analysis in Hepatocellular Carcinoma and Liver Cirrhosis. *Journal of Proteome Research* **2015**, *14* (12), 5388-5395. DOI: 10.1021/acs.jproteome.5b00792.
- (95) Lageveen-Kammeijer, G. S. M.; de Haan, N.; Mohaupt, P.; Wagt, S.; Filius, M.; Nouta, J.; Falck, D.; Wuhrer, M. Highly sensitive CE-ESI-MS analysis of N-glycans from complex

- biological samples. *Nature Communications* **2019**, *10* (1), 2137. DOI: 10.1038/s41467-019-09910-7.
- (96) Liu, H.; Zhang, N.; Wan, D.; Cui, M.; Liu, Z.; Liu, S. Mass spectrometry-based analysis of glycoproteins and its clinical applications in cancer biomarker discovery. *Clinical Proteomics* **2014**, *11* (1), 14. DOI: 10.1186/1559-0275-11-14.
- (97) Weiskopf, A. S.; Vouros, P.; Harvey, D. J. Electrospray ionization-ion trap mass spectrometry for structural analysis of complex N-linked glycoprotein oligosaccharides. *Anal Chem* **1998**, *70* (20), 4441-4447. DOI: 10.1021/ac980289r From NLM.
- (98) Su, Z.; Xie, Q.; Wang, Y.; Li, Y. Abberant Immunoglobulin G Glycosylation in Rheumatoid Arthritis by LTQ-ESI-MS. In *International Journal of Molecular Sciences*, 2020; Vol. 21.
- (99) March, R. E. An Introduction to Quadrupole Ion Trap Mass Spectrometry. *Journal of Mass Spectrometry* **1997**, *32*, 351-369.
- (100) Douglas, D. J.; Frank, A. J.; Mao, D. Linear ion traps in mass spectrometry. *Mass Spectrom Rev* **2005**, *24* (1), 1-29. DOI: 10.1002/mas.20004 From NLM.
- (101) Marshall, A. G.; Hendrickson, C. L.; Jackson, G. S. Fourier transform ion cyclotron resonance mass spectrometry: a primer. *Mass Spectrom Rev* **1998**, *17* (1), 1-35. DOI: 10.1002/(sici)1098-2787(1998)17:1<1::Aid-mas1>3.0.Co;2-k From NLM.
- (102) Nolting, D.; Malek, R.; Makarov, A. Ion traps in modern mass spectrometry. *Mass Spectrom Rev* **2019**, *38* (2), 150-168. DOI: 10.1002/mas.21549 From NLM.
- (103) Zubarev, R. A.; Makarov, A. Orbitrap Mass Spectrometry. *Analytical Chemistry* **2013**, *85* (11), 5288-5296. DOI: 10.1021/ac4001223.
- (104) Ruhaak, L. R.; Xu, G.; Li, Q.; Goonatilleke, E.; Lebrilla, C. B. Mass Spectrometry Approaches to Glycomic and Glycoproteomic Analyses. *Chem Rev* **2018**, *118* (17), 7886-7930. DOI: 10.1021/acs.chemrev.7b00732 From NLM.
- (105) Miller, P. E.; Denton, M. B. The quadrupole mass filter: Basic operating concepts. *Journal of Chemical Education* **1986**, *63* (7), 617. DOI: 10.1021/ed063p617.
- (106) Tsakalof, A.; Sysoev, A. A.; Vyatkina, K. V.; Eganov, A. A.; Eroshchenko, N. N.; Kiryushin, A. N.; Adamov, A. Y.; Danilova, E. Y.; Nosyrev, A. E. Current Role and Potential of Triple Quadrupole Mass Spectrometry in Biomedical Research and Clinical Applications. In *Molecules*, 2024; Vol. 29.
- (107) Mamyrin, B. A. Time-of-flight mass spectrometry (concepts, achievements, and prospects). *International Journal of Mass Spectrometry* **2001**, *206* (3), 251-266. DOI: https://doi.org/10.1016/S1387-3806(00)00392-4.
- (108) Silsirivanit, A.; Alvarez, M. R. S.; Grijaldo-Alvarez, S. J.; Gogte, R.; Kitkhuandee, A.; Piyawattanametha, N.; Seubwai, W.; Luang, S.; Panawan, O.; Mahalapbutr, P.; et al. Serum N-Glycomics with Nano-LC-QToF LC-MS/MS Reveals N-Glycan Biomarkers for Glioblastoma, Meningioma, and High-Grade Meningioma. *J Proteome Res* **2025**, *24* (3), 1402-1413. DOI: 10.1021/acs.jproteome.4c01090 From NLM.
- (109) Sagi, D.; Peter-Katalinic, J.; Conradt, H. S.; Nimtz, M. Sequencing of tri- and tetraantennary N-glycans containing sialic acid by negative mode ESI QTOF tandem MS. *Journal of the American Society for Mass Spectrometry* **2002**, *13* (9), 1138-1148. DOI: 10.1016/S1044-0305(02)00412-9.
- (110) Martin, A. J.; Synge, R. L. A new form of chromatogram employing two liquid phases: A theory of chromatography. 2. Application to the micro-determination of the higher

- monoamino-acids in proteins. *Biochem J* **1941**, *35* (12), 1358-1368. DOI: 10.1042/bj0351358 From NLM.
- (111) van Deemter, J. J.; Zuiderweg, F. J.; Klinkenberg, A. Longitudinal diffusion and resistance to mass transfer as causes of nonideality in chromatography. *Chemical Engineering Science* **1995**, *50* (24), 3869-3882. DOI: https://doi.org/10.1016/0009-2509(96)81813-6.
- (112) Gritti, F.; Guiochon, G. Diffusion models in chromatographic columns packed with fully and superficially porous particles. *Chemical Engineering Science* **2011**, *66* (17), 3773-3781. DOI: https://doi.org/10.1016/j.ces.2011.04.039.
- (113) Striegel, A. M. Longitudinal diffusion in size-exclusion chromatography: a stop-flow size-exclusion chromatography study. *Journal of Chromatography A* **2001**, *932* (1), 21-31. DOI: https://doi.org/10.1016/S0021-9673(01)01214-6.
- (114) Vreeker, G. C.; Wuhrer, M. Reversed-phase separation methods for glycan analysis. *Anal Bioanal Chem* **2017**, *409* (2), 359-378. DOI: 10.1007/s00216-016-0073-0 From NLM.
- (115) Dong, X.; Zhou, S.; Mechref, Y. LC-MS/MS analysis of permethylated free oligosaccharides and N-glycans derived from human, bovine, and goat milk samples. *Electrophoresis* **2016**, *37* (11), 1532-1548. DOI: 10.1002/elps.201500561 From NLM.
- (116) Hu, Y.; Zhou, S.; Khalil, S. I.; Renteria, C. L.; Mechref, Y. Glycomic profiling of tissue sections by LC-MS. *Anal Chem* **2013**, *85* (8), 4074-4079. DOI: 10.1021/ac400106x From NLM.
- (117) Zhou, S.; Hu, Y.; DeSantos-Garcia, J. L.; Mechref, Y. Quantitation of permethylated N-glycans through multiple-reaction monitoring (MRM) LC-MS/MS. *J Am Soc Mass Spectrom* **2015**, *26* (4), 596-603. DOI: 10.1007/s13361-014-1054-1 From NLM Medline.
- (118) West, C.; Elfakir, C.; Lafosse, M. Porous graphitic carbon: A versatile stationary phase for liquid chromatography. *Journal of Chromatography A* **2010**, *1217* (19), 3201-3216. DOI: https://doi.org/10.1016/j.chroma.2009.09.052.
- (119) Kawasaki, N.; Ohta, M.; Hyuga, S.; Hashimoto, O.; Hayakawa, T. Analysis of Carbohydrate Heterogeneity in a Glycoprotein Using Liquid Chromatography/Mass Spectrometry and Liquid Chromatography with Tandem Mass Spectrometry. *Analytical Biochemistry* **1999**, *269* (2), 297-303. DOI: https://doi.org/10.1006/abio.1999.4026.
- (120) Abrahams, J. L.; Campbell, M. P.; Packer, N. H. Building a PGC-LC-MS N-glycan retention library and elution mapping resource. *Glycoconjugate Journal* **2018**, *35* (1), 15-29. DOI: 10.1007/s10719-017-9793-4.
- (121) Bapiro, T. E.; Richards, F. M.; Jodrell, D. I. Understanding the Complexity of Porous Graphitic Carbon (PGC) Chromatography: Modulation of Mobile-Stationary Phase Interactions Overcomes Loss of Retention and Reduces Variability. *Anal Chem* **2016**, *88* (12), 6190-6194. DOI: 10.1021/acs.analchem.6b01167 From NLM.
- (122) Alpert, A. J. Hydrophilic-interaction chromatography for the separation of peptides, nucleic acids and other polar compounds. *Journal of Chromatography A* **1990**, 499, 177-196. DOI: https://doi.org/10.1016/S0021-9673(00)96972-3.
- (123) Dodds, J. N.; Baker, E. S. Ion Mobility Spectrometry: Fundamental Concepts, Instrumentation, Applications, and the Road Ahead. *J Am Soc Mass Spectrom* **2019**, *30* (11), 2185-2195. DOI: 10.1007/s13361-019-02288-2 From NLM.
- (124) Stow, S. M.; Causon, T. J.; Zheng, X.; Kurulugama, R. T.; Mairinger, T.; May, J. C.; Rennie, E. E.; Baker, E. S.; Smith, R. D.; McLean, J. A.; et al. An Interlaboratory Evaluation of Drift Tube Ion Mobility–Mass Spectrometry Collision Cross Section

- Measurements. *Analytical Chemistry* **2017**, *89* (17), 9048-9055. DOI: 10.1021/acs.analchem.7b01729.
- (125) Li, A.; Conant, C. R.; Zheng, X.; Bloodsworth, K. J.; Orton, D. J.; Garimella, S. V. B.; Attah, I. K.; Nagy, G.; Smith, R. D.; Ibrahim, Y. M. Assessing Collision Cross Section Calibration Strategies for Traveling Wave-Based Ion Mobility Separations in Structures for Lossless Ion Manipulations. *Anal Chem* **2020**, *92* (22), 14976-14982. DOI: 10.1021/acs.analchem.0c02829 From NLM.
- (126) Hynds, H. M.; Hines, K. M. MOCCal: A Multiomic CCS Calibrator for Traveling Wave Ion Mobility Mass Spectrometry. *Analytical Chemistry* **2024**, *96* (3), 1185-1194. DOI: 10.1021/acs.analchem.3c04290.
- (127) Liu, Y.; Clemmer, D. E. Characterizing Oligosaccharides Using Injected-Ion Mobility/Mass Spectrometry. *Analytical Chemistry* **1997**, *69* (13), 2504-2509. DOI: 10.1021/ac9701344.
- (128) Hofmann, J.; Pagel, K. Glycan Analysis by Ion Mobility-Mass Spectrometry. *Angew Chem Int Ed Engl* **2017**, *56* (29), 8342-8349. DOI: 10.1002/anie.201701309 From NLM.
- (129) Barroso, A.; Giménez, E.; Konijnenberg, A.; Sancho, J.; Sanz-Nebot, V.; Sobott, F. Evaluation of ion mobility for the separation of glycoconjugate isomers due to different types of sialic acid linkage, at the intact glycoprotein, glycopeptide and glycan level. *Journal of Proteomics* **2018**, *173*, 22-31. DOI: https://doi.org/10.1016/j.jprot.2017.11.020.
- (130) Manz, C.; Pagel, K. Glycan analysis by ion mobility-mass spectrometry and gas-phase spectroscopy. *Current Opinion in Chemical Biology* **2018**, *42*, 16-24. DOI: https://doi.org/10.1016/j.cbpa.2017.10.021.
- (131) Ben Faleh, A.; Warnke, S.; Bansal, P.; Pellegrinelli, R. P.; Dyukova, I.; Rizzo, T. R. Identification of Mobility-Resolved N-Glycan Isomers. *Analytical Chemistry* **2022**, *94* (28), 10101-10108. DOI: 10.1021/acs.analchem.2c01181.
- (132) Deng, L.; Ibrahim, Y. M.; Baker, E. S.; Aly, N. A.; Hamid, A. M.; Zhang, X.; Zheng, X.; Garimella, S. V. B.; Webb, I. K.; Prost, S. A.; et al. Ion Mobility Separations of Isomers based upon Long Path Length Structures for Lossless Ion Manipulations Combined with Mass Spectrometry. *ChemistrySelect* **2016**, *1* (10), 2396-2399. DOI: 10.1002/slct.201600460 From NLM.
- (133) Deng, L.; Ibrahim, Y. M.; Hamid, A. M.; Garimella, S. V.; Webb, I. K.; Zheng, X.; Prost, S. A.; Sandoval, J. A.; Norheim, R. V.; Anderson, G. A.; et al. Ultra-High Resolution Ion Mobility Separations Utilizing Traveling Waves in a 13 m Serpentine Path Length Structures for Lossless Ion Manipulations Module. *Anal Chem* **2016**, *88* (18), 8957-8964. DOI: 10.1021/acs.analchem.6b01915 From NLM.
- (134) Dyukova, I.; Ben Faleh, A.; Warnke, S.; Yalovenko, N.; Yatsyna, V.; Bansal, P.; Rizzo, T. R. A new approach for identifying positional isomers of glycans cleaved from monoclonal antibodies. *Analyst* **2021**, *146* (15), 4789-4795. DOI: 10.1039/d1an00780g From NLM.
- (135) Li, X.; Xu, Z.; Hong, X.; Zhang, Y.; Zou, X. Databases and Bioinformatic Tools for Glycobiology and Glycoproteomics. *Int J Mol Sci* **2020**, *21* (18). DOI: 10.3390/ijms21186727 From NLM.
- (136) Doubet, S.; Bock, K.; Smith, D.; Darvill, A.; Albersheim, P. The Complex Carbohydrate Structure Database. *Trends Biochem Sci* **1989**, *14* (12), 475-477. DOI: 10.1016/0968-0004(89)90175-8 From NLM.

- (137) Egorova, K. S.; Toukach, P. V. Carbohydrate Structure Database (CSDB): Examples of Usage. In *A Practical Guide to Using Glycomics Databases*, Aoki-Kinoshita, K. F. Ed.; Springer Japan, 2017; pp 75-113.
- (138) Kameyama, A.; Kikuchi, N.; Nakaya, S.; Ito, H.; Sato, T.; Shikanai, T.; Takahashi, Y.; Takahashi, K.; Narimatsu, H. A Strategy for Identification of Oligosaccharide Structures Using Observational Multistage Mass Spectral Library. *Analytical Chemistry* **2005**, 77 (15), 4719-4725. DOI: 10.1021/ac048350h.
- (139) Crowell, K. L.; Baker, E. S.; Payne, S. H.; Ibrahim, Y. M.; Monroe, M. E.; Slysz, G. W.; LaMarche, B. L.; Petyuk, V. A.; Piehowski, P. D.; Danielson, W. F., 3rd; et al. Increasing Confidence of LC-MS Identifications by Utilizing Ion Mobility Spectrometry. *Int J Mass Spectrom* **2013**, *354-355*, 312-317. DOI: 10.1016/j.ijms.2013.06.028 From NLM.
- (140) Wehr, T. Multidimensional liquid chromatography in proteomic studies. *LC GC Europe* **2003**, *16*, 154.
- (141) Evans, C. R.; Jorgenson, J. W. Multidimensional LC-LC and LC-CE for high-resolution separations of biological molecules. *Analytical and Bioanalytical Chemistry* **2004**, *378* (8), 1952-1961. DOI: 10.1007/s00216-004-2516-2.
- (142) Washburn, M. P.; Wolters, D.; Yates, J. R. Large-scale analysis of the yeast proteome by multidimensional protein identification technology. *Nature Biotechnology* **2001**, *19* (3), 242-247. DOI: 10.1038/85686.
- (143) Gilar, M.; Fridrich, J.; Schure, M. R.; Jaworski, A. Comparison of Orthogonality Estimation Methods for the Two-Dimensional Separations of Peptides. *Analytical Chemistry* **2012**, *84* (20), 8722-8732. DOI: 10.1021/ac3020214.
- (144) Schure, M. R.; Davis, J. M. Orthogonality measurements for multidimensional chromatography in three and higher dimensional separations. *J Chromatogr A* **2017**, *1523*, 148-161. DOI: 10.1016/j.chroma.2017.06.036 From NLM.
- (145) Gilar, M.; Olivova, P.; Daly, A. E.; Gebler, J. C. Orthogonality of Separation in Two-Dimensional Liquid Chromatography. *Analytical Chemistry* **2005**, *77* (19), 6426-6434. DOI: 10.1021/ac050923i.
- (146) Yeung, D.; Mizero, B.; Gussakovsky, D.; Klaassen, N.; Lao, Y.; Spicer, V.; Krokhin, O. V. Separation Orthogonality in Liquid Chromatography–Mass Spectrometry for Proteomic Applications: Comparison of 16 Different Two-Dimensional Combinations. *Analytical Chemistry* **2020**, *92* (5), 3904-3912. DOI: 10.1021/acs.analchem.9b05407.
- (147) Zhou, S.; Hu, Y.; Veillon, L.; Snovida, S. I.; Rogers, J. C.; Saba, J.; Mechref, Y. Quantitative LC-MS/MS Glycomic Analysis of Biological Samples Using AminoxyTMT. *Anal Chem* **2016**, *88* (15), 7515-7522. DOI: 10.1021/acs.analchem.6b00465 From NLM Medline.
- (148) Suzuki, N.; Abe, T.; Natsuka, S. Quantitative LC-MS and MS/MS analysis of sialylated glycans modified by linkage-specific alkylamidation. *Anal Biochem* **2019**, *567*, 117-127. DOI: 10.1016/j.ab.2018.11.014 From NLM Medline.
- (149) Ruhaak, L. R.; Miyamoto, S.; Lebrilla, C. B. Developments in the identification of glycan biomarkers for the detection of cancer. *Mol Cell Proteomics* **2013**, *12* (4), 846-855. DOI: 10.1074/mcp.R112.026799 From NLM Medline.
- (150) Jin, M.; Kim, J.; Ha, J.; Kim, A.; Lee, J.; Park, C. S.; Kang, M.; Kim, J.; Mun, C.; Kim, J.; et al. Identification and quantification of sialylated and core-fucosylated N-glycans in human transferrin by UPLC and LC-MS/MS. *Anal Biochem* **2022**, *647*, 114650. DOI: 10.1016/j.ab.2022.114650 From NLM Medline.

- (151) Tao, S.; Huang, Y.; Boyes, B. E.; Orlando, R. Liquid chromatography-selected reaction monitoring (LC-SRM) approach for the separation and quantitation of sialylated N-glycans linkage isomers. *Anal Chem* **2014**, *86* (21), 10584-10590. DOI: 10.1021/ac5020996 From NLM.
- (152) Hemstrom, P.; Irgum, K. Hydrophilic interaction chromatography. *J Sep Sci* **2006**, *29* (12), 1784-1821. DOI: 10.1002/jssc.200600199 From NLM Medline.
- (153) Failla, S.; Contò, M.; Miarelli, M. Variability of sialic acids in meat from alternative species to beef and pork. *Animal Frontiers* **2023**, *13* (6), 15-23. DOI: 10.1093/af/vfad058 (accessed 6/10/2025).
- (154) Tangvoranuntakul, P.; Gagneux, P.; Diaz, S.; Bardor, M.; Varki, N.; Varki, A.; Muchmore, E. Human uptake and incorporation of an immunogenic nonhuman dietary sialic acid. *Proc Natl Acad Sci U S A* **2003**, *100* (21), 12045-12050. DOI: 10.1073/pnas.2131556100 From NLM.
- (155) Dhar, C.; Sasmal, A.; Varki, A. From "Serum Sickness" to "Xenosialitis": Past, Present, and Future Significance of the Non-human Sialic Acid Neu5Gc. *Front Immunol* **2019**, *10*, 807. DOI: 10.3389/fimmu.2019.00807 From NLM.
- (156) Zauner, G.; Deelder, A. M.; Wuhrer, M. Recent advances in hydrophilic interaction liquid chromatography (HILIC) for structural glycomics. *Electrophoresis* **2011**, *32* (24), 3456-3466. DOI: 10.1002/elps.201100247 From NLM.
- (157) Bones, J.; Mittermayr, S.; O'Donoghue, N.; Guttman, A.; Rudd, P. M. Ultra Performance Liquid Chromatographic Profiling of Serum N-Glycans for Fast and Efficient Identification of Cancer Associated Alterations in Glycosylation. *Analytical Chemistry* **2010**, *82* (24), 10208-10215. DOI: 10.1021/ac102860w.
- (158) Shang, T. Q.; Saati, A.; Toler, K. N.; Mo, J.; Li, H.; Matlosz, T.; Lin, X.; Schenk, J.; Ng, C. K.; Duffy, T.; et al. Development and Application of a Robust N-Glycan Profiling Method for Heightened Characterization of Monoclonal Antibodies and Related Glycoproteins. *Journal of Pharmaceutical Sciences* **2014**, *103* (7), 1967-1978. DOI: https://doi.org/10.1002/jps.24004.
- (159) Segu, Z.; Todd, S.; Claudia, B.; Anthony, R.; Emma, D.; and Li, Y. A rapid method for relative quantification of N-glycans from a therapeutic monoclonal antibody during trastuzumab biosimilar development. *mAbs* **2020**, *12* (1), 1750794. DOI: 10.1080/19420862.2020.1750794.
- (160) Pallister, E. G.; Choo, M. S. F.; Walsh, I.; Tai, J. N.; Tay, S. J.; Yang, Y. S.; Ng, S. K.; Rudd, P. M.; Flitsch, S. L.; Nguyen-Khuong, T. Utility of Ion-Mobility Spectrometry for Deducing Branching of Multiply Charged Glycans and Glycopeptides in a High-Throughput Positive ion LC-FLR-IMS-MS Workflow. *Anal Chem* **2020**, *92* (23), 15323-15335. DOI: 10.1021/acs.analchem.0c01954 From NLM.
- (161) Wang, C.; Gao, X.; Gong, G.; Man, L.; Wei, Q.; Lan, Y.; Yang, M.; Han, J.; Jin, W.; Wei, M.; et al. A versatile strategy for high-resolution separation of reducing glycan mixtures as hydrazones by two-dimensional high-performance liquid chromatography. *Journal of Chromatography A* **2022**, *1685*, 463599. DOI: https://doi.org/10.1016/j.chroma.2022.463599.
- (162) Fenn, L. S.; McLean, J. A. Structural separations by ion mobility-MS for glycomics and glycoproteomics. *Methods Mol Biol* **2013**, *951*, 171-194. DOI: 10.1007/978-1-62703-146-2_12 From NLM.

- (163) Bansal, P.; Ben Faleh, A.; Warnke, S.; Rizzo, T. R. Identification of N-glycan positional isomers by combining IMS and vibrational fingerprinting of structurally determinant CID fragments. *Analyst* **2022**, *147* (4), 704-711. DOI: 10.1039/d1an01861b From NLM.
- (164) Jones, J. Y. a. A. Streamlined Workflows for N-Glycan Analysis of Biotherapeutics Using Agilent AdvanceBio Gly-X InstantPC and 2-AB Express Sample Preparation with LC/FLD/MS. Agilent Technologies, Inc.: 2021.
- (165) Manz, C.; Götze, M.; Frank, C.; Zappe, A.; Pagel, K. Dextran as internal calibrant for N-glycan analysis by liquid chromatography coupled to ion mobility-mass spectrometry. *Anal Bioanal Chem* **2022**, *414* (17), 5023-5031. DOI: 10.1007/s00216-022-04133-0 From NLM.
- (166) Li, A.; Conant, C. R.; Zheng, X.; Bloodsworth, K. J.; Orton, D. J.; Garimella, S. V. B.; Attah, I. K.; Nagy, G.; Smith, R. D.; Ibrahim, Y. M. Assessing Collision Cross Section Calibration Strategies for Traveling Wave-Based Ion Mobility Separations in Structures for Lossless Ion Manipulations. *Analytical Chemistry* **2020**, *92* (22), 14976-14982. DOI: 10.1021/acs.analchem.0c02829.
- (167) Palmisano, G.; Larsen, M. R.; Packer, N. H.; Thaysen-Andersen, M. Structural analysis of glycoprotein sialylation part II: LC-MS based detection. *RSC Advances* **2013**, *3* (45), 22706-22726, 10.1039/C3RA42969E. DOI: 10.1039/C3RA42969E.
- (168) Emily Betchy, B. B. a. R. O. Development of a Hydrophilic Interaction Liquid Chromatography Retention Model for Procainamide Tagged N-linked Glycans. *Chromatography Today* **2017**.
- (169) Seeberger, P. H.; Freedberg, D. I.; Cummings, R. D. Glycans in Biotechnology and the Pharmaceutical Industry. In *Essentials of Glycobiology*, 4th ed.; Varki, A., Cummings, R. D., Esko, J. D., Stanley, P., Hart, G. W., Aebi, M., Mohnen, D., Kinoshita, T., Packer, N. H., Prestegard, J. H., et al. Eds.; 2022; pp 771-784.
- (170) Santell, L.; Ryll, T.; Etcheverry, T.; Santoris, M.; Dutina, G.; Wang, A.; Gunson, J.; Warner, T. G. Aberrant metabolic sialylation of recombinant proteins expressed in Chinese hamster ovary cells in high productivity cultures. *Biochem Biophys Res Commun* **1999**, *258* (1), 132-137. DOI: 10.1006/bbrc.1999.0550 From NLM.
- (171) Lin, N.; Mascarenhas, J.; Sealover, N. R.; George, H. J.; Brooks, J.; Kayser, K. J.; Gau, B.; Yasa, I.; Azadi, P.; Archer-Hartmann, S. Chinese hamster ovary (CHO) host cell engineering to increase sialylation of recombinant therapeutic proteins by modulating sialyltransferase expression. *Biotechnol Prog* **2015**, *31* (2), 334-346. DOI: 10.1002/btpr.2038 From NLM.
- (172) Liu, S.; Gao, W.; Wang, Y.; He, Z.; Feng, X.; Liu, B. F.; Liu, X. Comprehensive N-Glycan Profiling of Cetuximab Biosimilar Candidate by NP-HPLC and MALDI-MS. *PLoS One* **2017**, *12* (1), e0170013. DOI: 10.1371/journal.pone.0170013 From NLM.
- (173) Váradi, C.; Jakes, C.; Bones, J. Analysis of cetuximab N-Glycosylation using multiple fractionation methods and capillary electrophoresis mass spectrometry. *Journal of Pharmaceutical and Biomedical Analysis* **2020**, *180*, 113035. DOI: https://doi.org/10.1016/j.jpba.2019.113035.
- (174) She, Y.-M.; Dai, S.; Tam, R. Y. Highly sensitive characterization of non-human glycan structures of monoclonal antibody drugs utilizing tandem mass spectrometry. *Scientific Reports* **2022**, *12* (1), 15109. DOI: 10.1038/s41598-022-19488-8.

- (175) Lu, G.; Crihfield, C. L.; Gattu, S.; Veltri, L. M.; Holland, L. A. Capillary Electrophoresis Separations of Glycans. *Chemical Reviews* **2018**, *118* (17), 7867-7885. DOI: 10.1021/acs.chemrev.7b00669.
- (176) Guo, R.-R.; Lageveen-Kammeijer, G. S. M.; Wang, W.; Dalebout, H.; Zhang, W.; Wuhrer, M.; Liu, L.; Heijs, B.; Voglmeir, J. Analysis of Immunogenic Galactose-α-1,3-galactose-Containing N-Glycans in Beef, Mutton, and Pork Tenderloin by Combining Matrix-Assisted Laser Desorption/Ionization-Mass Spectroscopy and Capillary Electrophoresis Hyphenated with Mass Spectrometry via Electrospray Ionization. *Journal of Agricultural and Food Chemistry* **2023**, *71* (9), 4184-4192. DOI: 10.1021/acs.jafc.2c08067.
- (177) Trappe, A.; Füssl, F.; Millán-Martín, S.; Ronan, R.; Zaborowska, I.; Bones, J. Correlative N-glycan and charge variant analysis of cetuximab expressed in murine, chinese hamster and human expression systems. *Journal of Chromatography B* **2022**, *1194*, 123186. DOI: https://doi.org/10.1016/j.jchromb.2022.123186.
- (178) Attah, I. K.; Nagy, G.; Garimella, S. V. B.; Norheim, R. V.; Anderson, G. A.; Ibrahim, Y. M.; Smith, R. D. Traveling-Wave-Based Electrodynamic Switch for Concurrent Dual-Polarity Ion Manipulations in Structures for Lossless Ion Manipulations. *Analytical Chemistry* **2019**, *91* (22), 14712-14718. DOI: 10.1021/acs.analchem.9b03987.
- (179) Nagy, G.; Attah, I. K.; Conant, C. R.; Liu, W.; Garimella, S. V. B.; Gunawardena, H. P.; Shaw, J. B.; Smith, R. D.; Ibrahim, Y. M. Rapid and Simultaneous Characterization of Drug Conjugation in Heavy and Light Chains of a Monoclonal Antibody Revealed by High-Resolution Ion Mobility Separations in SLIM. *Analytical Chemistry* **2020**, *92* (7), 5004-5012. DOI: 10.1021/acs.analchem.9b05209.
- (180) Walsh, G. Post-translational modifications of protein biopharmaceuticals. *Drug Discovery Today* **2010**, *15* (17), 773-780. DOI: https://doi.org/10.1016/j.drudis.2010.06.009.
- (181) Solá, R. J.; Griebenow, K. Glycosylation of therapeutic proteins: an effective strategy to optimize efficacy. *BioDrugs* **2010**, *24* (1), 9-21. DOI: 10.2165/11530550-000000000-00000 From NLM.
- (182) Li, H.; d'Anjou, M. Pharmacological significance of glycosylation in therapeutic proteins. *Current Opinion in Biotechnology* **2009**, *20* (6), 678-684. DOI: https://doi.org/10.1016/j.copbio.2009.10.009.
- (183) Zhang, P.; Woen, S.; Wang, T.; Liau, B.; Zhao, S.; Chen, C.; Yang, Y.; Song, Z.; Wormald, M. R.; Yu, C.; et al. Challenges of glycosylation analysis and control: an integrated approach to producing optimal and consistent therapeutic drugs. *Drug Discovery Today* **2016**, *21* (5), 740-765. DOI: https://doi.org/10.1016/j.drudis.2016.01.006.
- (184) Yang, X.; Bartlett, M. G. Glycan analysis for protein therapeutics. *Journal of Chromatography B* **2019**, *1120*, 29-40. DOI: https://doi.org/10.1016/j.jchromb.2019.04.031.
- (185) Oh, M. J.; Seo, Y.; Seo, N.; An, H. J. MS-Based Glycome Characterization of Biotherapeutics With N- and O-Glycosylation. *Mass Spectrom Rev* **2025**. DOI: 10.1002/mas.21925 From NLM.
- (186) Pallister, E. G.; Choo, M. S. F.; Walsh, I.; Tai, J. N.; Tay, S. J.; Yang, Y. S.; Ng, S. K.; Rudd, P. M.; Flitsch, S. L.; Nguyen-Khuong, T. Utility of Ion-Mobility Spectrometry for Deducing Branching of Multiply Charged Glycans and Glycopeptides in a High-Throughput Positive ion LC-FLR-IMS-MS Workflow. *Analytical Chemistry* **2020**, *92* (23), 15323-15335. DOI: 10.1021/acs.analchem.0c01954.

- (187) Manz, C.; Mancera-Arteu, M.; Zappe, A.; Hanozin, E.; Polewski, L.; Giménez, E.; Sanz-Nebot, V.; Pagel, K. Determination of Sialic Acid Isomers from Released N-Glycans Using Ion Mobility Spectrometry. *Anal Chem* **2022**, *94* (39), 13323-13331. DOI: 10.1021/acs.analchem.2c00783 From NLM.
- (188) Leijdekkers, A. G. M.; Huang, J.-H.; Bakx, E. J.; Gruppen, H.; Schols, H. A. Identification of novel isomeric pectic oligosaccharides using hydrophilic interaction chromatography coupled to traveling-wave ion mobility mass spectrometry. *Carbohydrate Research* **2015**, 404, 1-8. DOI: https://doi.org/10.1016/j.carres.2014.12.003.
- (189) Avcı, İ.; Mehmet, A.; Mehmet, K. H.; and Salih, B. Characterization of Monoclonal Antibody N-Glycan Conformations by Novel Hydrophilic Interaction Liquid Chromatography (HILIC) with Trapped Ion Mobility Mass Spectrometry (TIMS) and Fluorescence Detection (FLD). *Analytical Letters* **2025**, *58* (12), 2158-2173. DOI: 10.1080/00032719.2024.2384700.
- (190) Manabe, N.; Ohno, S.; Matsumoto, K.; Kawase, T.; Hirose, K.; Masuda, K.; Yamaguchi, Y. A Data Set of Ion Mobility Collision Cross Sections and Liquid Chromatography Retention Times from 71 Pyridylaminated N-Linked Oligosaccharides. *J Am Soc Mass Spectrom* **2022**, *33* (9), 1772-1783. DOI: 10.1021/jasms.2c00165 From NLM.
- (191) Campbell, M. P.; Royle, L.; Radcliffe, C. M.; Dwek, R. A.; Rudd, P. M. GlycoBase and autoGU: tools for HPLC-based glycan analysis. *Bioinformatics* **2008**, *24* (9), 1214-1216. DOI: 10.1093/bioinformatics/btn090 (accessed 6/9/2025).
- (192) Royle, L.; Campbell, M. P.; Radcliffe, C. M.; White, D. M.; Harvey, D. J.; Abrahams, J. L.; Kim, Y.-G.; Henry, G. W.; Shadick, N. A.; Weinblatt, M. E.; et al. HPLC-based analysis of serum N-glycans on a 96-well plate platform with dedicated database software. *Analytical Biochemistry* **2008**, *376* (1), 1-12. DOI: https://doi.org/10.1016/j.ab.2007.12.012.
- (193) Badgett, M. J.; Mize, E.; Fletcher, T.; Boyes, B.; Orlando, R. Predicting the HILIC Retention Behavior of the N-Linked Glycopeptides Produced by Trypsin Digestion of Immunoglobulin Gs (IgGs). *J Biomol Tech* **2018**, *29* (4), 98-104. DOI: 10.7171/jbt.18-2904-002 From NLM.
- (194) Stow, S. M.; Causon, T. J.; Zheng, X.; Kurulugama, R. T.; Mairinger, T.; May, J. C.; Rennie, E. E.; Baker, E. S.; Smith, R. D.; McLean, J. A.; et al. An Interlaboratory Evaluation of Drift Tube Ion Mobility-Mass Spectrometry Collision Cross Section Measurements. *Anal Chem* **2017**, *89* (17), 9048-9055. DOI: 10.1021/acs.analchem.7b01729 From NLM.
- (195) Hofmann, J.; Struwe, W. B.; Scarff, C. A.; Scrivens, J. H.; Harvey, D. J.; Pagel, K. Estimating Collision Cross Sections of Negatively Charged N-Glycans using Traveling Wave Ion Mobility-Mass Spectrometry. *Analytical Chemistry* **2014**, *86* (21), 10789-10795. DOI: 10.1021/ac5028353.
- (196) Kim, J. Y.; Kim, Y. G.; Lee, G. M. CHO cells in biotechnology for production of recombinant proteins: current state and further potential. *Appl Microbiol Biotechnol* **2012**, *93* (3), 917-930. DOI: 10.1007/s00253-011-3758-5 From NLM.
- (197) Tan, E.; Chin, C. S. H.; Lim, Z. F. S.; Ng, S. K. HEK293 Cell Line as a Platform to Produce Recombinant Proteins and Viral Vectors. *Front Bioeng Biotechnol* **2021**, *9*, 796991. DOI: 10.3389/fbioe.2021.796991 From NLM.
- (198) Chung Christine, H.; Mirakhur, B.; Chan, E.; Le, Q.-T.; Berlin, J.; Morse, M.; Murphy Barbara, A.; Satinover Shama, M.; Hosen, J.; Mauro, D.; et al. Cetuximab-Induced

- Anaphylaxis and IgE Specific for Galactose-α-1,3-Galactose. *New England Journal of Medicine 358* (11), 1109-1117. DOI: 10.1056/NEJMoa074943 (accessed 2025/06/09).
- (199) Ghaderi, D.; Taylor, R. E.; Padler-Karavani, V.; Diaz, S.; Varki, A. Implications of the presence of N-glycolylneuraminic acid in recombinant therapeutic glycoproteins. *Nature Biotechnology* **2010**, *28* (8), 863-867. DOI: 10.1038/nbt.1651.
- (200) Giddings, J. C. Maximum number of components resolvable by gel filtration and other elution chromatographic methods. *Analytical Chemistry* **1967**, *39* (8), 1027-1028. DOI: 10.1021/ac60252a025.
- (201) Horvath, C. G.; Lipsky, S. R. Peak capacity in chromatography. *Analytical Chemistry* **1967**, *39* (14), 1893-1893. DOI: 10.1021/ac50157a075.
- (202) Karpievitch, Y. V.; Polpitiya, A. D.; Anderson, G. A.; Smith, R. D.; Dabney, A. R. Liquid Chromatography Mass Spectrometry-Based Proteomics: Biological and Technological Aspects. *Ann Appl Stat* **2010**, *4* (4), 1797-1823. DOI: 10.1214/10-aoas341 From NLM.
- (203) Shi, Y.; Xiang, R.; Horváth, C.; Wilkins, J. A. The role of liquid chromatography in proteomics. *Journal of Chromatography A* **2004**, *1053* (1), 27-36. DOI: https://doi.org/10.1016/j.chroma.2004.07.044.
- (204) Hu, Y.; Mechref, Y. Comparing MALDI-MS, RP-LC-MALDI-MS and RP-LC-ESI-MS glycomic profiles of permethylated N-glycans derived from model glycoproteins and human blood serum. *Electrophoresis* **2012**, *33* (12), 1768-1777. DOI: 10.1002/elps.201100703 From NLM Medline.
- (205) Reusch, D.; Markus, H.; David, F.; Britta, P.; Bernd, M.; Jana, G.; Michaela, H.; Katharina, W.; Lea, B.; Patrick, B.; et al. Comparison of methods for the analysis of therapeutic immunoglobulin G Fc-glycosylation profiles—Part 2: Mass spectrometric methods. *mAbs* **2015**, *7* (4), 732-742. DOI: 10.1080/19420862.2015.1045173.
- (206) Gritti, F.; Guiochon, G. Optimization of the peak capacity per unit time. *Journal of Chromatography A* **2012**, *1263*, 125-140. DOI: https://doi.org/10.1016/j.chroma.2012.09.040.
- (207) Gilar, M.; Neue, U. D. Peak capacity in gradient reversed-phase liquid chromatography of biopolymers: Theoretical and practical implications for the separation of oligonucleotides. *Journal of Chromatography A* **2007**, *1169* (1), 139-150. DOI: https://doi.org/10.1016/j.chroma.2007.09.005.
- (208) Link, A. J.; Eng, J.; Schieltz, D. M.; Carmack, E.; Mize, G. J.; Morris, D. R.; Garvik, B. M.; Yates, J. R. Direct analysis of protein complexes using mass spectrometry. *Nature Biotechnology* **1999**, *17* (7), 676-682. DOI: 10.1038/10890.
- (209) Vivó-Truyols, G.; van der Wal, S.; Schoenmakers, P. J. Comprehensive Study on the Optimization of Online Two-Dimensional Liquid Chromatographic Systems Considering Losses in Theoretical Peak Capacity in First- and Second-Dimensions: A Pareto-Optimality Approach. *Analytical Chemistry* **2010**, *82* (20), 8525-8536. DOI: 10.1021/ac101420f.
- (210) Sarrut, M.; D'Attoma, A.; Heinisch, S. Optimization of conditions in on-line comprehensive two-dimensional reversed phase liquid chromatography. Experimental comparison with one-dimensional reversed phase liquid chromatography for the separation of peptides. *Journal of Chromatography A* **2015**, *1421*, 48-59. DOI: https://doi.org/10.1016/j.chroma.2015.08.052.
- (211) Giddings, J. C. Two-dimensional separations: concept and promise. *Analytical Chemistry* **1984**, *56* (12), 1258A-1270A. DOI: 10.1021/ac00276a003.

- (212) Zhu, K.; Pursch, M.; Eeltink, S.; Desmet, G. Maximizing two-dimensional liquid chromatography peak capacity for the separation of complex industrial samples. *Journal of Chromatography A* **2020**, *1609*, 460457. DOI: https://doi.org/10.1016/j.chroma.2019.460457.
- (213) Fairchild, J. N.; Horváth, K.; Guiochon, G. Approaches to comprehensive multidimensional liquid chromatography systems. *Journal of Chromatography A* **2009**, *1216* (9), 1363-1371. DOI: https://doi.org/10.1016/j.chroma.2008.12.073.
- (214) Motoyama, A.; Yates, J. R., III. Multidimensional LC Separations in Shotgun Proteomics. *Analytical Chemistry* **2008**, *80* (19), 7187-7193. DOI: 10.1021/ac8013669.
- (215) Stoll, D. R.; Carr, P. W. Two-Dimensional Liquid Chromatography: A State of the Art Tutorial. *Analytical Chemistry* **2017**, *89* (1), 519-531. DOI: 10.1021/acs.analchem.6b03506.
- (216) Valentine, S. J.; Plasencia, M. D.; Liu, X.; Krishnan, M.; Naylor, S.; Udseth, H. R.; Smith, R. D.; Clemmer, D. E. Toward Plasma Proteome Profiling with Ion Mobility-Mass Spectrometry. *Journal of Proteome Research* **2006**, *5* (11), 2977-2984. DOI: 10.1021/pr060232i.
- (217) Leijdekkers, A. G.; Huang, J. H.; Bakx, E. J.; Gruppen, H.; Schols, H. A. Identification of novel isomeric pectic oligosaccharides using hydrophilic interaction chromatography coupled to traveling-wave ion mobility mass spectrometry. *Carbohydr Res* **2015**, *404*, 1-8. DOI: 10.1016/j.carres.2014.12.003 From NLM.
- (218) Aguilar, M.-I.; Hearn, M. T. W. [1] High-resolution reversed-phase high-performance liquid chromatography of peptides and proteins. In *Methods in Enzymology*, Vol. 270; Academic Press, 1996; pp 3-26.
- (219) Josic, D.; Kovac, S. Reversed-phase High Performance Liquid Chromatography of proteins. *Curr Protoc Protein Sci* **2010**, *Chapter 8*, 8.7.1-8.7.22. DOI: 10.1002/0471140864.ps0807s61 From NLM.
- (220) Boersema, P. J.; Mohammed, S.; Heck, A. J. Hydrophilic interaction liquid chromatography (HILIC) in proteomics. *Anal Bioanal Chem* **2008**, *391* (1), 151-159. DOI: 10.1007/s00216-008-1865-7 From NLM.
- (221) Badgett, M. J.; Boyes, B.; Orlando, R. Peptide retention prediction using hydrophilic interaction liquid chromatography coupled to mass spectrometry. *J Chromatogr A* **2018**, *1537*, 58-65. DOI: 10.1016/j.chroma.2017.12.055 From NLM.